5-2009

Classification of subwatershed slopes and geotechnical characterization of steep slopes on reclaimed mine lands in East Tennessee

Patrick Hamilton White
University of Tennessee

To the Graduate Council:

I am submitting herewith a thesis written by Patrick Hamilton White entitled "Classification of subwatershed slopes and geotechnical characterization of steep slopes on reclaimed mine lands in East Tennessee." I have examined the final electronic copy of this thesis for form and content and recommend that it be accepted in partial fulfillment of the requirements for the degree of Master of Science, with a major in Civil Engineering.

Eric Drumm, Major Professor

We have read this thesis and recommend its acceptance:

Accepted for the Council:
Carolyn R. Hodges

Vice Provost and Dean of the Graduate School

(Original signatures are on file with official student records.)

To the Graduate Council:

I am submitting herewith a thesis written by Patrick Hamilton White entitled "Hill-slope Classification and Geotechnical Characterization of Steep Slopes in Reclaimed Mine Lands in East Tennessee." I have examined the final electronic copy of this thesis for form and content and recommend that it be accepted in partial fulfillment of the requirements for the degree of Master of Science with a major in Civil Engineering.

Dr. Eric Drumm, Major Professor

We have read this thesis
and recommend its acceptance:

Dr. Eric Drumm

Dr. John Schwartz

Dr. Baoshan Huang

Accepted for the Council:

Carolyn R. Hodges, Vice Provost and Dean of the Graduate School

Classification of Subwatershed Slopes and Geotechnical Characterization of Steep Slopes on Reclaimed Mine Lands in East Tennessee

A Thesis Presented for
the Master of Science
Degree
The University of Tennessee, Knoxville

Patrick Hamilton White
May 2009

ABSTRACT

Mining and logging activity in the Appalachian region create both excessive runoff and sedimentation in local streams and rivers. Also, the Surface Mining Control and Reclamation Act of 1977 led to over compaction of mine spoil which has led to reclaimed mine lands which will not grow economically viable native hardwood forests. In recent years a construction technique known as low compaction grading has allowed for suitable tree growth but stability and sedimentation have not yet been explored. The purpose of this paper is to create a rapid assessment method to classify the characteristics of watersheds based upon their geomorphology, and then to match this process to the established Rapid Geomorphic Assessment (RGA) method; these methods are intended to correspond to the tendency for a given slope to produce sediment. Also, this research attempts to match upland disturbance areas common in East Tennessee to sediment production characteristics. Lastly, mine spoil physical characteristics were determined and used to determine slope stability on steep reclaimed mine slopes using the low compaction grading technique, and to determine the medium's suitability for tree growth. No correlations were found between the developed Rapid Slope Assessment and the established RGA method. Sediment production characteristics were measured and compared for several land use disturbance areas common to East Tennessee and it was determined that logging roads were the most prone to high sediment production and then mining roads, logged areas, and mined areas followed in that order. Lastly, dry and wet unit weights, moisture contents, and grain size distributions were measured for reclaimed mine slopes using the low compaction grading method, and slope stability was assessed using an infinite slope analysis. It was determined that the nuclear density gauge was the most reliable and convenient way to measure unit weight. Furthermore the factor of safety against slope failure ranged from 1.9 to 1.4. These relatively low factors of safety are acceptable due to the low cost and consequence of slope failure on surface mine sites.

Table of Contents

I. Introduction

A. History of Surface Mining

Surface coal mining has been commercialized in the Appalachian region since the 1740's (Committee, 1981). Compared to underground coal mining, surface mining generally costs less, is safer for miners, and usually results in more complete recovery of the coal. However, it also results in much more extensive disturbance of the land, which can cause serious environmental problems unless proper controls are thoroughly followed and the mined land is carefully reclaimed (Angel et al. 2005). Prior to 1977 the overburden material, or spoil, was typically displaced downhill of the mining operation. This led to excessive sediment in stream and rivers near to mining operations and to the creation of the Surface Mining Control and Reclamation Act of 1977 (Angel et al. 2005).

The Surface Mining Control and Reclamation Act of 1977 requires operators to obtain a permit to mine and post a bond which will not be remitted until the reclamation performance standards are met (Angel et al. 2005). With tough standards in place the easy solution for mine operators was to heavily compact the spoil material into the area which had just been mined (Angel et al., 2005). This led to very stable slopes which would not grow economically viable native hardwood forests due to the over-compaction of the rooting medium. Because previously mined slopes were not being reclaimed into native forests, the Appalachian Regional Reforestation Initiative (ARRI) was created which advocates using the Forestry Reclamation Approach (Angel et al. 2005).

B. Appalachian Regional Reforestation Initiative

The Forestry Reclamation Approach calls for a suitable rooting medium at least four feet deep comprised of uncompacted topsoil, sandstone, or the best available material (Burger et al., 2005). This four feet thick layer of uncompacted material is normally obtained using the low compaction grading technique. Low compaction grading places the spoil material back into place creating a strong compacted core with a top layer of uncompacted material (Sweigard et al. 2007). The first step is to place a layer of uncompacted material onto the bench created from the mining operations. This layer is then compacted and graded so that the dump trucks can travel onto it to place another layer and to place the loose material which will cover the outside of the first layer. These steps are repeated until the necessary height is reached and then the loose material on top is graded once with a small bulldozer to obtain the required slope. This process is illustrated in Figures I.1 and I.2 shown below. Figure I.1 (left) shows the placement of loose material over the compacted layers. Figure I.2 (right) shows the final grading performed after the placement of all layers and loose materials.

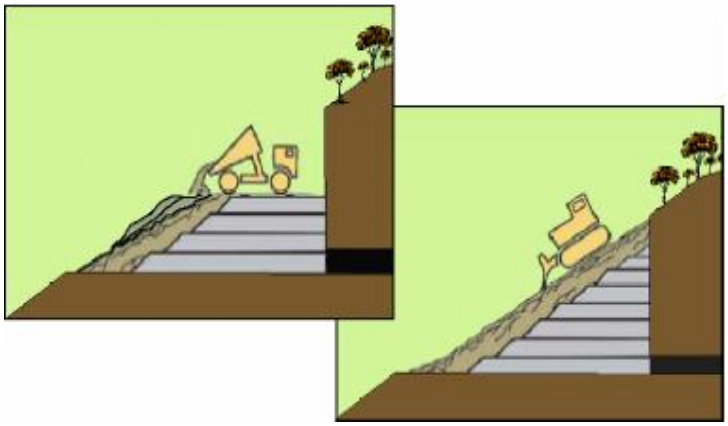

Figures I.1 and I.2 Low Compaction Grading Method (Sweigard et al, 2007)

C. Office of Surface Mining Applied Science Grants

The Office of Surface Mining (OSM) provided three research grants, under their applied science program, to the Department of Civil and Environmental Engineering to study runoff and stability issues in reclaimed surface mining areas. The first two of these three grants were an effort to improve models used for estimating sediment loads on a subwatershed scale. The objectives of these two grants were to identify different land-use disturbance areas to be used in a classification scheme and then to be related to GIS and field measurements. Also, the first two OSM applied science grants evaluated the use of a rapid geomorphic assessment technique and the models AnnAGNPS and ConCEPTS as sediment delivery and transport models respectively.

The third OSM applied science grant pertains to the bulk of this paper. Three reclaimed surface mine sites were chosen in East Tennessee to study stability, run-off, and sediment characteristics. These mine sites were all constructed using the low compaction grading technique discussed earlier and were constructed at a slope of 20 degrees or greater. The first site chosen was in Anderson County and was mined and constructed by Premium Coal Company. This site was a predominantly shale mix with some sandstone. The Premium site has a slope length of 120 feet and is divided by berms into four study areas which are approximately 75 feet in width. The average slope for this site was 28 degrees. The second site chosen was in Campbell County and was mined and constructed by National Coal Company. This site was a predominately sandstone mix with some shale, and had an average slope of 21 degrees. The National site has a slope length of 150 feet and is divided by berms into four study areas which are approximately 75 feet in width. The final site was in Claiborne County and was mined and constructed by Mountainside Coal Company. The Mountainside site is an even mix of sandstone and shale, and had an average slope of 28 degrees. This site has a slope length of 145 feet and is divided by berms into four study areas which are approximately 75 feet in width. Shown below in Figure I.3 are the coordinates for one of the three sites. All geographic coordinate data for all three sites may be seen in Appendix E.

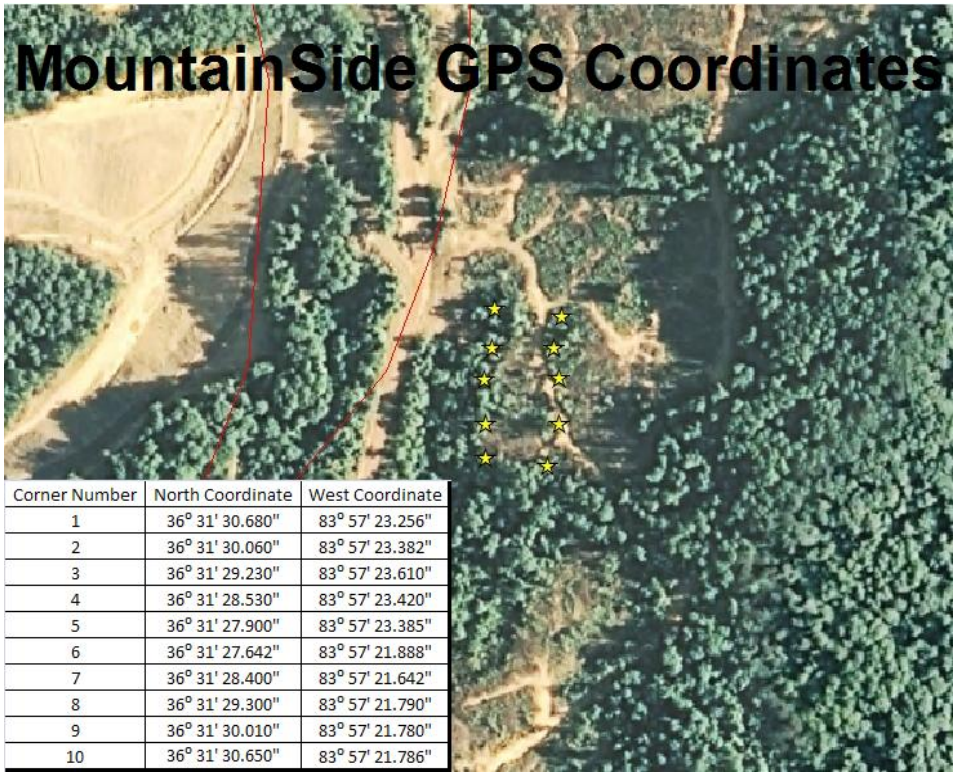

Corner Number	North Coordinate	West Coordinate
1	36° 31' 30.680"	83° 57' 23.256"
2	36° 31' 30.060"	83° 57' 23.382"
3	36° 31' 29.230"	83° 57' 23.610"
4	36° 31' 28.530"	83° 57' 23.420"
5	36° 31' 27.900"	83° 57' 23.385"
6	36° 31' 27.642"	83° 57' 21.888"
7	36° 31' 28.400"	83° 57' 21.642"
8	36° 31' 29.300"	83° 57' 21.790"
9	36° 31' 30.010"	83° 57' 21.780"
10	36° 31' 30.650"	83° 57' 21.786"

Figure I.3 Example of GPS Coordinates - Notice how the image was obtained prior to mining activity. All Raster images in GIS and Google Earth images used were the most up to date available.

D. Appalachian Spoil Characteristics

The expansion that occurs when overburden is excavated is responsible for the generation of much excess spoil (Committee, 1981). Excess spoil includes a variety of geologic materials ranging from rocks like sandstone, limestone, shale, claystone, and siltstone to unconsolidated materials like sand, silt, clay and soil. In Appalachia, spoil mostly consists of sandstone with some shale, claystone, and limestone. Most of the material is shale and sandstone (Committee, 1981).

Classification of Subwatershed Slopes

Abstract

Mining and logging activity in the Appalachian region create both excessive runoff and sedimentation in local streams and rivers. The New River Watershed was studied to determine the sediment production characteristics. A hill slope classification scheme was developed to characterize the sediment production of each subwatershed based upon its shape. The scheme was based on overall relief, gradient, and concavity. Also, samples were taken from several subwatersheds to determine the sediment production characteristics based upon a specific land use disturbance. Land uses which were tested include mining roads, logging roads, logged areas, and mined areas. No correlation was found between the developed Rapid Slope Assessment method and the established Rapid Geomorphic Assessment method. It was determined that logging roads were the most prone to high sediment production and then mining roads, logged areas, and mined areas followed in that order.

II. Classification of Subwatershed Slopes

A. Study Objectives

Mining and logging activity in the Appalachian region have created both excessive runoff and sedimentation in local streams and rivers. The New River Watershed was studied to determine the sediment production characteristics based upon the shape of the watershed. A hill slope classification scheme was developed to characterize the sediment production of each subwatershed based upon its shape. The scheme was based on overall relief, gradient, and concavity. Also, samples were taken from several subwatersheds to determine the sediment production characteristics based upon a specific land use disturbance. Land uses which were tested include mining roads, logging roads, logged areas, and mined areas.

B. Penetrometers

A Cole Parmer model EW-99039-00 pocket penetrometer and a Hogentogler model S-4615 cone penetrometer were used in this research to conclude the undrained shear strength of surface soils likely to contribute to sedimentation. The Cole Parmer pocket penetrometer is a lightweight, spring-operated penetrometer, which quickly measures the compressive soil strength (Cole Parmer, 2009). This tool reads out the approximate compressive strength of the soil in tons per square foot based on the resistance provided which is calibrated to the spring constant of the spring within the device. Shown below on the left in Figure II.1 is the Cole Parmer EW-99039-00 pocket penetrometer used in testing; on the right in Figure II.2 is the Hogentogler model S-4615 cone penetrometer used.

Figure II.1 Pocket Penetrometer

Figure II.2 Cone Penetrometer

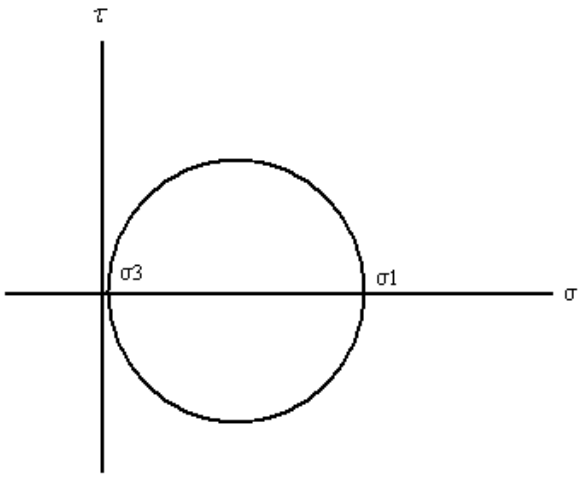

Figure II.3 Mohr's Circle for Near Surface Testing Using Penetrometers

The Hogentogler model S-4615 cone penetrometer measures the force required to push a 60 degree, 0.5 inch (12.7 mm) diameter, cone into the ground 1.16 inches measured by a proving ring. This can then be divided by the projected area of the cone to calculate the compressive strength of the soil (McCarthy, 2002). On a plot of shear stress versus normal stress the Mohr's Circle seen above in Figure II.3 can be created:

Where σ3 is the stress caused by overburden pressure, and therefore zero during surface testing, and σ1 is the compressive stress measured by the penetrometer. Through the geometry of this illustration it can be seen that the shear stress, τ , of the given soil will be half of the compressive stress measured by the penetrometer.

C. Sediment Production Assumptions

In Developing the hill-slope classification scheme discussed later and in the conclusion sections, certain assumptions were made about the sediment production characteristics of soils. These assumptions are listed as:

- Low plasticity clay content is an indicator of sediment production because this type of soil particle is not heavy and does not have enough plasticity to resist water run-off gradients.
- Low shear strength is an indicator of sediment production because soil uses its shear strength to overcome the forces of the water run-off gradient.
- Concave features are more likely to produce sediment than convex features because they collect water which increases the magnitude of the forces on the soil particles.
- Steeper slopes are more likely to produce sediment because of high velocity gradients applied to the soil particles.

These assumptions can be validated by common literature on the subject. The quantity and size of sediment material transported by channel flow are functions of flow velocity and turbulence, both of which increase as the slope steepens and the flow increases (Garcia, 2007). Increased accumulation of flow tends to increase erosion (Garcia, 2007). The larger the eroding material, the greater the velocity and turbulence must be to transport it (Garcia, 2007). The physical properties of the soil affect both the detachment and transportation characteristics during erosion (Garcia, 2007).

C. Hill-slope Classification Scheme

To classify the hill-slopes with respect to the tendency to produce sediment, a rapid slope assessment (RSA) method was developed. The system was modeled after the Rapid Geomorphic Assessment (RGA) method used to characterize the geomorphology of streambeds. The classification system was based on three elements determined from each of the 48 basins for which the RGA's were performed. RGA calculations were provided through OSM Applied Science Contract # CT612054 (Schwartz et al. 2008). Table A.1 found in Appendix A provides the correlation between the RSA basin identification numbers (1-48), the RGA site or field identification (FID) numbers, and name of the subwatershed associated with each. Table A.1 also provides the reverse correlation from RSA basin number to RGA site number in the right column. The RSA was estimated for the entire basin down to the RGA site. Not all RGA sites of the total 57 study sites were used for the RSA analysis because some RGA locations were too close in proximity and did not allow for notably different basin delineation.

Three elements or parameters were chosen as a reasonable representation of the geometry and shape of the landforms, yet they can be determined rapidly and relatively objectively from existing GIS layers. These elements are:

- Gradient or slope of the ground surface as determined from analysis within the GIS,
- Overall relief of the watershed, as determined as the difference in elevation from the outlet RGA point and the mean of 2 to 3 highest peaks found in the watershed, and,
- Proportion of the surface area that is judged to be concave along the length of the slope, expressed as a percentage of the total watershed (subwatershed) surface area.

Each of these elements is discussed below, followed by the discussion of the determination of the RSA score.

Gradient Score (GS): For each RSA/RGA basin, the 30 meter digital elevation map (DEM) data from the USGS Seamless Database was processed within the GIS to calculate the slope or gradient of the hill-slopes. The value of the gradient or change in slope over the 30 meter interval was expressed as a slope percentage and assigned to each area over which it was determined. An example of this can be seen in Figure II.4 below. The calculated gradients were then assigned to one of the ranges or "bins" of gradient values as shown in Table II.1. A score was assigned to each bin, with the greater slopes assigned a higher score reflecting the greater tendency to produce sediment.

The GS score was based on the integer 3 to the power of the bin value, factored by the proportion of the basin area with hill-slopes of that slope gradient value or:

$$\text{Gradient Score} = \text{GS} = \sum_{i=1}^{4} \left[3^{i} \times \text{Area}_{i}^{Normalized} \right]$$

where: i = Bin value = 1, 2, 3, or 4 depending upon the range in which the determined hill-slope gradient falls

$\text{Area}_i^{\text{Normalized}}$ = Area corresponding to bin i normalized by the total area of the RGA basin

Since all of the subwatersheds were predominantly in the range 8 to 35 percent slope, with only a relatively small percentage of surface area falling in the other ranges, the Gradient Scores did not cover a large range, varying only from about 20 to 28.

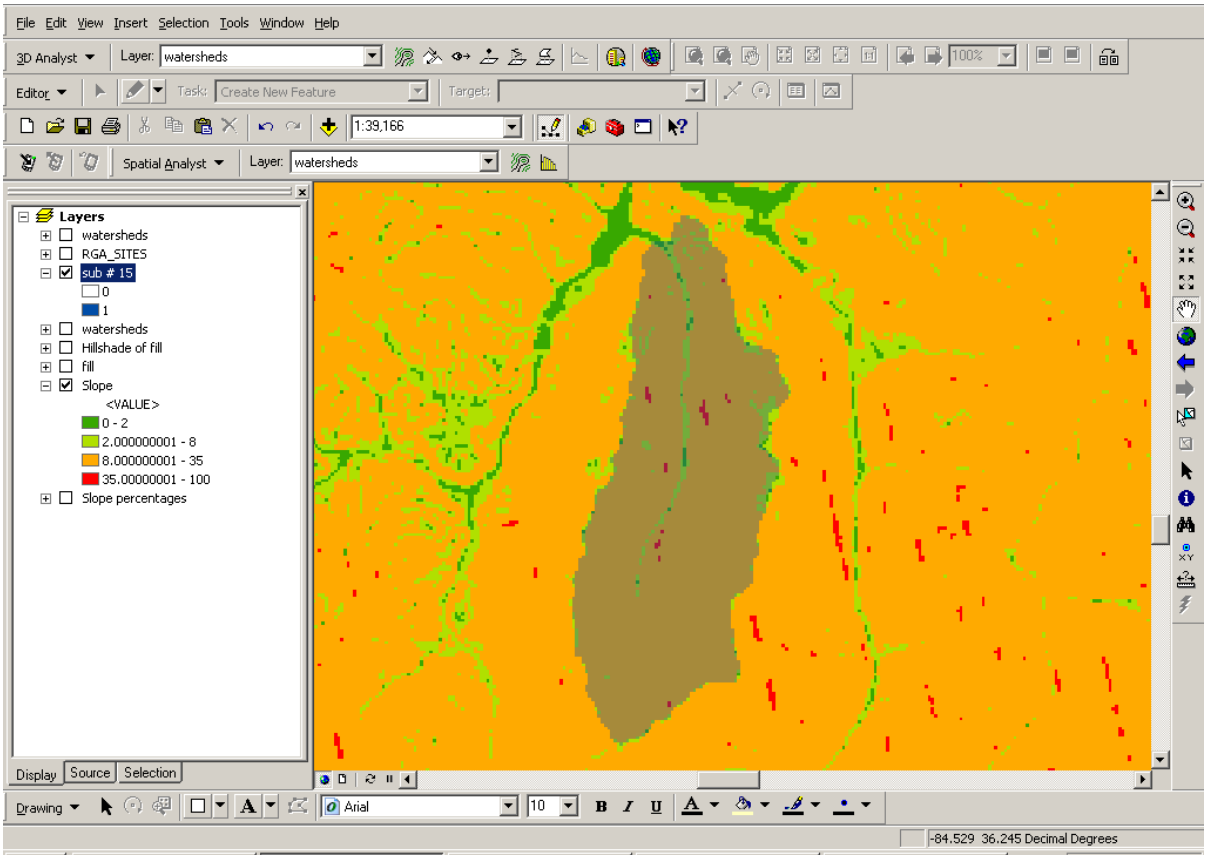

Figure II.4 Calculated Gradients and Associated Areas for RSA Basin #15. - The majority of Basin 15 (shaded in center of screen) is in the 8-35% slope range, but the basin shading has affected the orange coloring towards brown.

Table II.1. Determination of Gradient Score Assigned to Hill-Slopes.

Range of Gradients	Channel Morphology	Bin Value	Gradient Score
0 - 2 percent	Pool-riffle morphology	1	$3^1 = 3$
2 – 8 percent	Step pool morphology – low gradient headwaters	2	$3^2 = 9$
8 – 35 percent	Step pool morphology – high gradient headwaters	3	$3^3 = 27$
Greater than 35 percent	Approximation of 20-degree "steep" slope OSM definition	4	$3^4 = 81$

Relief Factor (RF): It was assumed that the greater the change in elevation or relief within a watershed, the more likely that sediment would be produced. The overall relief of the watershed was determined as the difference in elevation between the outlet RGA point and the mean of 2 to 3 highest peaks found in the watershed. The Relief Factor was determined as:

$$\text{Relief Factor} = RF = \frac{\text{relief (in feet)}}{1000\,\text{feet}}$$

Valley Score (VS): For each RGA basin, a sufficient number of coordinates to define the boundaries of the basin were located in the Google Earth web-based GIS. The Terrain feature was used, and the view was tilted and rotated to view the basin looking upstream from the RGA point. Examples of this are shown below in Figures II.5 and II.6. Based on this view, a virtual "fly-over" of the watershed could be performed. The percentage of the surface area thought to be of concave or valley shape, illustrated in Figure II.7, was then estimated, and the percentage assigned to a range or "bin" as summarized in Table II.2.

The areas considered to be concave are highlighted in the examples shown in Figures II.5 and II.6. While the estimation of the percent of a basin area determined to be concave may be somewhat subjective, because the percentages were placed in bins it was not important that the exact area be determined, only the appropriate bin or range. For example, in Figure II.5 the concave areas were determined to be between 20 and 30 percent of the total basin area, while the concave areas in Figure II.6 are less than 20 percent falling in the 10 to 20 percent range.

The Valley Score was determined for each subwatershed as:

$$\text{Valley Score} = \text{VS} = 3^i$$

where: i = Bin value = 1, 2, 3, or 4 depending upon the range in which the valley percentage was determined

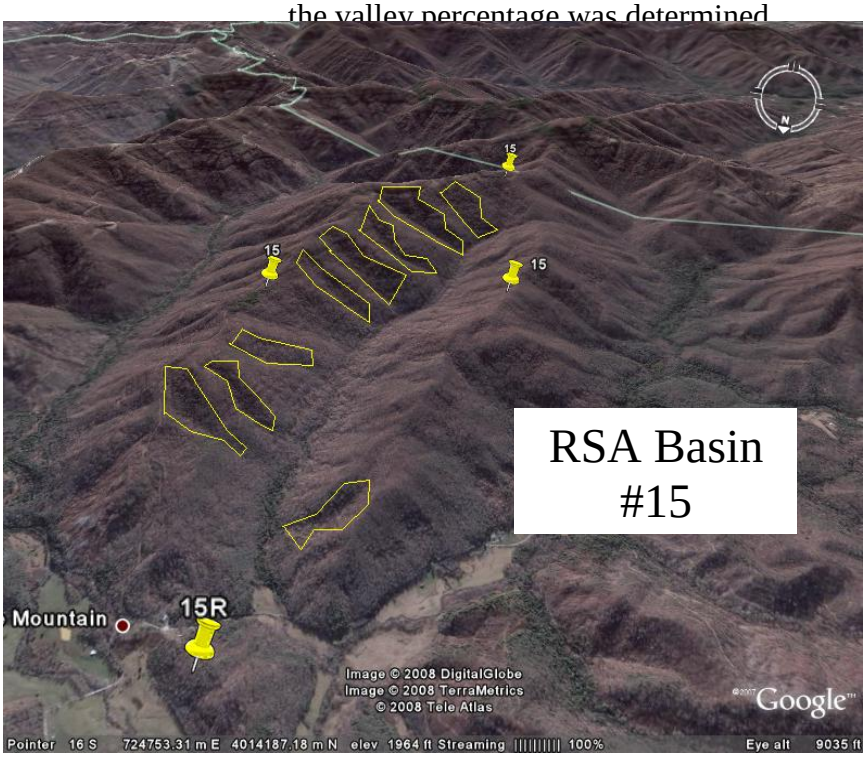

Figure II.5. Typical View of RSA Basin #15 Looking Upstream From the RGA Point Used to Determine the Valley Score (Google Earth with the Terrain Tilted).

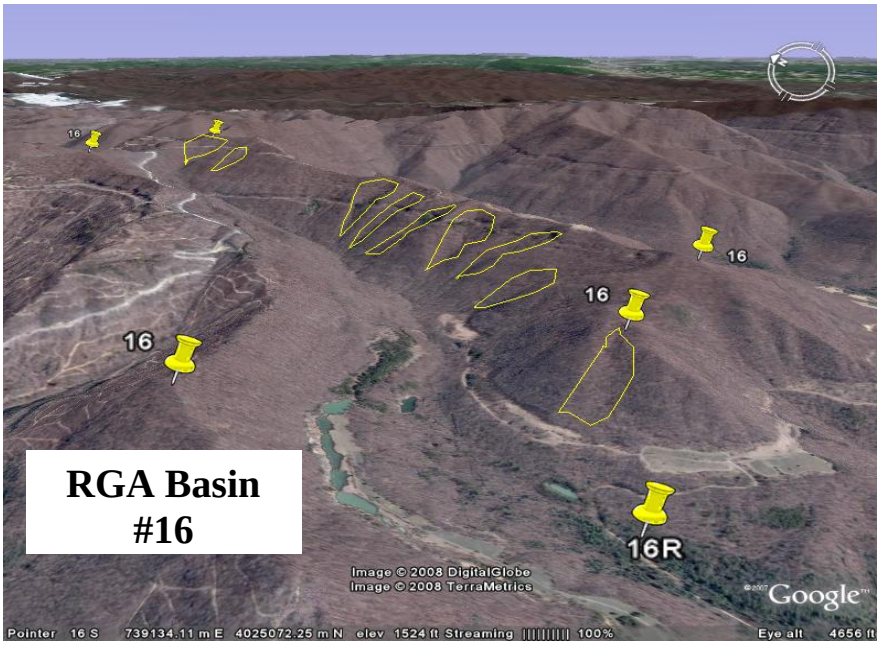

Figure II.6. Typical View of RSA Basin #16 Looking Upstream From the RGA Point Used to Determine the Valley Score (Google Earth with Terrain Tilted).

Figure II.8 is a frequency diagram of the Valley Score results, indicating the number of basins that were scored in each of the ranges of percent concave area. For example, 25 of the 48 basins scored in range 3 corresponding to 20 to 30 % concave area.

Rapid Slope Assessment Score. The RSA total score was then determined from the GS, RF, and VS sub-scores as:

$$RSA = GS + (\text{RF} * \text{VS})$$

where:

GS = Gradient Score
RF = Relief Factor
VS = Valley Score

The total RSA scores for the 48 subwatersheds ranged from 21 to 160, as depicted in Figure II.9. The results for each basin are summarized in Table A.2 found in Appendix A. Figure II.10 is a frequency diagram of the final RSA values.

a) Convex b) Concave

Figure II.7. Assumed Definitions of Convex and Concave Slope Geometry.

Table II.2. Determination of Valley Score.

Range of percent concave or valley area	Bin Value	Valley Score
0 – 10 percent	1	$3^1 = 3$
10 -20 percent	2	$3^2 = 9$
20 – 30 percent	3	$3^3 = 27$
Greater than 30 percent	4	$3^4 = 81$

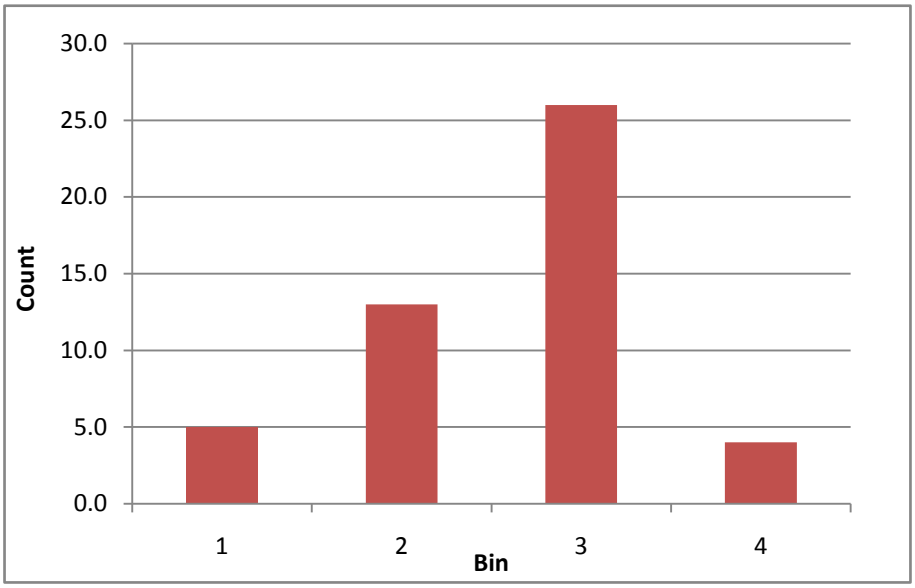

Figure II.8. Frequency Graph of Valley Score Watershed Count for Various Bin Values (Bin 1 = 0-10%, Bin 2 = 10-20%, Bin 3 = 20-30%, and Bin 4 = >30%).

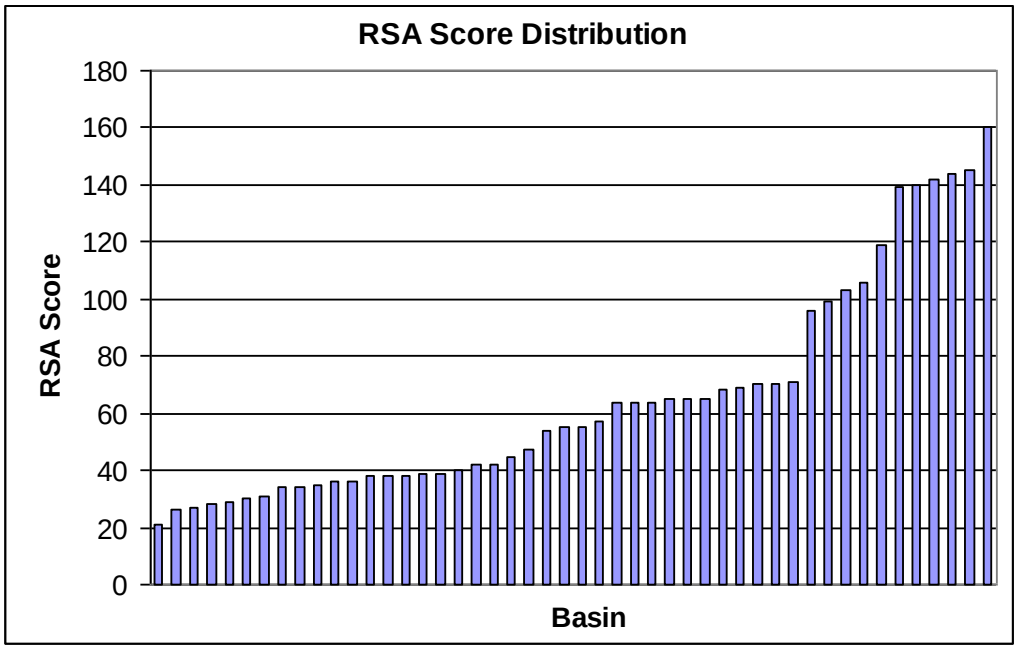

Figure II.9. Distribution of RSA Scores Sorted from Low to High.

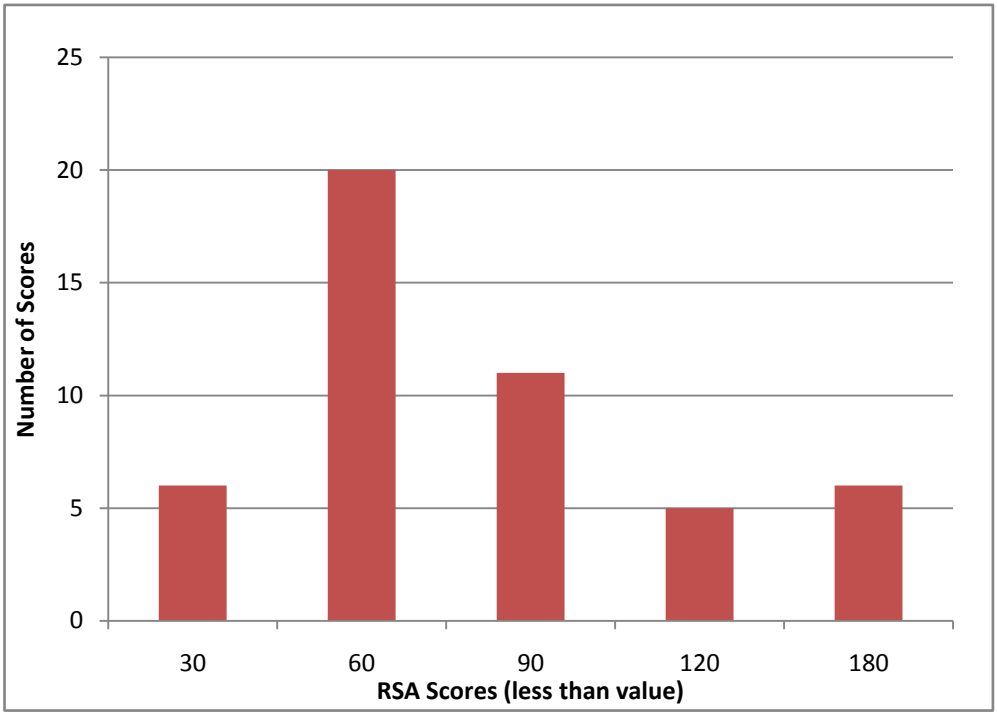

Figure II.10. Frequency Graph of Final RSA Scores.

E. Upland Sampling

The Montgomery Fork, Brimstone Creek, and Smokey Creek subwatersheds within the New River Basin were chosen for uplands sampling, and four sample sites were identified in each subwatershed. These sites were selected to target the four areas which are believed to be the main sediment producers: logging, mining, dirt roads, and gravel roads. Each test site was chosen to be representative of the overall conditions, of each of the four parameters, of the subwatershed. Other factors which effected the sampling and testing site locations were accessibility and proximity to RGA points.

Shown below in Figure II.11 is a typical map of one of the subwatersheds chosen for uplands sampling and testing. On the map can be seen the land uses in the subwatershed along with the test site locations and RGA site locations. All of the subwatershed maps can be seen in Appendix B.

Table II.3 summarizes the site location data. Note that the site descriptions may not exactly match those seen in the subwatershed maps in Appendix B, because the conditions may have changed since the preparation of the raster images. The site description in Table II.3 reflects the actual site conditions that existed at the time the sample was taken. For example, some of the logging operations are less than one year old and may be described as 75% logging in Table II.3, but appear as no logging on the raster image used to create the subwatershed map.

Table II.3 Uplands Site and Sample identification

Subwatershed	Site ID	Coordinates (lat, long)	Site Description
Brimstone Creek	BR-1	36.26, -84.50	Active Logging Road
Brimstone Creek	BR-2	36.26, -84.51	25% Logged Area
Brimstone Creek	BR-3	36.23, -84.48	75% Reclaimed Mine
Brimstone Creek	BR-4	36.25, -84.48	Active Mining Road
Montgomery Fork	MF-1	36.33, -84.34	100% Logged Area
Montgomery Fork	MF-2	36.34, -84.35	50% Reclaimed Mine
Montgomery Fork	MF-3	36.34, -84.36	Active Logging Road
Montgomery Fork	MF-4	36.34, -84.35	Active Mining Road
Smokey Creek	SC-1	36.20, -84.41	50% Reclaimed Mine
Smokey Creek	SC-2	36.21, -84.42	Inactive Un-reclaimed Logging Road
Smokey Creek	SC-3	36.23, -84.44	75% Logged Area
Smokey Creek	SC-4	36.19, -84.42	Inactive Un-reclaimed Mining Road

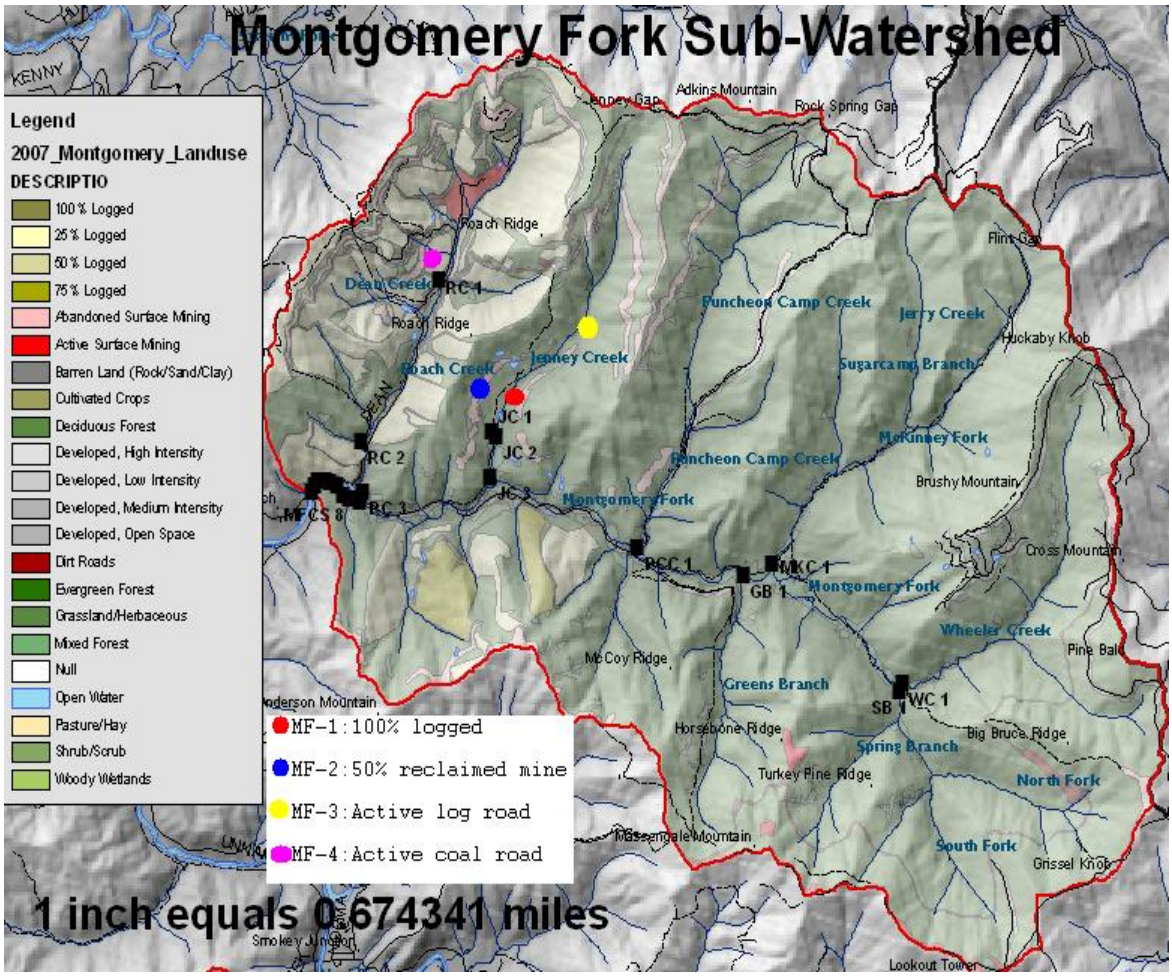

Figure II.11 Map of Montgomery Fork Subwatershed with the Location of the Four Uplands Sample Sites, Each Representing a Different Land Use Category (Schwartz et al. 2008)

After choosing each location, any forest litter, or debris was cleared from the surface. This ranged anywhere from 0.5 to 2 inches of material removed depending on the location. As little of the topsoil was removed as possible, to ensure the sample was of material which had a high chance of becoming runoff sediment. Next, at least 10 pocket penetrometer readings were taken using a Cole Parmer model EW-99039-00, which yields an approximate measure of the soil compressive strength, which can then be divided by 2 to yield the undrained shear strength in non-cohesive soils. This is illustrated with Mohr's Circle found in the literature review section. Tests were conducted within an area no smaller than 1 square foot. After this, at least 10 cone penetrometer tests were conducted using a Hogentogler model S-4615 in the same area, which yields a measure of the force required to push the cone into the soil for a distance of 1.16 inches. This cone resistance can then be correlated to shear strength as well. Outlaying data was discarded and an average was calculated for both the Pocket and Cone Penetrometers. Lastly, a soil sample to a depth no greater than 3 inches below the penetrometer tests was taken for index property tests, grain size distribution analysis, and soil classification.

Figure II.12 is a plot of the pocket penetrometer readings of tons per square foot, versus the cone penetrometer readings of pounds. As can be seen, the correlation is strong with an R-squared value of 0.9606, which is not surprising since both are indirect measures of the soil shear strength. The cone penetrometer, which has a slightly larger contact with the soil than does the pocket penetrometer, may represent the strength of a larger volume of soil.

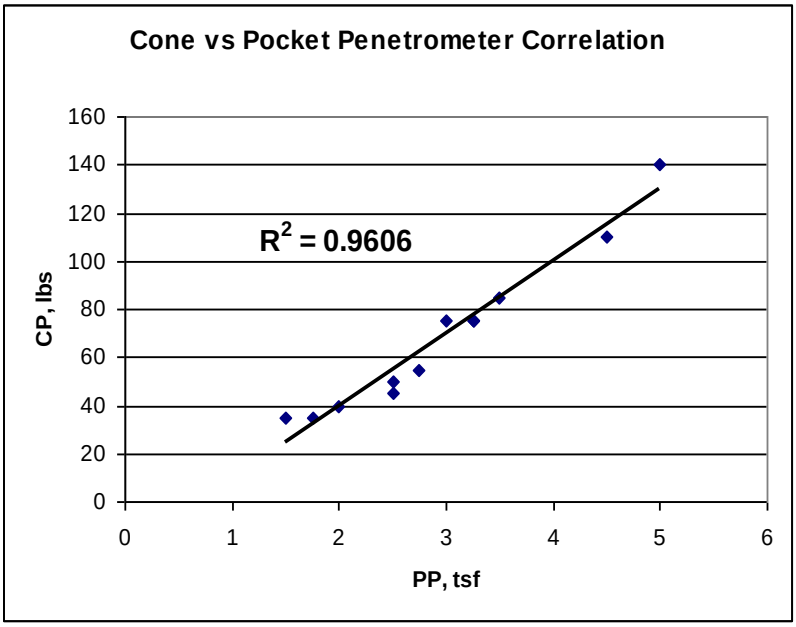

Figure II.12 Comparison of Cone Penetration and Pocket Penetration Strength Measures for Near Surface Uplands Samples from All Three Subwatersheds.

The soil samples were tested in general accordance with ASTM D 4318 to determine the Atterberg limits and ASTM D 422 to determine the Unified Soil Classification. Table II.4 and II.5 summarize the soil properties determined by laboratory testing of the upland samples.

Table II.4 Upland Sample Data

Sample ID	Shear Strength (PP, tsf)	Shear Resistance (CP, lbs)	Plastic Limit	Liquid Limit	Plasticity Index
SC-1	3.25	75	32	40	8
SC-2	5	140	24	33	9
SC-3	2.5	45	NP	NP	NP
SC-4	3	75	NP	NP	NP
MF-1	1.75	35	NP	NP	NP
MF-2	2.75	55	43	55	12
MF-3	4.5	110	32	33	1
MF-4	2.5	50	NP	NP	NP
BR-1	3.25	75	NP	NP	NP
BR-2	2	40	NP	NP	NP
BR-3	3.5	85	NP	NP	NP
BR-4	1.5	35	NP	NP	NP

Table II.5 Upland Sample Data Continued

Sample ID	% finer than 200	% clay	D50 (mm)	D84 (mm)	USCS Classification
SC-1	45	13	0.3	6	SM
SC-2	51	14	0.07	4	ML
SC-3	67	20	0.022	2.5	ML
SC-4	41	8	0.2	9	SM
MF-1	52	14	0.07	10.5	ML
MF-2	26	7	6	11.7	GM
MF-3	58	22	0.03	4	ML
MF-4	60	28	0.02	1.8	ML
BR-1	61	16	0.035	1	ML
BR-2	57	9	0.05	0.25	ML
BR-3	39	10	0.85	8	SM
BR-4	56	19	0.04	11.5	ML

III. Part I Conclusions

The normal distribution of Figures II.8 and II.9 suggest that the RSA method provides good resolution of the score based on the three selected elements, in spite of the fact that the gradient score data was all within a relatively narrow range.

The Rapid Slope Assessment is a convenient means to quantify how the shape of the ground surface may contribute to the production of sediment. Although the RSA method is quick and convenient, there was no correlation found between the developed RSA method and the established RGA method.

Assuming a high low plasticity clay content and low shear strength are indicators that sediment production is likely, as discussed earlier, then the following conclusions can be made:

The shear strength data collected within the reclaimed mining areas fell near the average for all of the studied areas. In addition to these areas having average strengths they also had the lowest low plasticity clay contents. This suggests that these areas should be less prone than other studied areas to producing high sediment loads

The highest shear strength data was collected within the logging roads. Although these areas had the highest strengths they also had higher than average low plasticity clay contents. This suggests that these areas should be slightly less prone to producing sediment loads than the other studied areas.

The shear strength data from the mining roads was below average for the studied areas. In addition to low strength data these areas also had higher than average low plasticity clay contents. This suggests that these areas should be more prone to producing sediment than the logging road areas.

The lowest shear strength data was collected within the logged areas. In addition to low strength data these areas had the highest low plasticity clay contents. This suggests that these areas should be more prone to producing sediment than the mining road areas.

List of References

Cole Parmer, 2009.
http://www.coleparmer.com/catalog/product_view.asp?sku=9903900. February 24, 2009

Committee on Disposal of Excess Spoil, Board on Mineral and Energy Resources, Commission on Natural Resources, and National Research Council. 1981. Disposal of Excess Spoil from Coal Mining and the Surface Mining Control and Reclamation Act of 1977. National Academy Press., Washington D.C.

Angel, P., V. Davis, J. Burger, D. Graves, and C. Zipper (2005) "The Appalachian Regional Reforestation Initiative." U.S. Office of Surface Mining. Forest Reclamation Advisory Number 1.

Burger, J., D. Graves, P. Angel,, V. Davis, , and C. Zipper (2005) "The Forestry Reclamation Approach." U.S. Office of Surface Mining. Forest Reclamation Advisory Number 2.

McCarthy, David F. 2002. Essentials of Soil Mechanics and Foundations. Prentice Hall, Columbus, Ohio.

Sweigard, R., J. Burger, C. Zipper, J. Skousen, C. Barton, and P. Angel (2005) "Low Compaction Grading to Enhance Reforestation Success on Coal Surface Mines." U.S. Office of Surface Mining. Forest Reclamation Advisory Number 3.

Sweigard, R., V. Badaker, and K. Hunt. 2007. "Development of a Field Procedure to Evaluate the Reforestation Potential of Reclaimed Surface-Mined Land." University of Kentucky, Department of Mining Engineering.

Schwartz, J., E. Drumm, M. Massey, D. Johnson, J. Baines, W. Cantrell. 2008 "Development of a Rapid Geomorphic Assessment Technique to Support the CHIA/PHC Progress: A Focus on Model Improvement for Estimating Sediment Loads". Department of Civil and Environmental Engineering. University of Tennessee, Knoxville.

Garcia, Marcelo H. 2007. Sedimentation Engineering. American Society for Civil Engineers. Reston, Virginia

Geotechnical Characterization of Steep Slopes on Reclaimed Mined Lands in East Tennessee

Abstract

Over compaction of mine spoil after the Surface Mining Control and Reclamation Act of 1977 has led to reclaimed mine lands which will not grow economically viable native hardwood forests. This has been remedied by using the low compaction grading technique. This construction technique attempts to balance stability which utilizes compaction and tree growth which needs a looser growing medium. The physical characteristics of reclaimed mine slopes using the low compaction grading technique were studied. Several different methods to measure unit weight were examined including using a nuclear density gauge and two different replacement methods similar to the sand cone density test. Also, grain size distributions were calculated for the three areas studied. The in-situ angle of the material and the internal friction angle of the material were measured and used in a simple infinite slope analysis to determine slope stability. It was found that the unit weight reading were highly variable which is mainly due to the variable nature of the material tested. Also, it was found that there was no correlation between density and depth which suggests that the material had not been heavily compacted. Next, it was found that the low compaction grading technique provides a suitable tree root growth medium due to low unit weights and high void ratios. Lastly, it was found that the infinite slope analysis provided factor of safety values with an upper bound of 1.9 to 1.4 and a lower bound of 0.7. These values were acceptable because of the low cost and consequences of failure of a surface mine slope.

IV. Geotechnical Characterization of Steep Slopes on Reclaimed Mined Lands in East Tennessee

A. Study Objectives

Over compaction of mine spoil after the Surface Mining Control and Reclamation Act of 1977 has led to reclaimed mine lands which will not grow economically viable native hardwood forests. This has been remedied by using the low compaction grading technique. This construction technique attempts to balance stability which utilizes compaction and tree growth which needs a looser growing medium. The physical characteristics of reclaimed mine slopes using the low compaction grading technique were studied. Several different methods to measure unit weight were examined including using a nuclear density gauge and two different replacement methods similar to the sand cone density test. Also, grain size distributions were calculated for the three areas studied. The in-situ angle of the material and the internal friction angle of the material were measured and used in a simple infinite slope analysis to determine slope stability.

B. Nuclear Density Gauge

Surface-type nuclear-moisture density equipment is currently in widespread use for performing density tests on compacted backfill and asphaltic concrete, replacing the sand-cone and rubber-balloon methods, primarily because of the rapid results which can be obtained (Troxler, 1997). The principle elements in a nuclear density apparatus are the nuclear source, which emits gamma rays, a detector to pick up the gamma rays passing through the tested soil and a counter for determining the rate at which the gamma rays are reaching the detector (Troxler, 1997).

A Troxler 3411 B nuclear gauge was used in this research, which has both a cesium-137 source, which emits gamma rays for determining unit weight, and a americium-241 beryllium source which emits alpha particles for determining moisture content. This device can be seen later in Figure IV.2. When the equipment is in use the gamma rays are emitted from a probe rod which has been placed into the ground. Although density readings can be taken on the surface of the material, the most accurate results are provided when the source rod is placed into the material by utilizing a punched or drilled hole (Troxler, 1997). This setup can be seen in Figure IV.1 below.

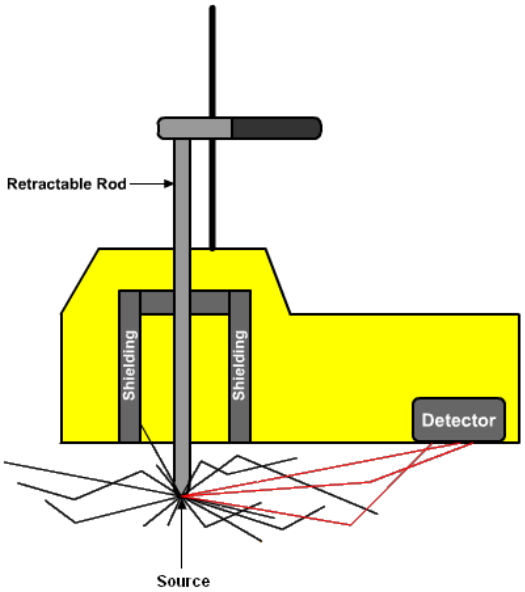

Figure IV.1 Nuclear Gauge Illustration

The gamma rays penetrate into the soil where some are absorbed, but some reach the detector by direct transmission or after reflecting off of soil mineral electrons. The amount of gamma radiation reaching the detector is inversely proportional to the density of the soil (Troxler, 1997). Densities are determined by obtaining a nuclear count rate and then relating this count rate to the known density of a calibration reading. The density reading is of a bulk wet unit weight of the entire material. A calibration block was provided by Troxler which calibrates both the density and the moisture content measurements because of its known hydrogen atom content and density.

Moisture determinations are obtained using the alpha particles emitted from the americium-241 beryllium source. The americium-241 bombards the beryllium which causes the beryllium to emit fast neutrons which lose velocity if they strike hydrogen atoms (Troxler, 1997). The velocity of these atoms can be measured and then related to the standard count provided by the calibration block, and then a moisture percentage can be calculated. This moisture percentage can then be used to determine the dry unit weight of the soil.

C. University of Kentucky Research

The University of Kentucky has been performing research on the surface mining reclamation process for several years. One of its most recent reports on an OSM research grant had the following three major objectives (Sweigard et al. 2007):

- Establish initial values for comparison of depth to refusal and soil resistance using both the static and dynamic cone penetrometers.
- Compare the effectiveness of the dynamic cone penetrometer (DCP) to the static cone penetrometer (SCP) on various construction types of reclaimed spoil.
- Develop a standard procedure that can be applied in the field under all circumstances, to evaluate the physical characteristics of the root growth medium as it relates to reforestation success.

This research tested three different types of construction with both the DCP and the SCP. The SCP was only used where tractor access was available which would limit its use, especially in the mountainous Appalachian region (Sweigard et al. 2007). The three types of construction techniques tested were loose-dumped, struck-off, and compacted. Undisturbed areas were also tested in this study. The results of this research were variable. The first round of testing with the SCP indicated that the struck-off material gave more resistance than the compacted material, and there was only a slight decrease from loose-dumped to struck-off and from struck-off to compacted with the DCP (Sweigard et al. 2007). The second round of testing in the same area yielded results which were more anticipated in that the maximum penetration depth decreased from undisturbed to loose-dumped to struck-off to compacted. Although both soil penetration resistance and maximum penetration depth were reported, no density measurements were given for any of the test plots or construction methods. Even though no density measurements were reported they did report the use of a nuclear density gauge and recommended a maximum bulk density of 98 pounds per cubic foot (pcf) at a two inch depth and 113 pcf at a 12 inch depth (Sweigard et al. 2007).

The conclusions of this report suggested that the DCP was an acceptable means of measuring the physical characteristics of the tree growth medium when a SCP could not be used because of terrain restrictions (Sweigard et al. 2007). Also concluded was that there was no correlation found between the SCP and the DCP because of rocks in the medium tested, and that the SCP seemed more suitable for soils without rocks present.

This research seems incomplete due to the following reasons:

- The maximum testing depth of the DCP and SCP was 16 inches and the ARRI calls for an uncompacted layer 48 inches thick.
- SCP and DCP equipment are not meant to measure resistance in rocky conditions.
- Density testing recommendations are not backed up by testing data.
- No testing was done on steep slopes or any terrain other than flat constructed areas.
- Other than cone resistance, no other soil characterization parameters were reported

D. Sampling Methods

A type of random sampling was used to determine unit weight on the three sites. First, for each site, a five meter square grid was laid out in an area which was judged to be representative of the entire site. Then, blocks within this grid which were judged to be unrepresentative of the overall unit weight were not included in the sampling area. An example of this would be areas with noticeably higher rock contents that were not tested because this might skew the readings towards the unit weight of the rock material. After this tests were conducted at random within the testing grid. This sampling method is consistent with stratified random sampling.

Stratified random sampling uses prior information about the area or process to create groups that are sampled independently using a random process (U.S. EPA, 2008). These groups can be based on spatial or temporal proximity, or on preexisting information or professional judgment (U.S. EPA, 2008). Stratified Random Sampling can be used for any objective such as estimating means, values, proportions, etc., delineating boundaries, etc. This sampling method can be useful when (U.S. EPA, 2008):

- the area or process can be divided based on prior knowledge, professional judgment, or using a surrogate that is highly correlated with the item of interest;
- the target area or process is heterogeneous;
- there is a need to ensure representativeness by distributing the samples throughout the spatial and or temporal dimensions of the area or process;
- there is a need to ensure that rare groups (e.g., shrimps clustering in large but scattered schools, unevenly distributed contamination, rare and endangered species) of the area or process are sampled sufficiently (i.e., you take enough samples to draw conclusions about these groups);
- costs and or methods of sampling differ within the area or process, or
- there is a need for information about the entire area or process and specific subgroups, yet the entire area is too large to be sampled.

E. Unit Weight

For each of the three sites which were constructed using the low compaction grading technique, a series of tests were conducted to determine the Bulk Wet Unit Weight, Bulk Dry Unit Weight, Grain Size Distribution, and Soil Classification. Unit Weight was measured using three different methods. The first method is called the Water Replacement Method and is similar to the sand cone method. It should be noted that the logistics of the sites as well as voids within the strata made sand cone testing impractical. First, a sampling area is chosen and leveled by hand to simplify the measurement. Next, a mass of soil is removed from this area, weighed, and taken to the lab for moisture determination. The area excavated was approximately one foot in diameter and was taken to as deep as a shovel could penetrate into the strata. Lastly, the void space is lined with plastic and filled with a measured amount of water to determine the volume.

Shown below in Tables IV.1, IV.2, and IV.3 are the values from the three sites using the replacement method to determine unit weight. All unit weight testing was conducted within the areas that used stratified random sampling techniques. The soil samples were tested in general accordance with ASTM D 4959 to determine moisture percentage and ASTM D 5030 to determine unit weight.

Table IV.1 Replacement Method Data – Mountainside Coal Site

Test #	Moisture (%)	Wet Unit Weight (pcf)	Dry Unit Weight (pcf)	Wet Unit Weight (kN/m^3)	Dry Unit Weight (kN/m^3)
1	10.6	85.6	77.4	13.4	12.2
2	8.6	130.7	120.4	20.5	18.9
3	12.1	108.9	97.1	17.1	15.3
4	9.5	95.7	87.4	15.0	13.7
5	9.4	112.2	102.6	17.6	16.1
6	8.9	117.6	108.0	18.5	17.0
7	8.4	112.7	104.0	17.7	16.3
8	8.2	115.1	106.4	18.1	16.7
9	9.9	120.0	109.2	18.8	17.1
Time	9.5	110.9	101.4	17.4	15.9
S.D.	1.3	13.3	12.7	2.1	2.0

Table IV.2 Replacement Method Data – Premium Coal Site

Test #	Moisture (%)	Wet Unit Weight (pcf)	Dry Unit Weight (pcf)	Wet Unit Weight (kN/m^3)	Dry Unit Weight (kN/m^3)
1	15.1	96.0	83.3	15.1	13.1
2	15.0	77.4	67.3	12.1	10.6
3	13.7	84.5	74.3	13.3	11.7
4	16.4	100.1	86.0	15.7	13.5
5	13.9	105.5	92.6	16.6	14.5
Mean	14.8	92.7	80.7	14.5	12.7
S.D.	1.1	11.5	10.0	1.8	1.6

Table IV.3 Replacement Method Data – National Coal Site

Test #	Moisture (%)	Wet Unit Weight (pcf)	Dry Unit Weight (pcf)	Wet Unit Weight (kN/m^3)	Dry Unit Weight (kN/m^3)
1	10.7	107.9	97.5	16.9	15.3
2	9.7	122.7	111.8	19.3	17.6
3	9.3	100.4	91.8	15.8	14.4
4	9.4	117.5	107.3	18.4	16.9
5	8.5	113.8	105.0	17.9	16.5
6	10.3	107.4	97.4	16.9	15.3
Mean	9.6	111.6	101.8	17.5	16.0
S.D.	0.8	8.0	7.5	1.3	1.2

The second method for unit weight measurement was to use a Troxler 3411 B nuclear density gauge. First, a test area was chosen and leveled by hand. Each test site was leveled because if the nuclear gauge is not flush with the ground then it will take the air beneath it into account during its calculations. Next, a pilot hole for the probe rod was created using a pin and rubber mallet. After that, the gauge is set onto the test site, the probe rod is lowered into the pilot hole and the depth of the pilot hole is programmed into the gauge. Lastly, the gauge reads wet unit weight, dry unit weight, and moisture in terms of percentage. Tests were conducted at the deepest point attainable by the pilot hole because more soil is characterized per test the deeper the probe rod goes. Shown below in Tables IV.4, IV.5, and IV.6 are values from the three sites using the nuclear density gauge to determine unit weight. All Nuclear density tests used stratified random sampling techniques. The test were conducted in general accordance with ASTM D 2927 to determine moisture percentage and unit weight. Shown below in Figure IV.2 is a picture of the nuclear density gauge set into the leveled area with the probe rod set into the pilot hole. As can be seen the gauge is as flush to the ground as possible for this terrain.

Figure IV.2 Nuclear Density Gauge Testing on Reclaimed Mine Slope

Table IV.4 Nuclear Density Gauge Data – Mountainside Coal Site

Test #	Depth (in.)	Depth (mm)	Moisture %	Wet Unit Weight (pcf)	Dry Unit Weight (pcf)	Wet Unit Weight kN/m3	Dry Unit Weight kN/m3
1	12	304.8	12.4	110.6	98.4	17.4	15.4
2	8	203.2	9.4	107.2	98	16.8	15.4
3	8	203.2	10.6	108.7	98.3	17.1	15.4
4	2	50.8	8.6	107.2	98.6	16.8	15.5
5	4	101.6	8.7	104.5	96.1	16.4	15.1
Mean	6.8	172.7	9.9	107.6	97.9	16.9	15.4
S.D.	3.9	99.0	1.6	2.2	1.0	0.4	0.2

Table IV.5 Nuclear Density Gauge Data – Premium Coal Site

Test #	Depth (in.)	Depth (mm)	Moisture %	Wet Unit Weight (pcf)	Dry Unit Weight (pcf)	Wet Unit Weight kN/m3	Dry Unit Weight kN/m3
1	8	203.2	16.2	100.1	86.2	15.7	13.5
2	10	254	13.5	107.6	94.8	16.9	14.9
3	12	304.8	18.2	94.1	79.7	14.8	12.5
4	8	203.2	17.1	107.6	91.9	16.9	14.4
5	6	152.4	23.4	102.9	83.4	16.2	13.1
6	8	203.2	24.7	96.7	77.5	15.2	12.2
7	12	304.8	22.2	99.7	81.6	15.7	12.8
Mean	9.1	232.2	19.3	101.2	85.0	15.9	13.3
S.D.	2.3	57.6	4.2	5.1	6.4	0.8	1.0

Table IV.6 Nuclear Density Gauge Data – National Coal Site

Test #	Depth (in.)	Depth (mm)	Moisture %	Wet Unit Weight (pcf)	Dry Unit Weight (pcf)	Wet Unit Weight kN/m3	Dry Unit Weight kN/m3
1	8	203.2	13.1	112.6	99.5	17.7	15.6
2	10	254	11.0	117.6	105.9	18.5	16.6
3	12	304.8	12.7	116.9	103.7	18.4	16.3
4	8	203.2	13.4	110.7	97.6	17.4	15.3
5	6	152.4	11.5	106.3	95.3	16.7	15.0
6	8	203.2	13.7	111.3	97.9	17.5	15.4
7	12	304.8	12.3	114.2	101.7	17.9	16.0
Mean	9.1	232.2	12.5	112.8	100.2	17.7	15.7
S.D.	2.1	52.5	1.1	4.2	4.0	0.7	0.6

The third method used for measuring unit weight was called the Auger Replacement Method and is a replacement method similar to the first method. In this method a hand auger was used to drill a hole, at most 36 inches deep. The soil removed from the hole was weighed and taken to the lab to determine moisture content. Then the hole was measured and a volume was calculated. Testing using the auger method was not performed in areas defined by the stratified random sampling techniques. Instead, sampling was done through convenience where testing tubes were being placed for future collection of tree growth data (Franklin et al. 2008). Shown below in Tables IV.7, IV.8, and IV.9 are values from the three sites for unit weight using the auger replacement method.

Table IV.7 Example of Auger Replacement Data – Mountainside Coal Site

Test #	Depth (in.)	Depth (mm)	Moisture %	Wet Unit Weight (pcf)	Dry Unit Weight (pcf)	Wet Unit Weight kN/m3	Dry Unit Weight kN/m3
1	10 - 19	254 - 482.6	16.1	77.6	66.9	12.2	10.5
2	11 - 24	279.4 - 609.6	13.1	79.1	69.9	12.4	11.0
3	24 - 35	609.6 - 889	9.7	102.5	93.5	16.1	14.7
4	2 - 13	50.8 - 330.2	15.6	120.6	104.4	18.9	16.4
5	10 - 21.5	254 - 546.1	14.5	128.8	112.5	20.2	17.7
6	4 - 14	101.6 - 355.6	10.2	119.5	108.4	18.8	17.0
7	14 -26.5	355.6 - 673.1	14.2	85.5	74.9	13.4	11.8
8	11 - 23	279.4 - 584.2	10.5	120.3	108.8	18.9	17.1
9	23 - 33	584.2 - 838.2	10.6	121.7	110.0	19.1	17.3
AverageSample Depth > 20 Inches		Mean	11.5	103.3	92.8	16.2	14.6
		S.D.	2.4	18.1	17.6	2.8	2.8
Average Sample Depth < 20 Inches		Mean	13.3	107.7	95.2	16.9	14.9
		S.D.	2.5	22.9	20.9	3.6	3.3

Table IV.8 Example of Auger Replacement Data – Premium Coal Site

Test #	Depth (in.)	Depth (mm)	Moisture %	Wet Unit Weight (pcf)	Dry Unit Weight (pcf)	Wet Unit Weight kN/m3	Dry Unit Weight kN/m3
1	9 - 24	228.6 - 609.6	7.9	91.9	85.2	14.4	13.4
2	7 - 20	177.8 - 508	6.5	89.4	83.9	14.0	13.2
3	10 - 20	254 - 508	15.6	101.5	87.8	15.9	13.8
4	20 - 35	508 - 889	20.4	113.6	94.4	17.8	14.8
5	9 - 19.5	228.6 - 495.3	17.7	92.6	78.7	14.5	12.4
6	5 - 20	127 - 508	5.8	81.8	77.3	12.8	12.1
7	20 - 27	508 - 685.8	5.2	99.1	94.2	15.6	14.8
8	8 - 26	203.2 - 660.4	11.4	75.0	67.3	11.8	10.6
AverageSample Depth		Mean	12.8	106.4	94.3	16.7	14.8
> 20 Inches		S.D.	10.7	10.3	0.2	1.6	0.0
Average Sample Depth		Mean	10.8	88.7	80.0	13.9	12.6
< 20 Inches		S.D.	5.0	9.2	7.4	1.4	1.2

Table IV.9 Example of Auger Replacement Data – National Coal Site

Test #	Depth (in.)	Depth (mm)	Moisture %	Wet Unit Weight (pcf)	Dry Unit Weight (pcf)	Wet Unit Weight kN/m3	Dry Unit Weight kN/m3
1	8 - 20.5	203.2 - 520.7	15.0	113.0	98.2	17.7	15.4
2	8.5 - 19.5	215.9 - 495.3	15.3	133.6	115.9	21.0	18.2
3	19.5 - 30.5	495.3 - 774.7	17.0	141.3	120.7	22.2	19.0
4	6 - 18	152.4 - 457.2	16.4	133.8	115.0	21.0	18.1
5	18 - 30.5	457.2 - 774.7	17.9	114.4	97.0	18.0	15.2
6	9 - 21	228.6 - 533.4	13.7	121.0	106.4	19.0	16.7
7	10 - 24	254 - 609.6	15.3	113.3	98.2	17.8	15.4
8	24 - 35.5	609.6 - 901.1	15.3	105.3	91.3	16.5	14.3
Average Sample Depth		Mean	16.7	120.3	103.0	18.9	16.2
> 20 Inches		S.D.	1.3	18.7	15.6	2.9	2.5
Average Sample Depth		Mean	15.1	122.9	106.7	19.3	16.8
< 20 Inches		S.D.	1.0	10.3	8.6	1.6	1.4

Figures IV.3, IV.4, and IV.5 shown below, illustrate the differences in the data from the three testing methods. Figure IV.6 and IV.7 below, show the error range for each testing method at each site. It can be seen in these figures that the replacement and auger methods have a higher variability between individual test results. Also, it should be noticed that the averages for all three test methods at all three sites fall within ten percent of each other.

All unit weight testing methods found values which were within the expected range. No test gave a unit weight reading greater than that of the unit weight of the rock, approximately 160 pounds per cubic foot, which was excavated during the mining operation. Also, the average readings of all three methods gave a unit weight less than that of natural undisturbed soils in the area.

Shale found in the testing areas has a lower unit weight than the sandstone in the same areas. Areas of higher shale content, the Premium Coal site particularly, were found to have more subsurface voids. This higher void content and higher shale content led to lower readings than the other two sites. The high void content may have also led to the high variability of the readings.

Assuming a specific gravity of solids of 2.65 for undisturbed materials in the area, a void ratio, e, and porosity, n, can be calculated based on the mean dry unit weight measurements by the following equation (McCarthy, 2002):

$$e = \frac{2.65}{\frac{\gamma_{dry,measured}}{\gamma_{water}}} - 1; \quad n = \frac{e}{1+e}$$

Values of void ratio and porosity can be seen in Figures IV.8 and IV.9 below.

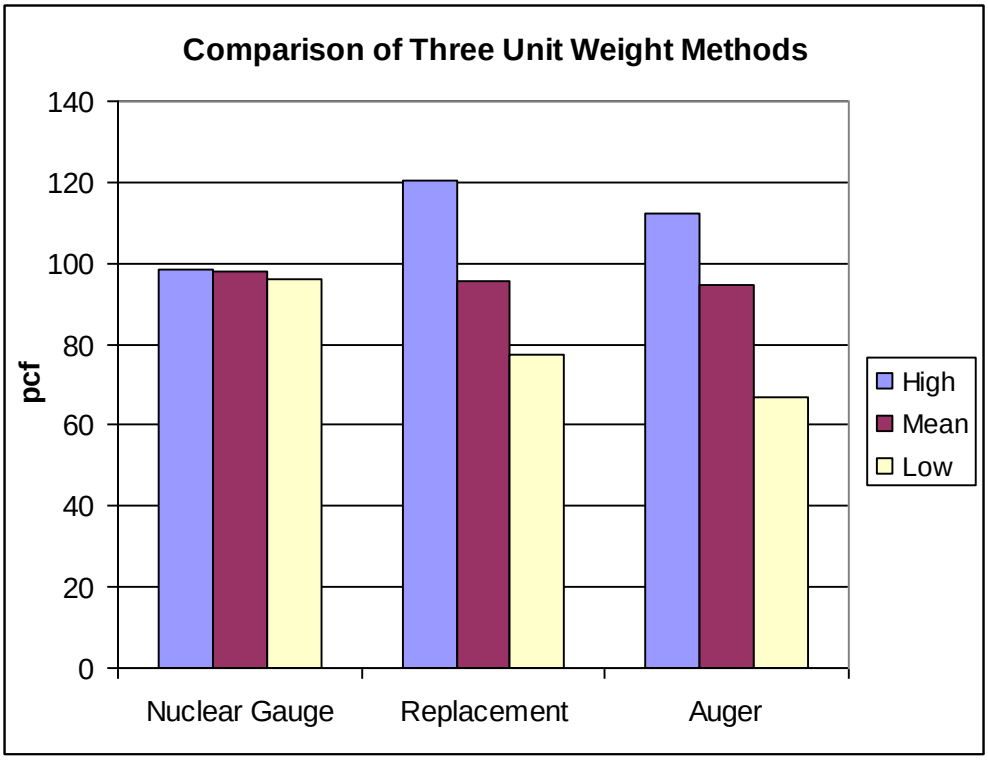

Figure IV.3 Comparison of Unit Weight Test Methods at Mountainside Coal Site.

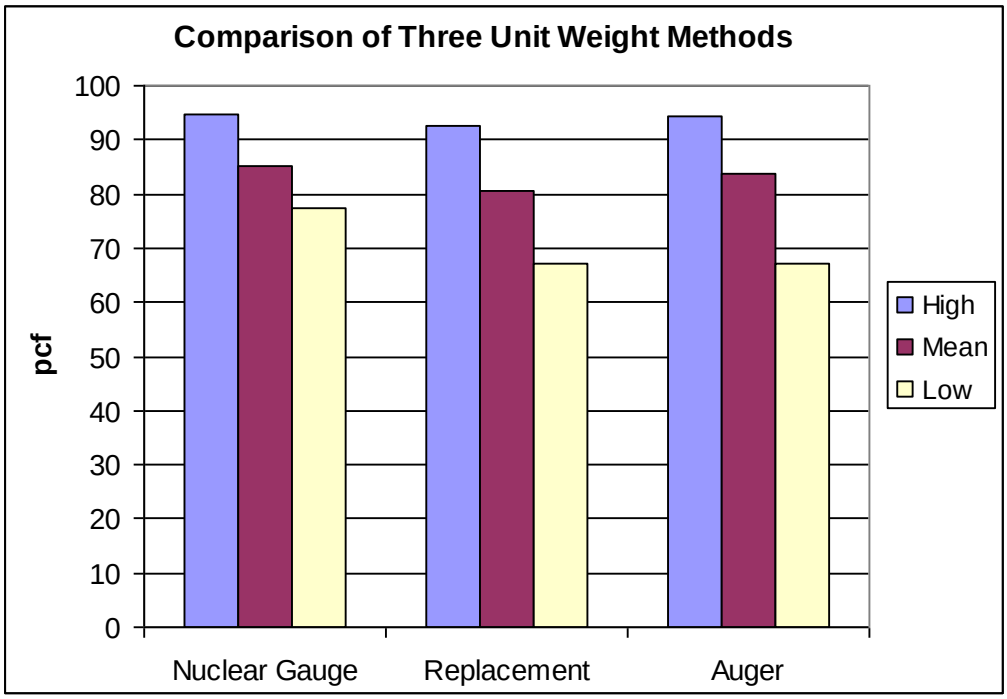

Figure IV.4 Comparison of Unit Weight Test Methods at Premium Coal Site.

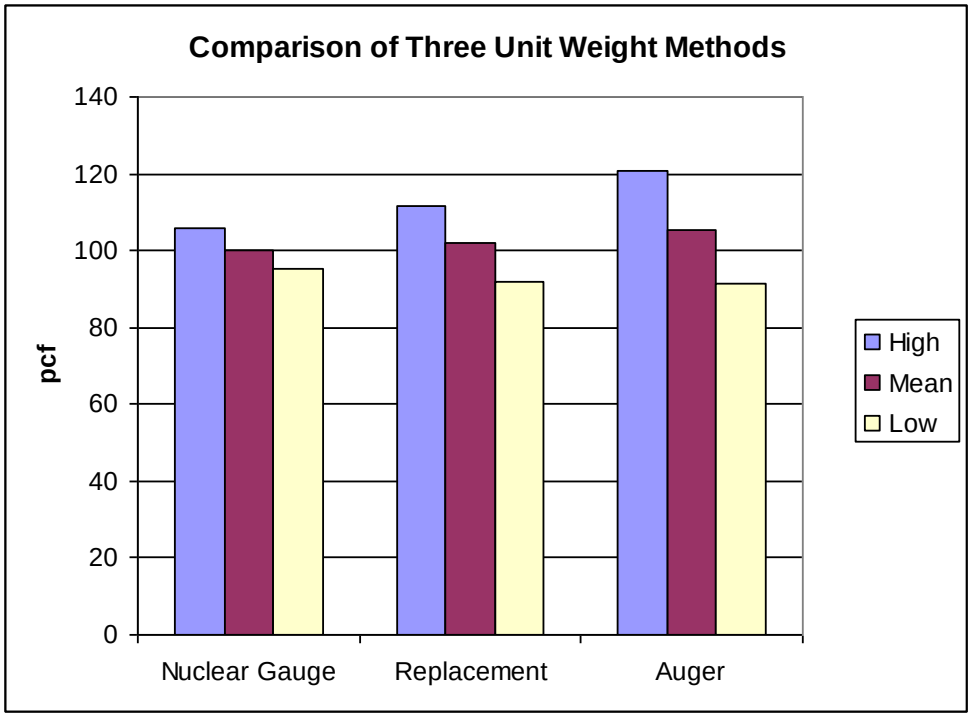

Figure IV.5 Comparison of Unit Weight Test Methods at National Coal Site.

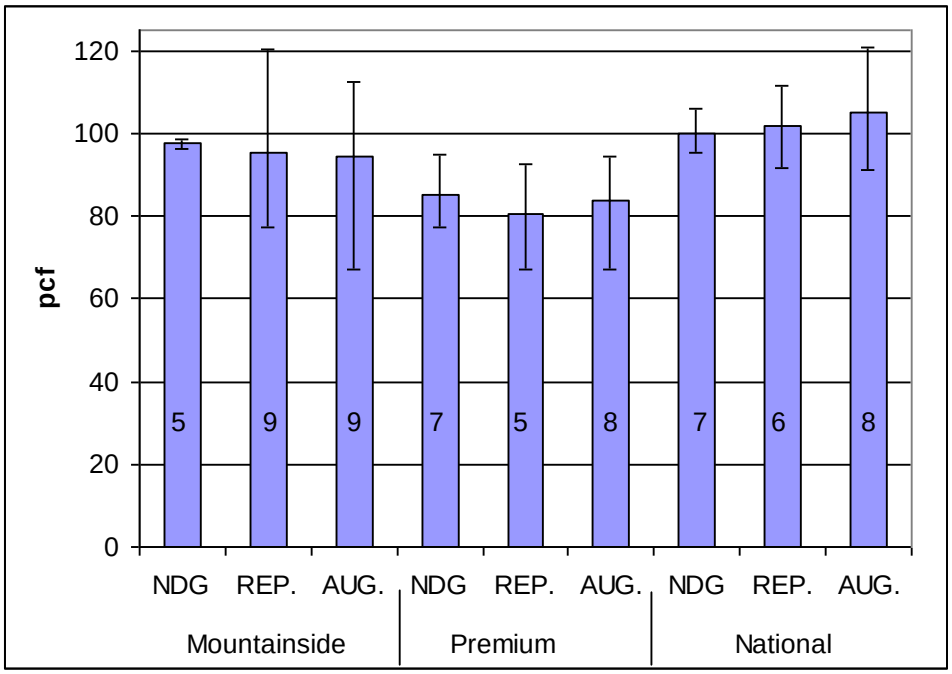

Figure IV.6 Comparison of Three Testing Methods (English Units) – mean value shown with error bars indicating high and low values measured. Also shown within the bars is the number of samples taken

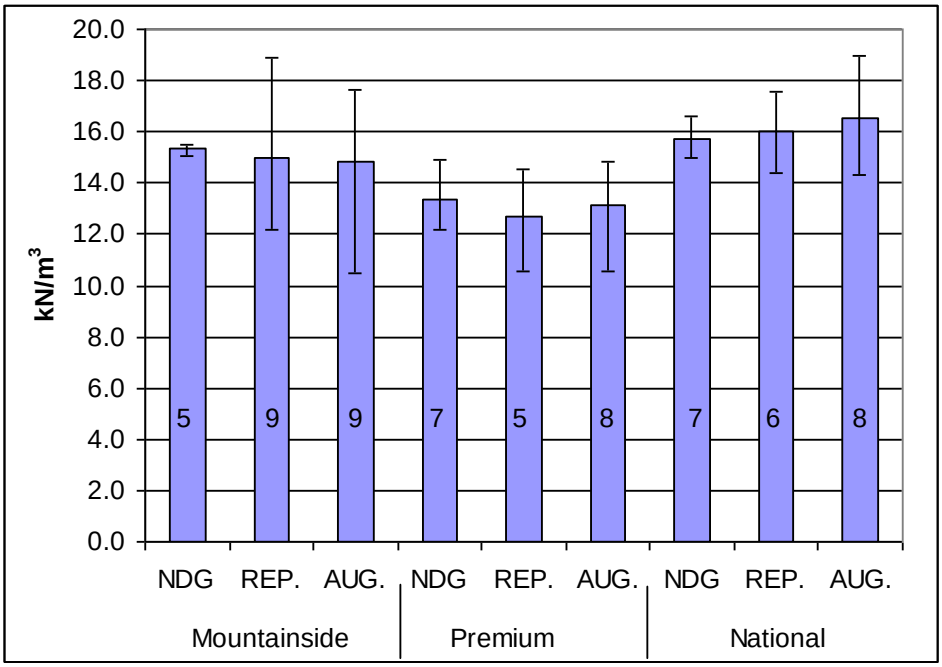

Figure IV.7 Comparison of Three Testing Methods (SI Units) – mean value shown with error bars indicating high and low values measured. Also shown within the bars is the number of samples taken

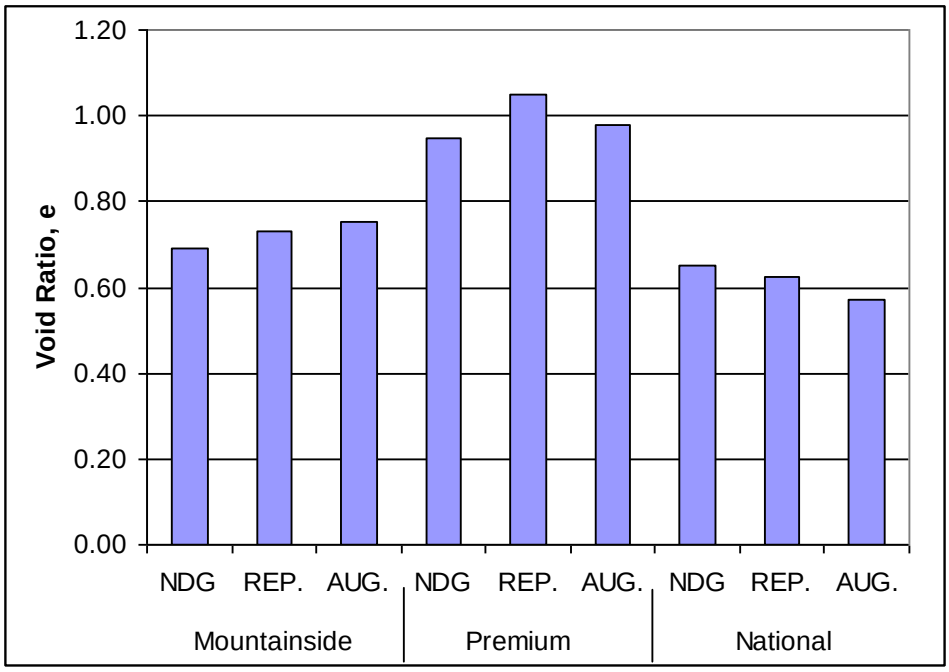

Figure IV.8 Void Ratio Calculations

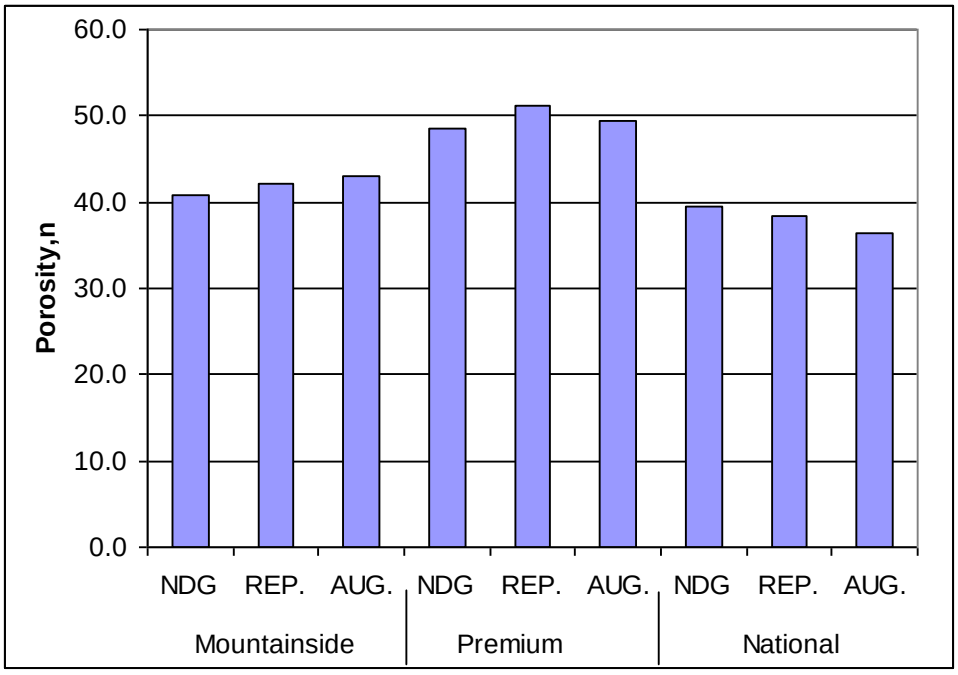

Figure IV.9 Porosity Calculations

F. Grain Size Distribution

Samples from each site were taken to conduct a grain size distribution analysis. These samples were collected using the same hand auger which was used to measure unit weight. This ensured that the sample taken would not contain large rocks, but only soil and small rock fragments. Samples with no large rocks (larger than two inches, or 50 mm, in diameter), can be easily analyzed and then the large rock fraction of the medium can be accounted for later if needed. Shown below in Figure IV.10 is a typical grain size distribution chart resulting from one of the samples taken from the Mountainside Coal site. All grain size distribution charts from all three sites may be seen in Appendix C. Table IV.10 summarizes soil index properties measured by the grain size distribution analysis. Note that the soils index properties measured are only for the fraction less than 2 inches in diameter. Also, it should be noted that the smallest fraction measured was that smaller than a number 100 sieve or 0.15 mm. This was chosen because this is the smallest fraction which can be dry sieved and the percent of particles smaller than 0.15 mm was seen as less than 13 percent of the fraction less than 2 inches (50 mm) and less than 7 percent of the overall grain size distribution. When classifying the material it was assumed that the percent finer than the number 200 sieve would always be less than the percent finer than the number 100 sieve.

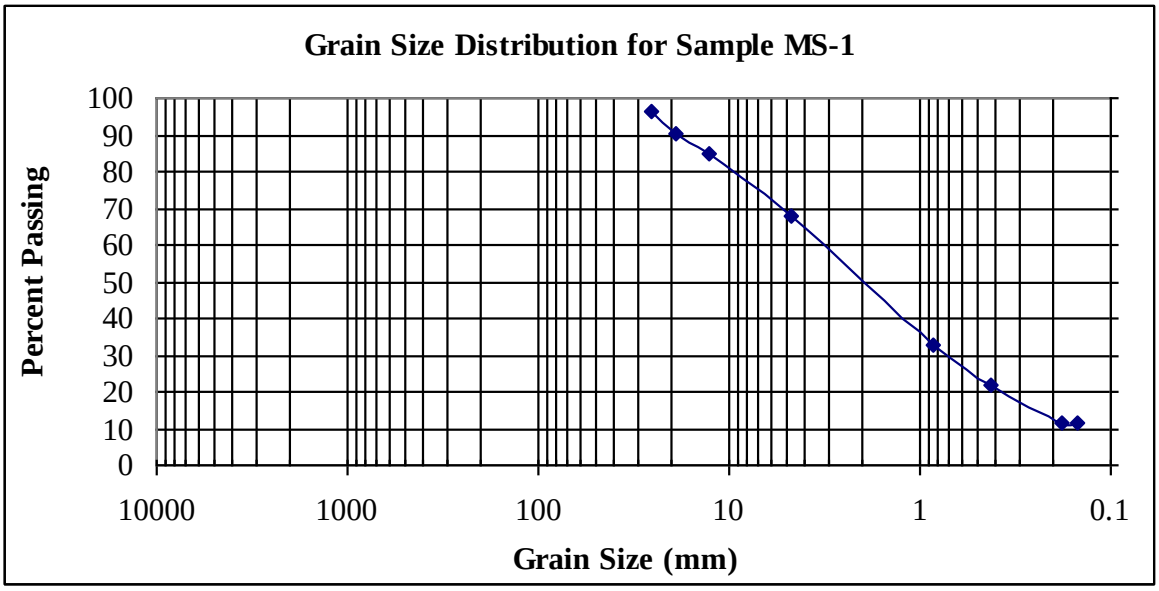

Site ID	Site	% finer than #100	D50 (mm)	D84 (mm)	USCS Classification
MS-1	Mountainside	11.4	2	10.5	SW - SM

Figure IV.10 Grain Size Distribution Number One from Mountainside Site – Portion < 2 Inches (50 mm)

Table IV.10 Summary of Soil Index Properties for Samples with Particles > Two Inches (50 mm) Removed

Site ID	Site	% finer than #100	D50 (mm)	D84 (mm)	USCS Classification
P-1	**Premium**	5.2	2.5	10	SW
P-2	**Premium**	6.1	2.5	10	SW
P-3	**Premium**	4.3	3.5	10.5	SW
P-4	**Premium**	6.6	2.5	10.5	SW
P-5	**Premium**	6.8	3	10	SW
N-1	**National**	12.9	2	11	SW - SM
N-2	**National**	9.7	1.5	10	SW - SM
N-3	**National**	7.2	1.5	6.5	SW - SM
N-4	**National**	9.3	1.5	9	SW - SM
N-5	**National**	9.6	2	11	SW - SM
MS-1	**Mountainside**	11.4	2	10.5	SW - SM
MS-2	**Mountainside**	10.9	2	10.5	SW - SM
MS-3	**Mountainside**	9.7	2.5	11.5	SW - SM
MS-4	**Mountainside**	11.3	2	10.5	SW - SM
MS-5	**Mountainside**	8.6	2.5	11.5	SW - SM

In addition to measuring the grain size distribution of the particles less than two inches, an estimate of the overall grain size distribution was created. It should be noted that directly measuring the grain size distribution is impractical because at some sites the maximum particle size is larger than four feet. The estimated particle size distribution was created by using the same grid used by the stratified random sampling technique, but in this case every grid was sampled. A photograph of each square within the grid was taken, and this was used to estimate percentages of particles larger than 2 inches (50 mm). The percentage of particles larger than 2 and 12 inches was estimated for the entire site and then the largest particle size for the site was identified. Once this data was collected the data from the less than 2 inch samples could be adjusted, based on the estimate of percent of particles greater than two inches, to reflect the overall grain size distribution. Shown below in Figures IV.11 and IV.12 are some examples of estimating the percentage of particles larger than one foot. Also seen below in Figures IV.13, IV.14, and IV.15 are the adjusted grain size distributions for the three sites. Lastly, Figure IV.16, shown below, shows a site picture with the grid layout used in the adjusted grain size distributions as well as the stratified random sampling technique. All of the grid layout pictures may be seen in Appendix F.

Figure IV.11 (Left) Photograph Used to Estimate 15 % Larger than 12 Inches
Figure IV.12 (Right) Photograph Used to Estimate 20 % Larger than 12 Inches

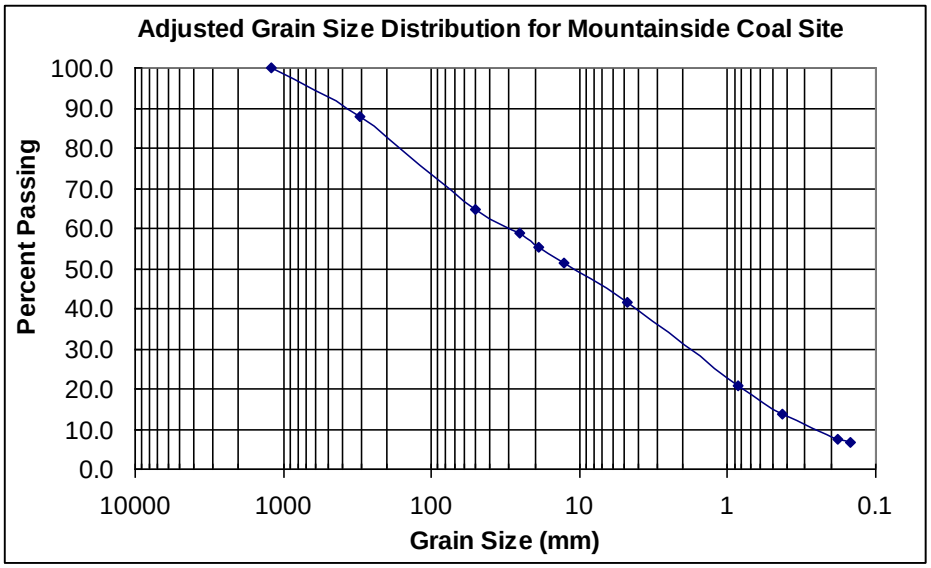

Site	% finer than 2 in.	% finer than #100	D50 (mm)	D84 (mm)
Mountainside Coal	64.6	6.7	10	110

Figure IV.13 Adjusted Grain Size Distribution for Mountainside Coal Site

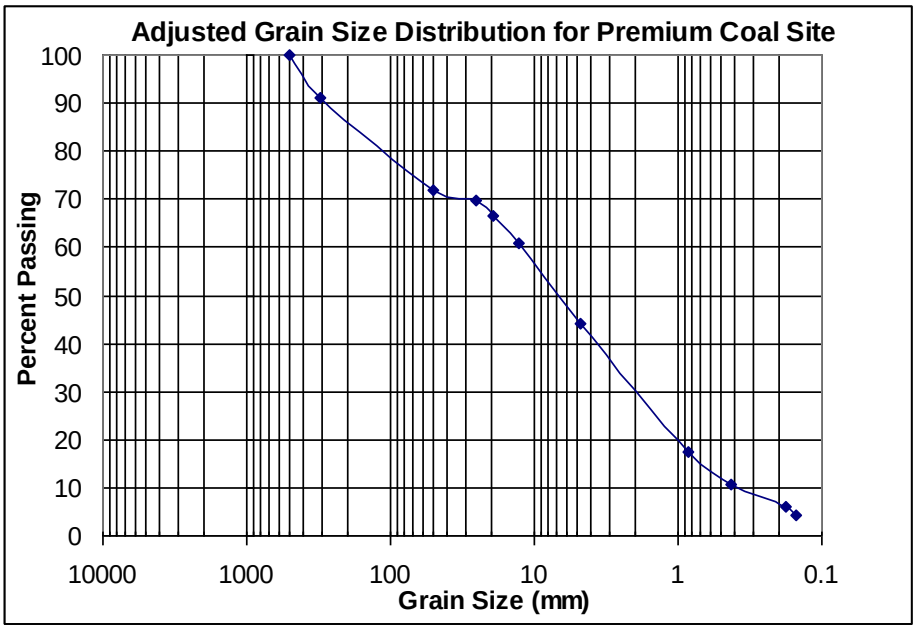

Site	% finer than 2 in.	% finer than #100	D50 (mm)	D84 (mm)
Premium Coal	71.8	4.2	6.5	105

Figure IV.14 Adjusted Grain Size Distribution for Premium Coal Site

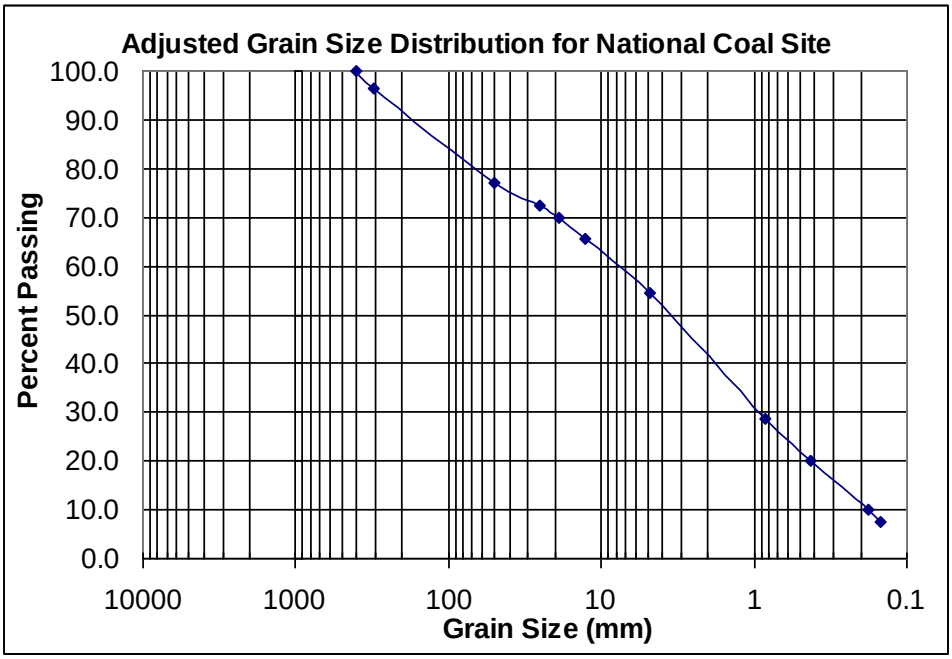

Site	% finer than 2 in.	% finer than #100	D50 (mm)	D84 (mm)
National Coal	77.2	7.5	3.5	100

Figure IV.15 Adjusted Grain Size Distribution for National Coal Site

Figure IV.16 Five Meter Square Grid Photograph at Mountainside Coal Site

G. Slope Stability

i. Angle of Repose

For each site the in-situ angle of the slope, q, was measured using a Suunto Mechanical Inclinometer model PM-5/360PC. Each site was measured along each berm and then the largest value was used for each site because this represents the worst case scenario and yields the most conservative calculation. Shown Below in Figures IV.17, IV.18, and IV.19 are aerial views of the three sites with the slope measurements shown in degrees.

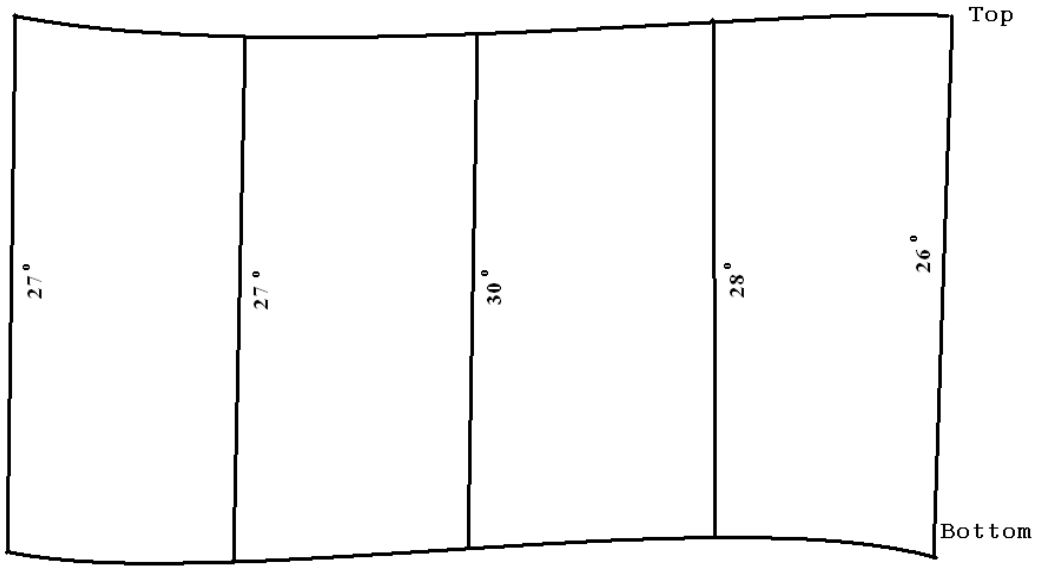

Figure IV.17 Berm Slope Measurements at Mountainside Site

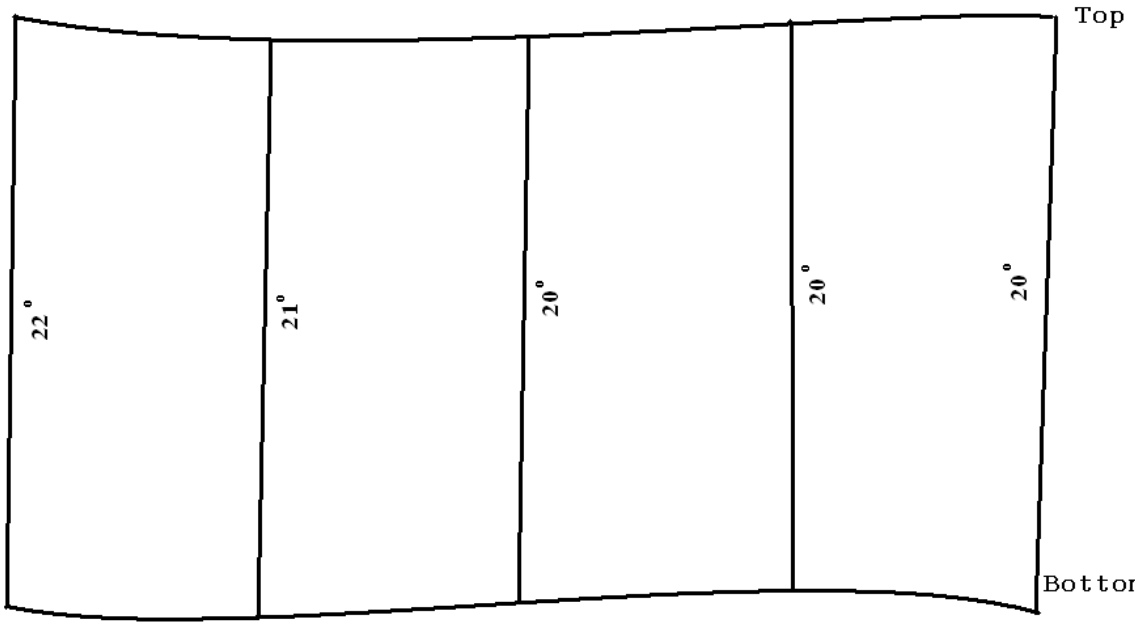

Figure IV.18 Berm Slope Measurements at National Site

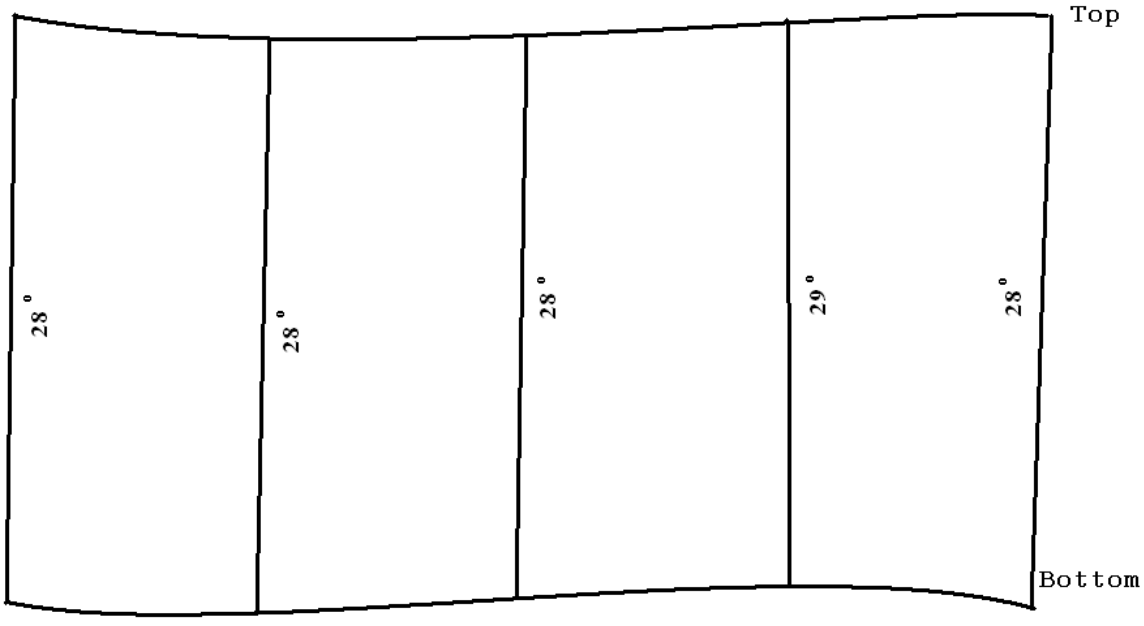

Figure IV.19 Berm Slope Measurements at Premium Site

The method for measuring the angle of repose, which can be assumed to be equal to the internal friction angle for a loose state, is referred to as the tipping test. This process involves dumping material into a pile and measuring the steepness at which it holds itself in place. This was already being conducted in the construction of the slopes, but it was unsafe to measure this angle using an inclinometer during construction. So, to measure this angle, a picture was taken of the slope using a hand held level to ensure the picture is parallel with the ground. Then in photo editing software this angle can be marked and measured. This process is repeated several times at each site to ensure a large enough sampling size to guarantee an accurate angle of repose.

Shown below in Figure IV.20 is an example of this process for the National Coal Site during construction. The slope length in Figure IV.20 is approximately 75 feet (23 meters). All Pictures used in the infinite slope analysis can be seen in Appendix D. Also seen below in Table IV.11 are the values for all measurements taken at each site.

Figure IV.20 Example of Measured Angle of Repose at National Coal Site

Table IV.11 Values Used in Infinite Slope Analysis

Site	Sample #	Angle of Repose, Degrees	Highest In-Situ Angle
National	1	36	22
National	2	38	22
National	3	37	22
National	4	36	22
Premium	1	38	29
Premium	2	38	29
Premium	3	37	29
Premium	4	39	29
Mountainside	1	38	30
Mountainside	2	39	30
Mountainside	3	37	30
Mountainside	4	38	30

ii. Infinite Slope Analysis

To determine slope stability a simple infinite slope analysis was used for all three sites. As implied by its name, in the infinite slope procedure the slope is assumed to extend infinitely in all directions and sliding is assumed to occur along a plane parallel to the face of the slope (Duncan et al. 2005). Because the slope is infinite, the stresses will be the same on any two planes that are perpendicular to the slope, such as the planes A-A' and B-B' seen in Figure IV.21 below (Duncan et al. 2005). Equilibrium equations can then be derived by considering the rectangular block created by sections A-A' and B-B'. Because the forces on the end of the block will be equal in magnitude and opposite in direction they may be ignored (Duncan et al. 2005). Summing forces in directions perpendicular and parallel to the slip plane gives the following expressions for the shear force S, and the normal force N:

$$S = W \sin q$$

$$N = W \cos q$$

Where q is the inclination of the slope, in degrees, as shown and W is the weight of the rectangular block for a given thickness acting downward in the vertical direction. For a given depth to the slip surface, z, W can then be calculated as (Duncan et al. 2005):

$$W = \gamma/z \cos q$$

Where γ is the unit weight of the soil.

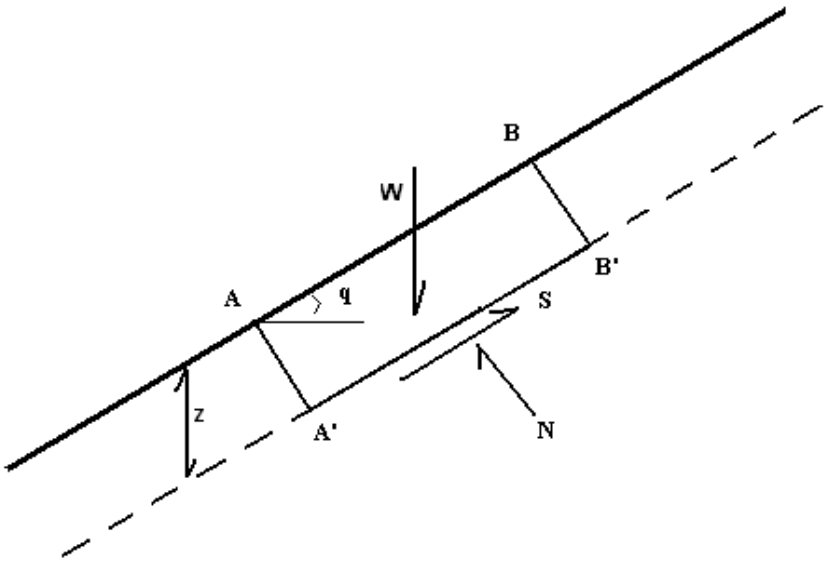

Figure IV.21 Infinite Slope Illustration

Shear stress, τ , and normal stress, σ can then be calculated by dividing the shear force and normal force by the area of the plane, which yields (Duncan et al. 2005):

$$\tau = \gamma * z \cos q \sin q$$
$$\sigma = \gamma * z \cos^2 q$$

Then a factor of safety can be calculated by dividing the available shear strength by the equilibrium shear stress (Duncan et al. 2005). Note that the depth term, z, drops out. The available shear strength can then be expressed by the Mohr-Coulomb equation as follows (Duncan et al. 2005):

$$s' = c + \sigma \tan \phi$$

Where c is the cohesion of the material and ϕ is the internal friction angle of the material. For a cohesionless soil the factor of safety can then be calculated as (Duncan et al. 2005):

$$FS = \frac{\tan \phi}{\tan q}$$

Table IV.12 Factor of Safety Data

Site	Mean Angle of Repose °	Highest In-Situ Angle °	Mean Upper Bound F.S.	Mean Lower Bound F.S.
Mountainside	**38**	**30**	**1.4**	**0.7**
National	**37**	**22**	**1.9**	**0.95**
Premium	**38**	**29**	**1.4**	**0.7**

These factor of safety values assume no cohesion in the spoil material which is a conservative assumption because the material does have some small measure of cohesion. Also, assuming a cohesionless material is valid when considering long term drained conditions because under these conditions the boundary pore pressures will remain constant.

While these safety factors are conservative as a simple infinite slope analysis procedure they do not take into account seepage, or water flow within the spoil, parallel to the surface. This seepage parallel to the slope face is often reached in the lower portions of natural slopes (Lambe et al. 1969). Seepage changes the infinite slope procedure because the effective normal stress, described as σ earlier, is proportional to the buoyant unit weight (Lambe et al. 1969). Since the buoyant unit weight can be as much as about one half of the normal unit weight, the factor of safety can then be reduced by as much as one half for severe seepage conditions. This can be seen in the following equation where the unit weight of water, γw, is taken as 62.4 pounds per cubic foot and the unit weight of soil, γs is taken as 120 pounds per cubic foot and therefore γw divided by γs is approximately 0.5:

$$FS_{w/\,seepage} = FS_{w/o \quad seepage}\left[\frac{\gamma_w}{\gamma_s}\right] \cong 0.5FS_{w/o \quad seepage}$$

Table IV.12, shown above, provides an upper bound for the factor of safety which assumes no seepage and a lower bound which assumes major seepage parallel to the slope surface.

Safety factors usually range from one to three depending on the uncertainties involved in calculation and the consequences of failure (Duncan et al. 2005). The larger the uncertainty and consequence of failure then the larger the factor of safety should be for a given situation (Duncan et al. 2005). If the engineer has been conservative in the calculation of the internal friction angle a factor of safety of one can be used for slopes (Lambe et al. 1969). Safety factors of two are typical for structures such as gravity retaining walls and small foundations (Lambe et al. 1969). Common factor of safety values vary from about 1.1 for low probability seismic loading to 3.0 for full water level static loading in dam structures (National Research Council, 1983).

V. Part II Conclusions

The high variability in the unit weight readings is partly due to human error in testing, but is mainly due to the nature of the material tested. Certain tests with higher readings than average may have had higher rock contents. Lower readings may be due to voids in the subsurface which were found to be common during testing, especially in areas of higher shale content as discussed earlier.

There was no correlation found between unit weight and depth in the first three feet of material during the auger unit weight testing. This is consistent with testing performed by the University of Kentucky. This may suggest that at least the top three feet of material has not been compacted by machinery.

The most useful method to determine the unit weight of reclaimed mine spoils was to use a nuclear density gauge. Other methods were determined to be equally as accurate but had a higher variability among tests within the same area. Also, the nuclear density gauge is the fastest test and has the lowest human error factor.

Due to the average unit weight readings being less than that of typical natural undisturbed soils for the area, and to the relatively high void ratios, it is concluded that the soil mediums tested would be sufficient for tree growth, assuming all other tree growth soil properties are sufficient.

The low compaction grading technique, when applied properly, should yield soils with unit weights similar to those reported from the three sites studied. Therefore the low compaction grading technique should yield a sufficient medium for tree growth, assuming all other tree growth soil properties are sufficient.

The infinite slope procedure is convenient as a quick way to measure slope stability, but should not be used in final design of a reclaimed mine slope. The assumption of cohesion-less soil is shown to be conservative by the grain size distributions which yielded no greater than 13 percent clay content of the material less than two inches and no greater than 7 percent clay content of the adjusted overall grain size distribution.

The simple infinite slope analysis is a convenient and quick way to asses the stability of any slope in question. It could also be a quick way to assess what in-situ slope angle should be constructed based on the angle of repose of the material.

The slope stability of the three sites is within the expected range of values. The lowest factor of safety of 0.7 is the worst case scenario of the steepest slope, the least resistive material, and very high seepage rates, which makes this calculation very conservative in nature.

List of References

Duncan, Michael J. and Wright, Stephen G.. 2005. Soil Strength and Soil Stability. John
Wiley and Sons, Inc., Hoboken, New Jersey

Sweigard, R., J. Burger, C. Zipper, J. Skousen, C. Barton, and P. Angel (2005) "Low Compaction Grading to Enhance Reforestation Success on Coal Surface Mines." U.S. Office of Surface Mining. Forest Reclamation Advisory Number 3.

U.S. EPA. 2008. Selecting a Sampling Design. http://www.epa.gov/quality/qksampl.html. February, 24, 2009.

Sweigard, R., V. Badaker, and K. Hunt. 2007. "Development of a Field Procedure to Evaluate the Reforestation Potential of Reclaimed Surface-Mined Land." University of Kentucky, Department of Mining Engineering.

Lambe, T. and R. Whitman. 1969. Soil Mechanics. John Wiley and Sons. New York

Troxler Electronic Laboratories, Inc. 1997. "Nuclear Gauge Safety Training Program, 8th edition". Troxler Electronic Laboratories. Research Triangle Park, NC.

Franklin, J. and D. Buckley. 2008. "Reforestation of Steep Reclaimed Slopes: Forest Establishment and Function." Department of Forestry, Wildlife and Fisheries. University of Tennessee, Knoxville.

National Research Council. 1983. Safety of Existing Dams: Evaluation and Improvement, Committee on Safety of Existing Dams, Water Science and Technology Board, Commission on Engineering and Technical Systems. National Academy Press. Washington D.C.

McCarthy, David F. 2002. Essentials of Soil Mechanics and Foundations. Prentice Hall, Columbus, Ohio.

Appendices

Appendix A: Hill-slope Classification Data

Table A.1: Correlation of RSA Basins and RGA Basins with Associated Subwatersheds Used in the Classification of Hill-Slopes.

RGA/FID Basin Number and corresponding RSA Basin Number					RSA Basin Number and corresponding RGA/FID Basin Number			
RGA or FID Basin Number	SITE ID	RSA Basin ID Number	Sub-Watershed		RSA Basin ID Number	SITE ID	RGA or FID Basin Number	Sub-Watershed
0	BBC 1	17	Montgomery Fork		1	GCR 1	9	Bull Creek
1	BBC 2	46	Smokey Creek		2	GCR 3	11	Bull Creek
2	BBC 3	3	Bull Creek		3	BBC 3	2	Bull Creek
3	BC 1	10	Greasy Creek		4	MFCS 1	28	Bull Creek
4	BSC 1	18	Brimstone		5	MFCS 10	29	Brimstone
5	BSC 2	28	Ligias Fork		6	LF 2	23	Brimstone
6	BSC 3	11	Greasy Creek		7	GCR 2	10	Brimstone
7	FB 1	37	Montgomery Fork		8	LBC 2	19	Ligias Fork
8	GB 1	26	Ligias Fork		9	RC 3	37	Montgomery Fork
9	GCR 1	1	Bull Creek		10	BC 1	3	Greasy Creek
10	GCR 2	7	Brimstone		11	BSC 3	6	Greasy Creek
11	GCR 3	2	Bull Creek		12	SC 1	39	Greasy Creek
12	GGB 1	41	Smokey Creek		13	SF 1	45	Ligias Fork
13	GGB 2	32	Frozen Head		14	JC 3	16	Ligias Fork
14	IC 1	22	Bull Creek		15	LBC 1	18	Brimstone
15	JC 2	27	Ligias Fork		16	PCC 1	34	Montgomery Fork
16	JC 3	14	Ligias Fork		17	BBC 1	0	Montgomery Fork
17	JOE 1	24	Ligias Fork		18	BSC 1	4	Brimstone
18	LBC 1	15	Brimstone		19	SC 2	40	Bull Creek
19	LBC 2	8	Ligias Fork		20	RC 2	36	Bull Creek
20	LBC 3	29	Montgomery Fork		21	LBC 4	21	Bull Creek
21	LBC 4	21	Bull Creek		22	IC 1	14	Bull Creek
22	LF 1	23	Ligias Fork		23	LF 1	22	Ligias Fork
23	LF 2	6	Brimstone		24	JOE 1	17	Ligias Fork
24	LF 3	39	Montgomery Fork		25	SC 3	41	Ligias Fork
25	LF 4	40	Smokey Creek		26	GB 1	8	Ligias Fork
26	LF 5	30	Montgomery Fork		27	JC 2	15	Ligias Fork
27	LF 6	42	Smokey Creek		28	BSC 2	5	Ligias Fork
28	MFCS 1	4	Bull Creek		29	LBC 3	20	Montgomery Fork
29	MFCS 10	5	Brimstone		30	LF 5	26	Montgomery Fork
30	MKC 1	45	Smokey Creek		31	SC 5	43	Montgomery Fork
31	NPFF 1	43	Smokey Creek		32	GGB 2	13	Frozen Head
32	NPFF 2	48	Montgomery Fork		33	SHC 1	46	Frozen Head
33	NPFF 3	34	Frozen Head		34	NPFF 3	33	Frozen Head
34	PCC 1	16	Montgomery Fork		35	SC 4	42	Montgomery Fork
35	RC 1	38	Montgomery Fork		36	SC 6	44	Montgomery Fork
36	RC 2	20	Bull Creek		37	FB 1	7	Montgomery Fork
37	RC 3	9	Montgomery Fork		38	RC 1	35	Montgomery Fork
38	SB 1	47	Smokey Creek		39	LF 3	24	Montgomery Fork
39	SC 1	12	Greasy Creek		40	LF 4	25	Smokey Creek
40	SC 2	19	Bull Creek		41	GGB 1	12	Smokey Creek
41	SC 3	25	Ligias Fork		42	LF 6	27	Smokey Creek
42	SC 4	35	Montgomery Fork		43	NPFF 1	31	Smokey Creek
43	SC 5	31	Montgomery Fork		44	WC 1	47	Smokey Creek
44	SC 6	36	Montgomery Fork		45	MKC 1	30	Smokey Creek
45	SF 1	13	Ligias Fork		46	BBC 2	1	Smokey Creek
46	SHC 1	33	Frozen Head		47	SB 1	38	Smokey Creek
47	WC 1	44	Smokey Creek		48	NPFF 2	32	Montgomery Fork

Table A.2. Summary of RSA Basin Scores.

RGA or FID Basin Number	Sub-Watershed	RSA Basin ID Number	SITE ID	RSA Sub-Basin	Gradient Score	RF = Relief Factor	Valley Score	RSA Score
0	Montgomery Fork	17	BBC 1	17	25.5	0.42	9	29
1	Smokey Creek	46	BBC 2	46	26.1	1.41	27	64
2	Bull Creek	3	BBC 3	3	25.0	0.35	27	34
3	Greasy Creek	10	BC 1	10	21.5	0.62	9	27
4	Brimstone	18	BSC 1	18	25.1	1.39	9	38
5	Ligias Fork	28	BSC 2	28	26.9	1.67	9	42
6	Greasy Creek	11	BSC 3	11	20.1	0.18	3	21
7	Montgomery Fork	37	FB 1	37	26.4	0.98	81	106
8	Ligias Fork	26	GB 1	26	25.7	1.05	9	35
9	Bull Creek	1	GCR 1	1	25.9	1.43	81	142
10	Brimstone	7	GCR 2	7	25.0	1.07	27	54
11	Bull Creek	2	GCR 3	2	24.7	1.25	9	36
12	Smokey Creek	41	GGB 1	41	26.2	1.40	27	64
13	Frozen Head	32	GGB 2	32	28.0	0.58	3	30
14	Bull Creek	22	IC 1	22	26.5	1.11	27	57
15	Ligias Fork	27	JC 2	27	25.1	1.61	27	68
16	Ligias Fork	14	JC 3	14	23.7	0.82	3	26
17	Ligias Fork	24	JOE 1	24	25.7	1.19	9	36
18	Brimstone	15	LBC 1	15	26.2	1.08	27	55
19	Ligias Fork	8	LBC 2	8	26.5	1.46	81	145
20	Montgomery Fork	29	LBC 3	29	25.1	0.79	3	28
21	Bull Creek	21	LBC 4	21	26.4	0.58	27	42
22	Ligias Fork	23	LF 1	23	25.9	1.43	9	39
23	Brimstone	6	LF 2	6	25.9	1.40	81	139
24	Montgomery Fork	39	LF 3	39	27.2	1.64	81	160
25	Smokey Creek	40	LF 4	40	26.0	1.44	27	65
26	Montgomery Fork	30	LF 5	30	26.4	0.94	81	103
27	Smokey Creek	42	LF 6	42	25.4	1.48	27	65
28	Bull Creek	4	MFCS 1	4	24.1	1.10	9	34
29	Brimstone	5	MFCS 10	5	23.5	0.90	81	96
30	Smokey Creek	45	MKC 1	45	27.2	1.62	27	71
31	Smokey Creek	43	NPFF 1	43	26.5	1.53	9	40
32	Montgomery Fork	48	NPFF 2	48	27.1	1.58	27	70
33	Frozen Head	34	NPFF 3	34	27.1	1.44	81	144
34	Montgomery Fork	16	PCC 1	16	27.5	1.14	9	38
35	Montgomery Fork	38	RC 1	38	26.4	0.67	27	45
36	Bull Creek	20	RC 2	20	24.2	0.83	27	47
37	Montgomery Fork	9	RC 3	9	26.6	1.04	27	55
38	Smokey Creek	47	SB 1	47	27.1	1.60	27	70
39	Greasy Creek	12	SC 1	12	25.1	1.42	81	140
40	Bull Creek	19	SC 2	19	26.2	0.90	81	99
41	Ligias Fork	25	SC 3	25	27.1	1.37	27	64
42	Montgomery Fork	35	SC 4	35	26.8	1.23	9	38
43	Montgomery Fork	31	SC 5	31	27.3	1.54	27	69
44	Montgomery Fork	36	SC 6	36	26.1	1.15	81	119
45	Ligias Fork	13	SF 1	13	26.1	1.64	3	31
46	Frozen Head	33	SHC 1	33	27.7	1.37	27	65
47	Smokey Creek	44	WC 1	44	26.0	1.41	9	39

Appendix B: Uplands Sample Data

Table B.1 "Master Table"

Subwatershed	Site ID	Coordinates (lat, long)	Site Description
Brimstone Creek	BR-1	36.26, -84.50	Active Logging Road
Brimstone Creek	BR-2	36.26, -84.51	25% Logged Area
Brimstone Creek	BR-3	36.23, -84.48	75% Reclaimed Mine
Brimstone Creek	BR-4	36.25, -84.48	Active Mining Road
Montgomery Fork	MF-1	36.33, -84.34	100% Logged Area
Montgomery Fork	MF-2	36.34, -84.35	50% Reclaimed Mine
Montgomery Fork	MF-3	36.34, -84.36	Active Logging Road
Montgomery Fork	MF-4	36.34, -84.35	Active Mining Road
Smokey Creek	SC-1	36.20, -84.41	50% Reclaimed Mine
Smokey Creek	SC-2	36.21, -84.42	Inactive Un-reclaimed Logging Road
Smokey Creek	SC-3	36.23, -84.44	75% Logged Area
Smokey Creek	SC-4	36.19, -84.42	Inactive Un-reclaimed Mining Road

Sample ID	Shear Strength (PP, tsf)	Shear Resistance (CP, lbs)	Plastic Limit	Liquid Limit	Plasticity Index
BR-1	3.25	75	NP	NP	NP
BR-2	2	40	NP	NP	NP
BR-3	3.5	85	NP	NP	NP
BR-4	1.5	35	NP	NP	NP

Sample ID	% finer than 200	% clay	D50 (mm)	D84 (mm)	USCS Classification
BR-1	61	16	0.035	1	ML
BR-2	57	9	0.05	0.25	ML
BR-3	39	10	0.85	8	SM
BR-4	56	19	0.04	11.5	ML

Sample ID	Shear Strength (PP, tsf)	Shear Resistance (CP, lbs)	Plastic Limit	Liquid Limit	Plasticity Index
MF-1	1.75	35	NP	NP	NP
MF-2	2.75	55	43	55	12
MF-3	4.5	110	32	33	1
MF-4	2.5	50	NP	NP	NP

Sample ID	% finer than 200	% clay	D50 (mm)	D84 (mm)	USCS Classification
MF-1	52	14	0.07	10.5	ML
MF-2	26	7	6	11.7	GM
MF-3	58	22	0.03	4	ML
MF-4	60	28	0.02	1.8	ML

Sample ID	Shear Strength (PP, tsf)	Shear Resistance (CP, lbs)	Plastic Limit	Liquid Limit	Plasticity Index
SC-1	3.25	75	32	40	8
SC-2	5	140	24	33	9
SC-3	2.5	45	NP	NP	NP
SC-4	3	75	NP	NP	NP

Sample ID	% finer than 200	% clay	D50 (mm)	D84 (mm)	USCS Classification
SC-1	45	13	0.3	6	SM
SC-2	51	14	0.07	4	ML
SC-3	67	20	0.022	2.5	ML
SC-4	41	8	0.2	9	SM

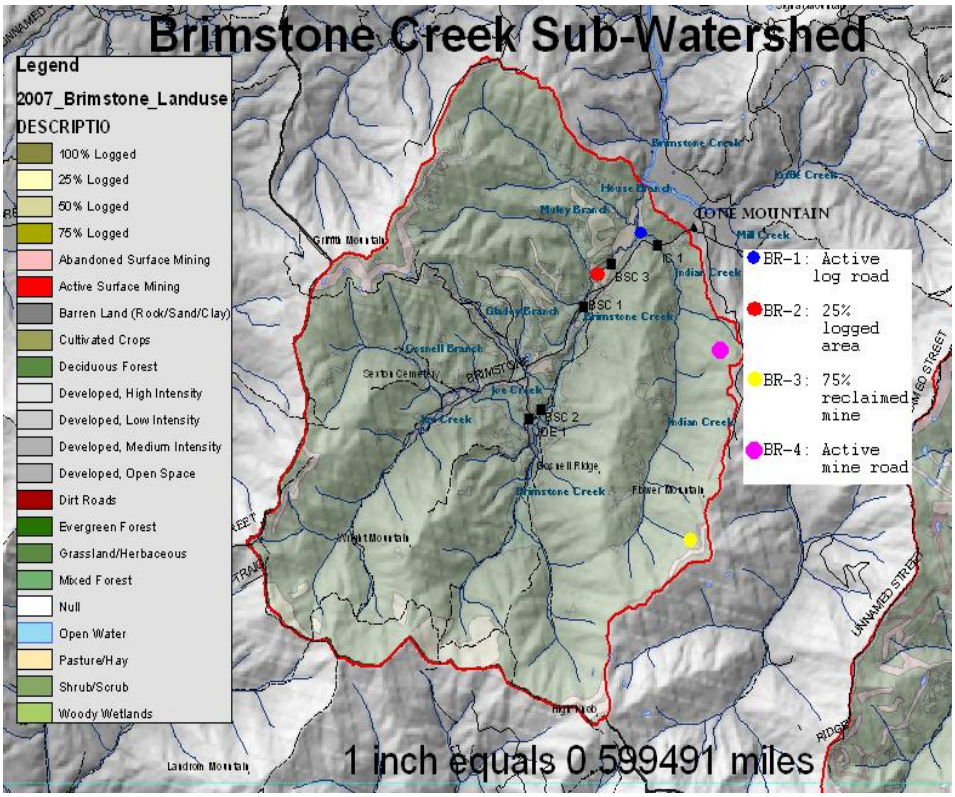

Figure B.1 Map of Brimstone Creek Subwatershed with the Location of the Four Uplands Sample Sites, Each Representing a Different Land Use Category

Table B.2 Upland Sample Data

Sample ID	Shear Strength (PP, tsf)	Shear Resistance (CP, lbs)	Plastic Limit	Liquid Limit	Plasticity Index
BR-1	3.25	75	NP	NP	NP
BR-2	2	40	NP	NP	NP
BR-3	3.5	85	NP	NP	NP
BR-4	1.5	35	NP	NP	NP

Table B.3 Upland Sample Data Continued

Sample ID	% finer than 200	% clay	D50 (mm)	D84 (mm)	USCS Classification
BR-1	61	16	0.035	1	ML
BR-2	57	9	0.05	0.25	ML
BR-3	39	10	0.85	8	SM
BR-4	56	19	0.04	11.5	ML

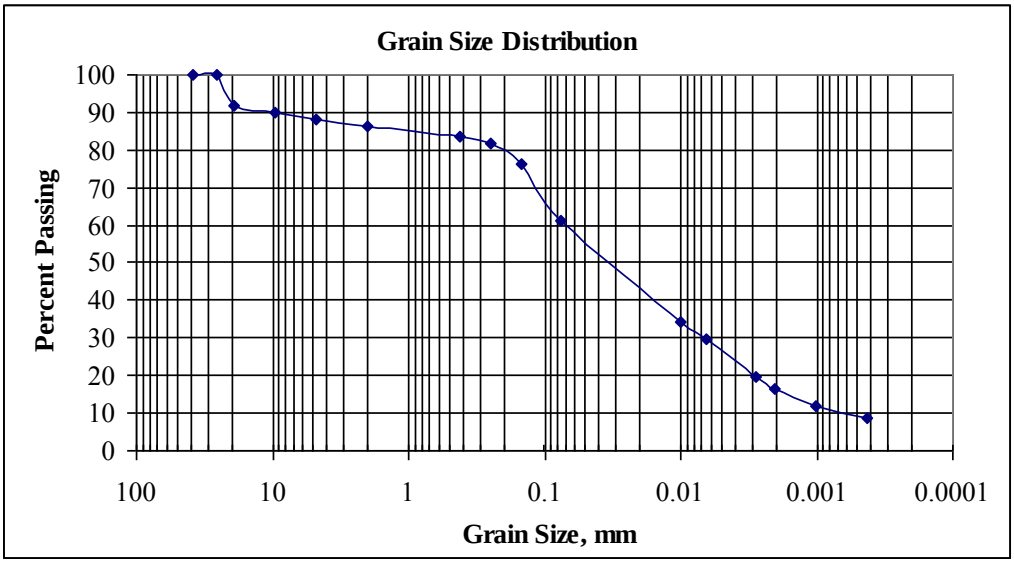

Site ID	Watershed	% finer than 200	% clay	D50 (mm)	D84 (mm)	USCS Classification
BR-1	Brimstone Creek	61	16	0.035	1	ML

Figure B.2 Grain Size Distribution BR-1

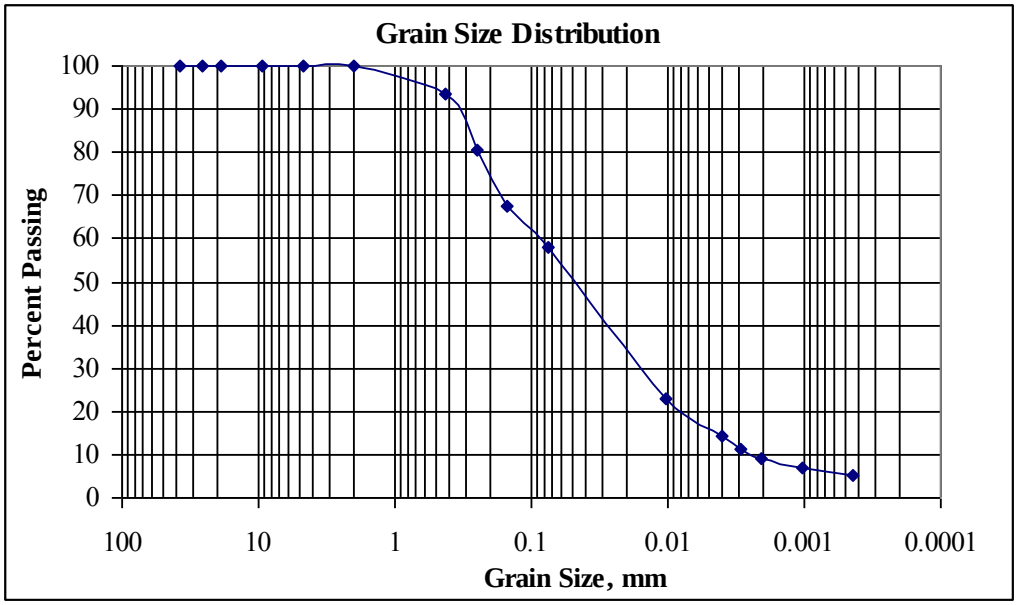

Site ID	Watershed	% finer than 200	% clay	D50 (mm)	D84 (mm)	USCS Classification
BR-2	Brimstone Creek	57	9	0.05	0.25	ML

Figure B.3 Grain Size Distribution BR-2

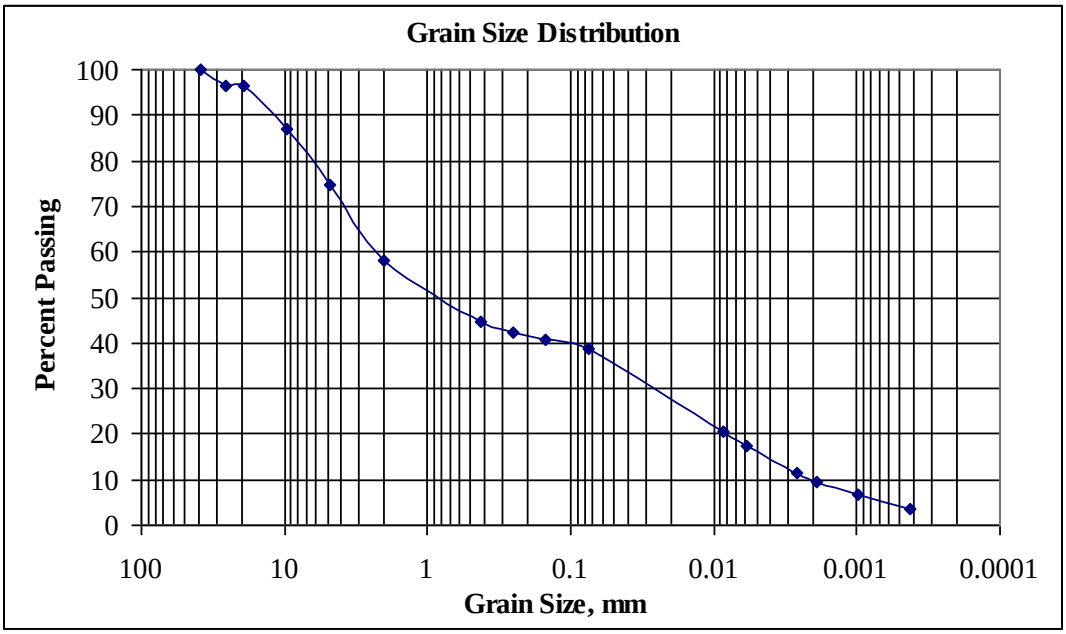

Site ID	Watershed	% finer than 200	% clay	D50 (mm)	D84 (mm)	USCS Classification
BR-3	Brimstone Creek	39	10	0.85	8	SM

Figure B.4 Grain Size Distribution BR-3

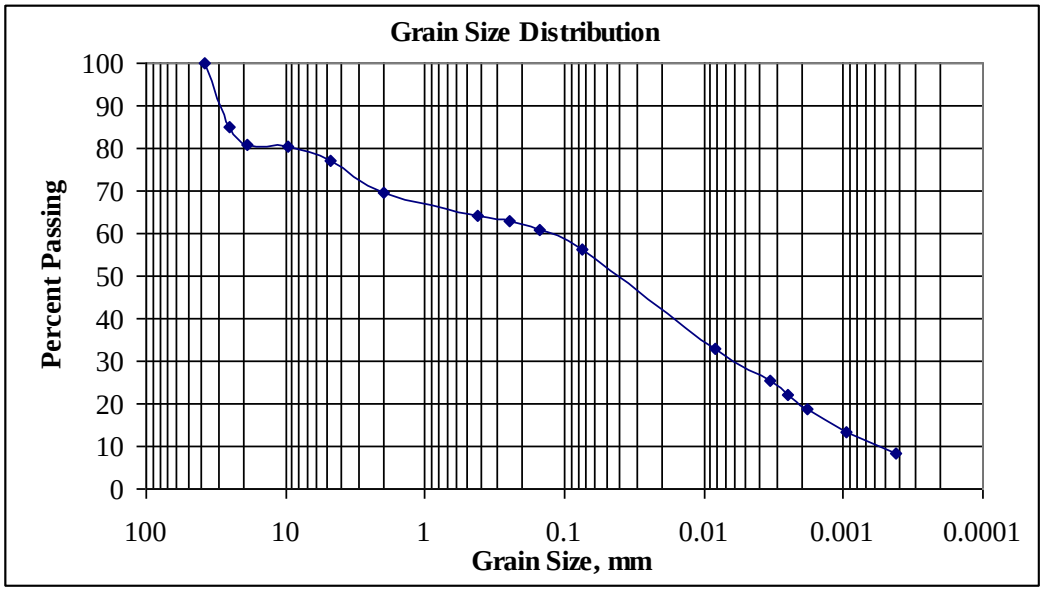

Site ID	Watershed	% finer than 200	% clay	D50 (mm)	D84 (mm)	USCS Classification
BR-4	Brimstone Creek	56	19	0.04	11.5	ML

Figure B.5 Grain Size Distribution BR-4

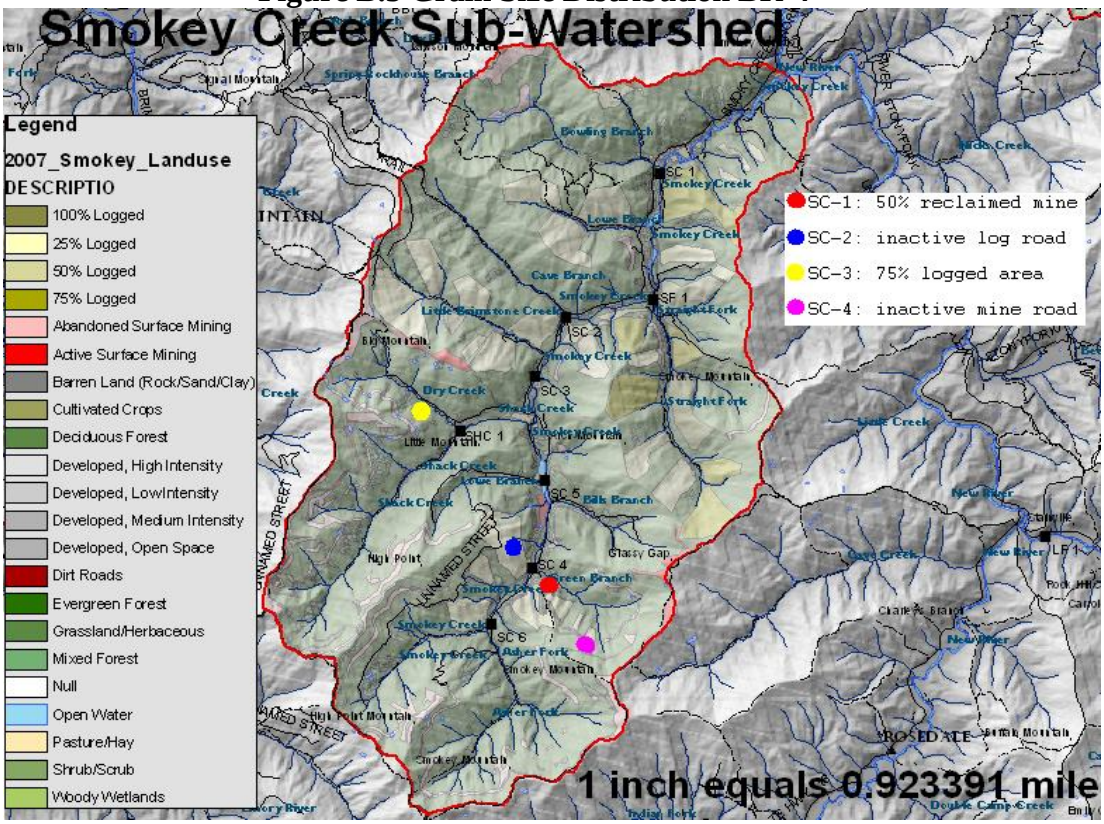

Figure B.6 Map of Smokey Creek Subwatershed with the Location of the Four Uplands Sample Sites, Each Representing a Different Land Use Category

Table B.4 Upland Sample Data

Sample ID	Shear Strength (PP, tsf)	Shear Resistance (CP, lbs)	Plastic Limit	Liquid Limit	Plasticity Index
SC-1	3.25	75	32	40	8
SC-2	5	140	24	33	9
SC-3	2.5	45	NP	NP	NP
SC-4	3	75	NP	NP	NP

Table B.5 Upland Sample Data Continued

Sample ID	% finer than 200	% clay	D50 (mm)	D84 (mm)	USCS Classification
SC-1	45	13	0.3	6	SM
SC-2	51	14	0.07	4	ML
SC-3	67	20	0.022	2.5	ML

SC-4	41	8	0.2	9	SM

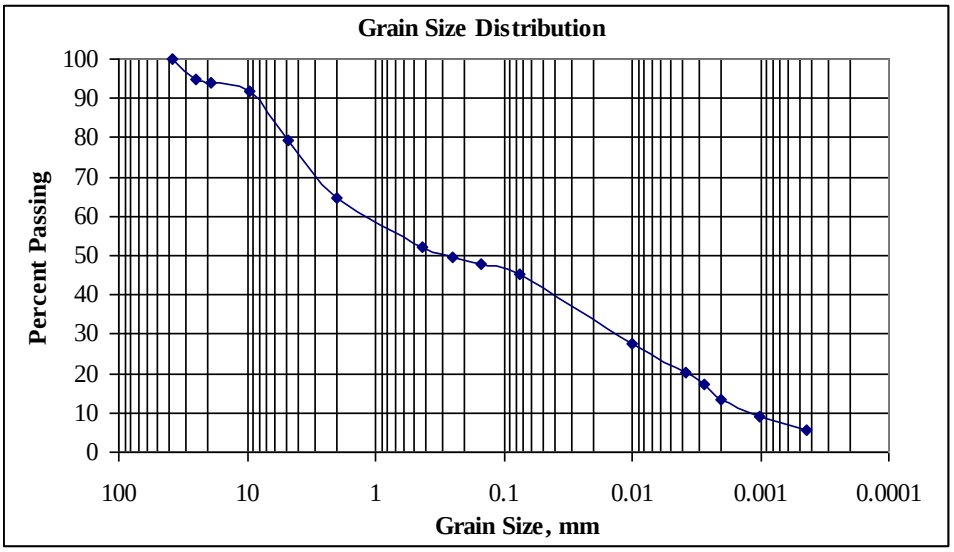

Site ID	Watershed	% finer than 200	% clay	D50 (mm)	D84 (mm)	USCS Classification
SC-1	**Smokey Creek**	45	13	0.3	6	SM

Figure B.7 Grain Size Distribution SC-1

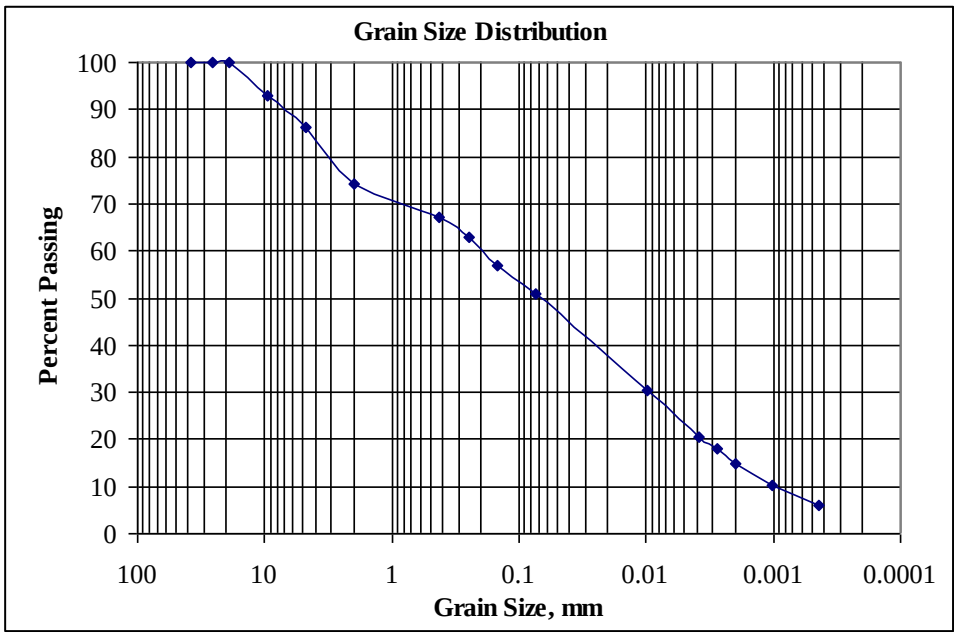

Site ID	Watershed	% finer than 200	% clay	D50 (mm)	D84 (mm)	USCS Classification
SC-2	**Smokey Creek**	51	14	0.07	4	ML

Figure B.8 Grain Size Distribution SC-2

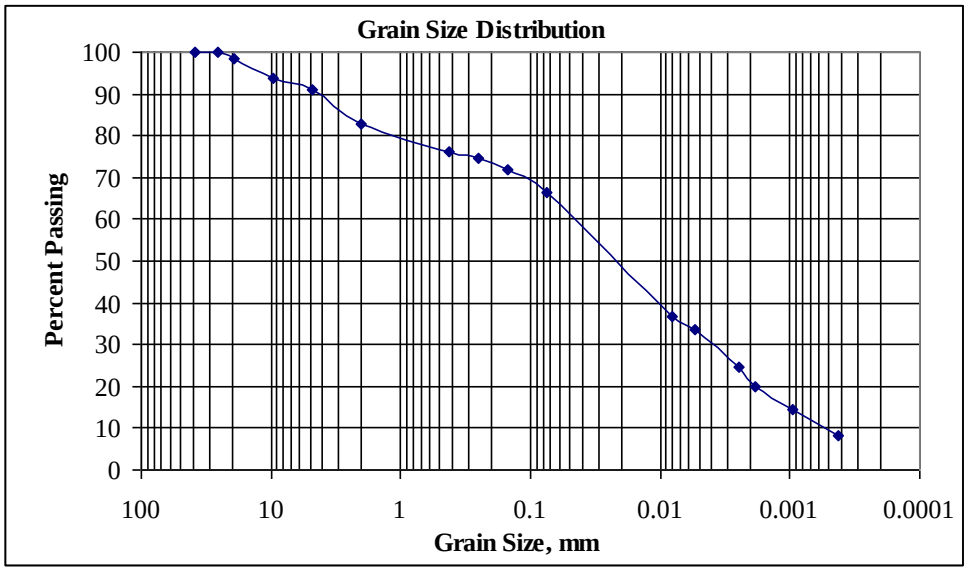

Site ID	Watershed	% finer than 200	% clay	D50 (mm)	D84 (mm)	USCS Classification
SC-3	Smokey Creek	67	20	0.022	2.5	ML

Figure B.9 Grain Size Distribution SC-3

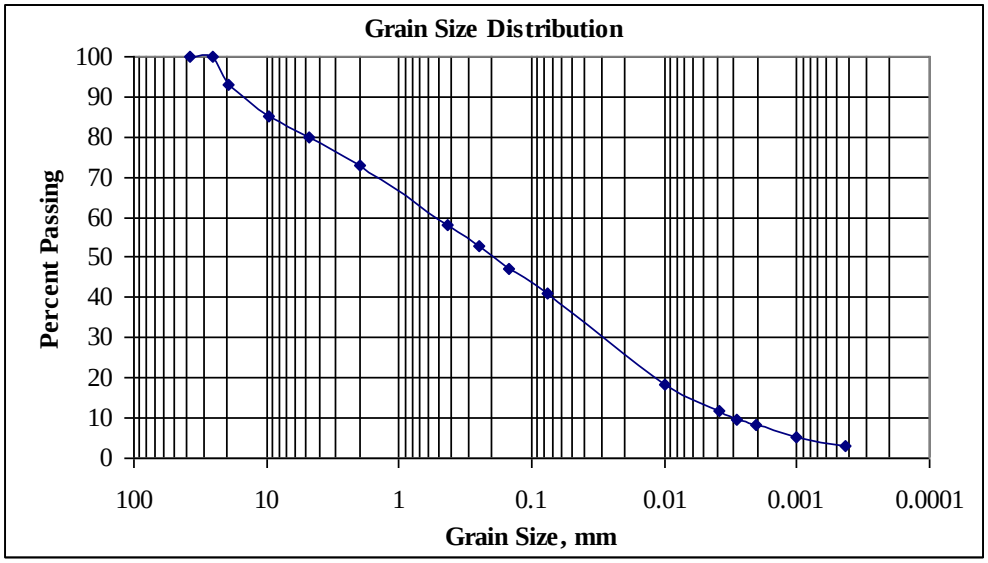

Site ID	Watershed	% finer than 200	% clay	D50 (mm)	D84 (mm)	USCS Classification
SC-4	Smokey Creek	41	8	0.2	9	SM

Figure B.10 Grain Size Distribution SC-4

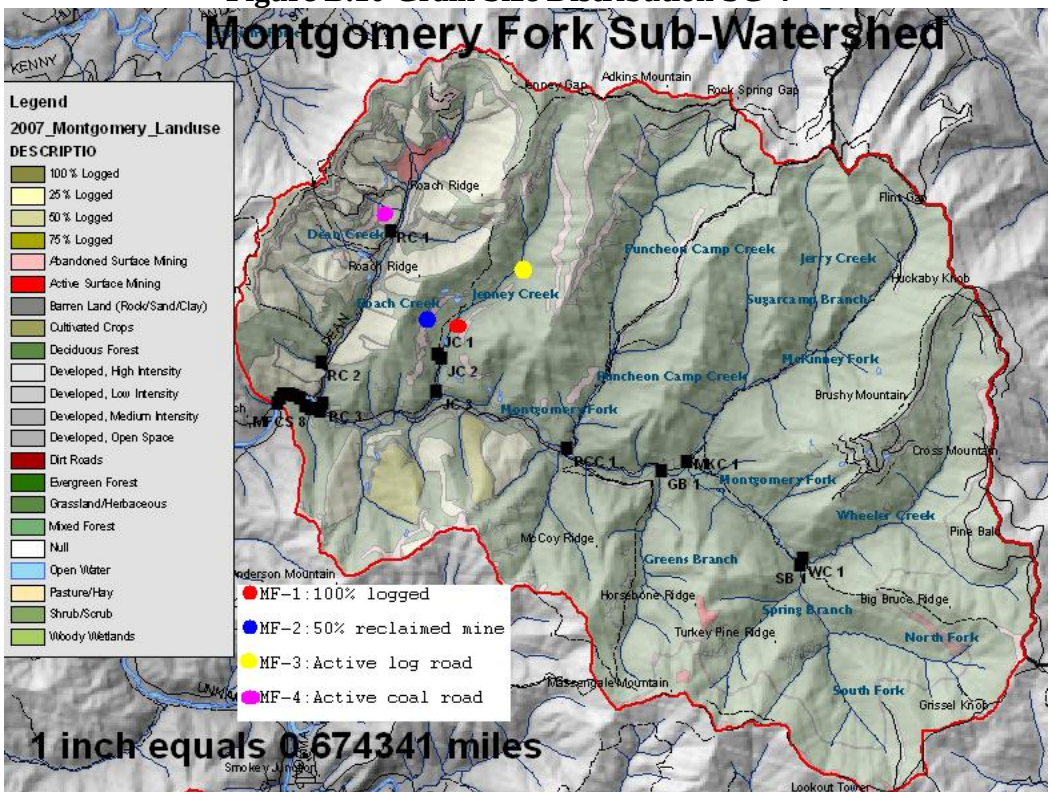

Figure B.11 Map of Montgomery Fork Subwatershed with the Location of the Four Uplands Sample Sites, Each Representing a Different Land Use Category

Table B.6 Upland Sample Data

Sample ID	Shear Strength (PP, tsf)	Shear Resistance (CP, lbs)	Plastic Limit	Liquid Limit	Plasticity Index
MF-1	1.75	35	NP	NP	NP
MF-2	2.75	55	43	55	12
MF-3	4.5	110	32	33	1
MF-4	2.5	50	NP	NP	NP

Table B.7 Upland Sample Data Continued

Sample ID	% finer than 200	% clay	D50 (mm)	D84 (mm)	USCS Classification
MF-1	52	14	0.07	10.5	ML
MF-2	26	7	6	11.7	GM
MF-3	58	22	0.03	4	ML

MF-4	60	28	0.02	1.8	ML

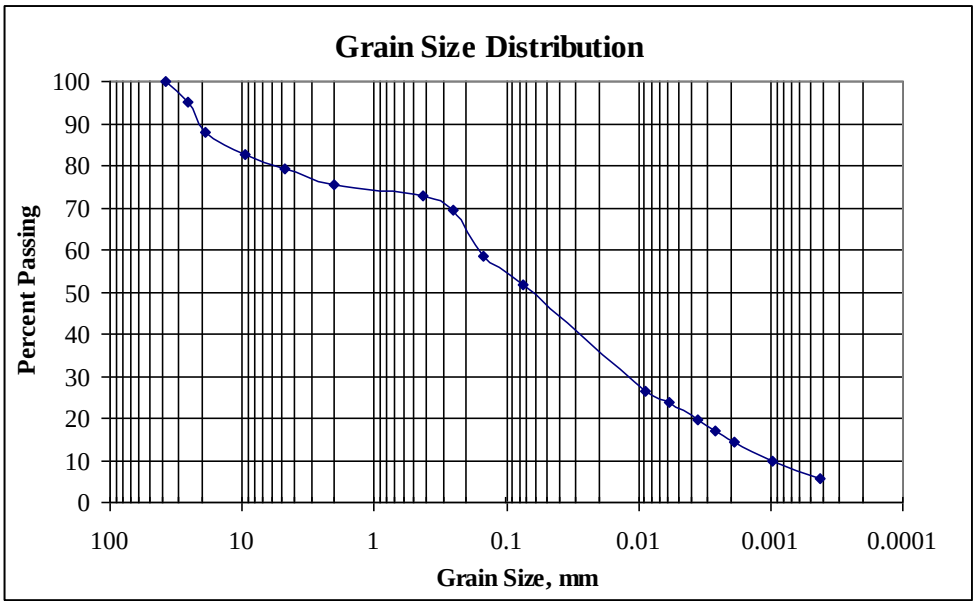

Site ID	Watershed	% finer than 200	% clay	D50 (mm)	D84 (mm)	USCS Classification
MF-1	**Montgomery Fork**	52	14	0.07	10.5	ML

Figure B.12 Grain Size Distribution MF-1

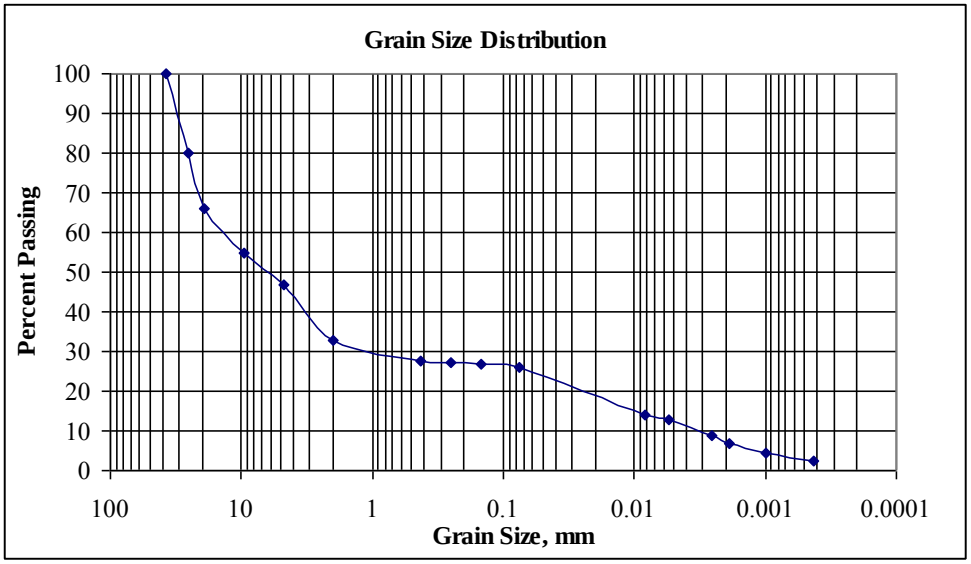

Site ID	Watershed	% finer than 200	% clay	D50 (mm)	D84 (mm)	USCS Classification
MF-2	**Montgomery Fork**	26	7	6	11.7	GM

Figure B.13 Grain Size Distribution MF-2

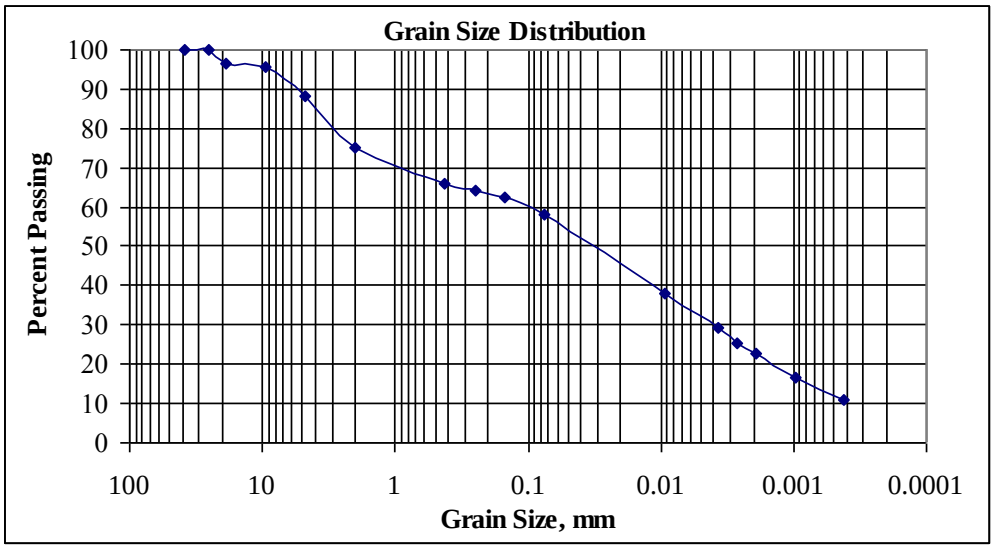

Site ID	Watershed	% finer than 200	% clay	D50 (mm)	D84 (mm)	USCS Classification
MF-3	Montgomery Fork	58	22	0.03	4	ML

Figure B.14 Grain Size Distribution MF-3

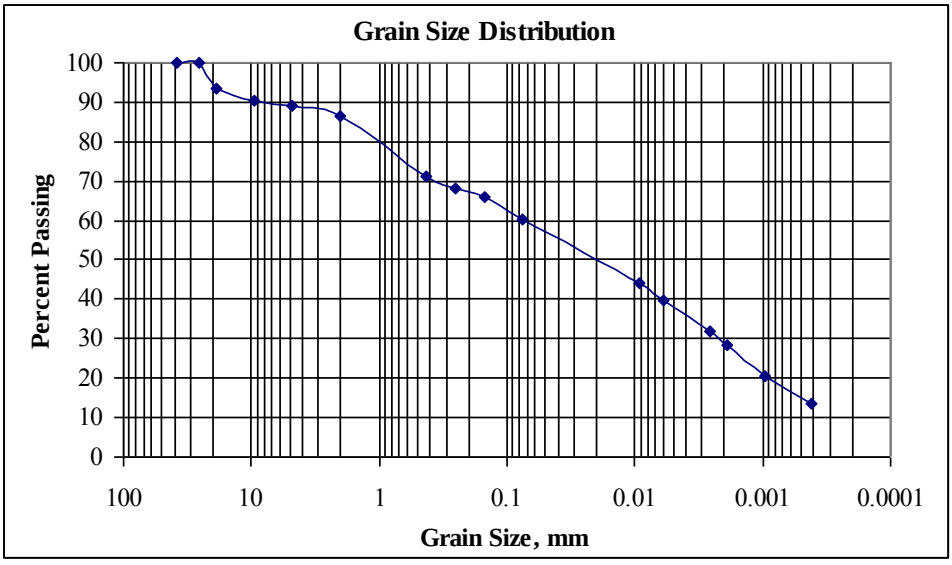

Site ID	Watershed	% finer than 200	% clay	D50 (mm)	D84 (mm)	USCS Classification
MF-4	Montgomery Fork	60	28	0.02	1.8	ML

Figure B.15 Grain Size Distribution MF-4

Appendix C: Grain Size Distribution for Part II

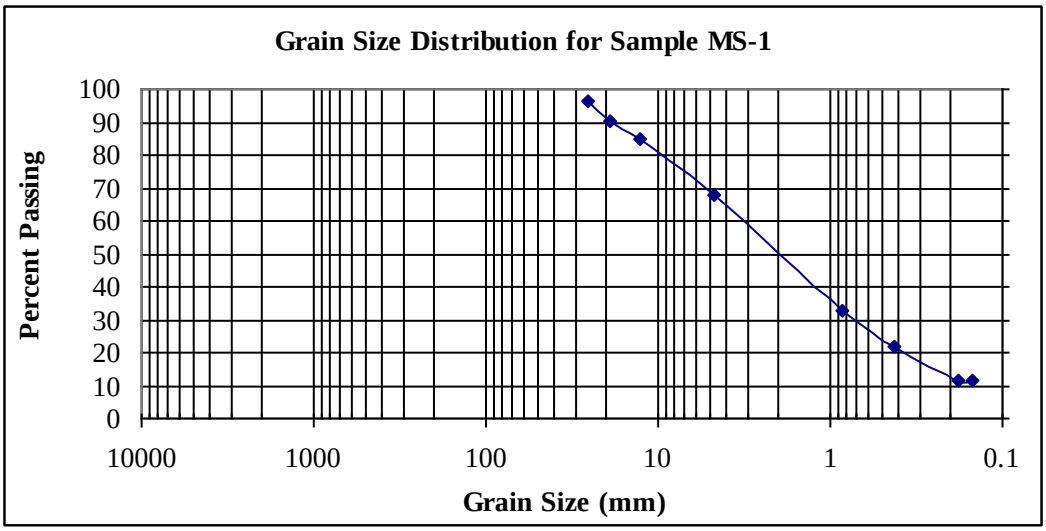

Site ID	Site	% finer than #100	D50 (mm)	D84 (mm)	USCS Classification
MS-1	Mountainside	11.4	2	10.5	SW - SM

Figure C.1 Grain Size Distribution for MS-1

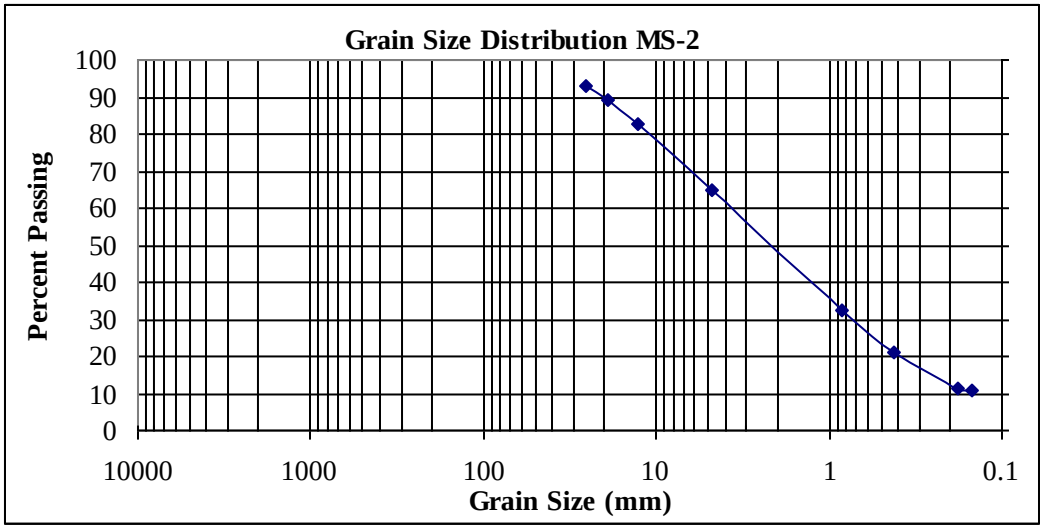

Site ID	Site	% finer than #100	D50 (mm)	D84 (mm)	USCS Classification
MS-2	Mountainside	10.9	2	10.5	SW - SM

Figure C.2 Grain Size Distribution for MS-2

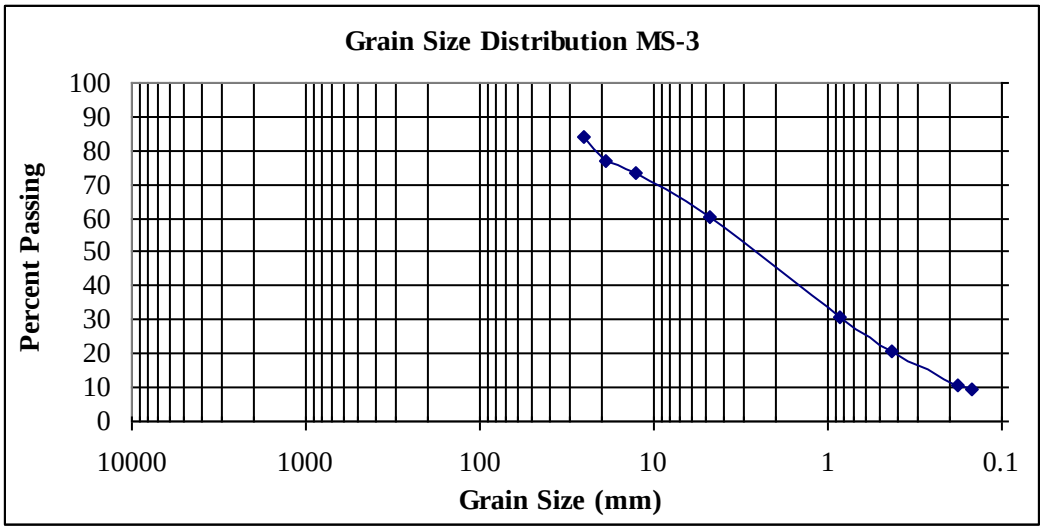

Site ID	Site	% finer than #100	D50 (mm)	D84 (mm)	USCS Classification
MS-3	Mountainside	9.7	2.5	11.5	SW - SM

Figure C.3 Grain Size Distribution for MS-3

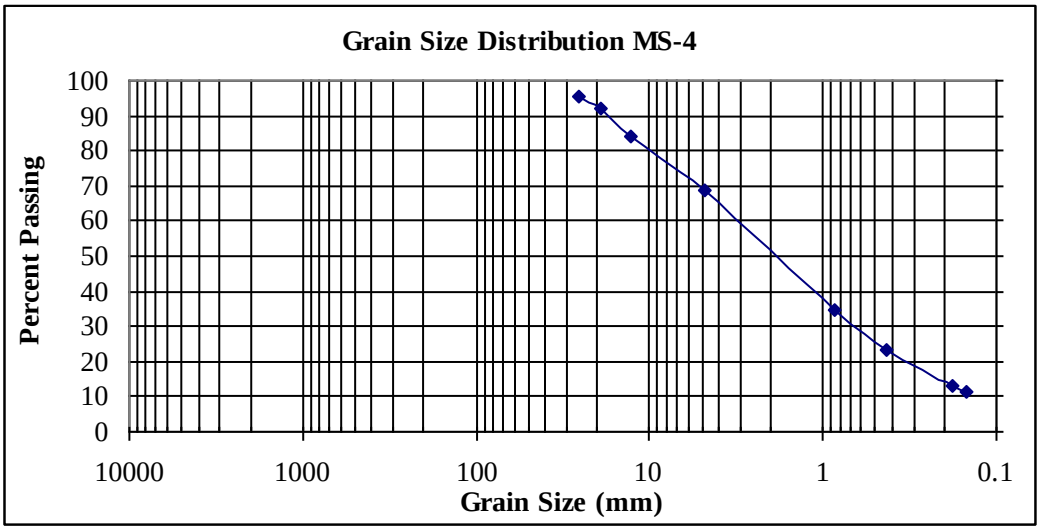

Site ID	Site	% finer than #100	D50 (mm)	D84 (mm)	USCS Classification
MS-4	Mountainside	11.3	2	10.5	SW - SM

Figure C.4 Grain Size Distribution for MS-4

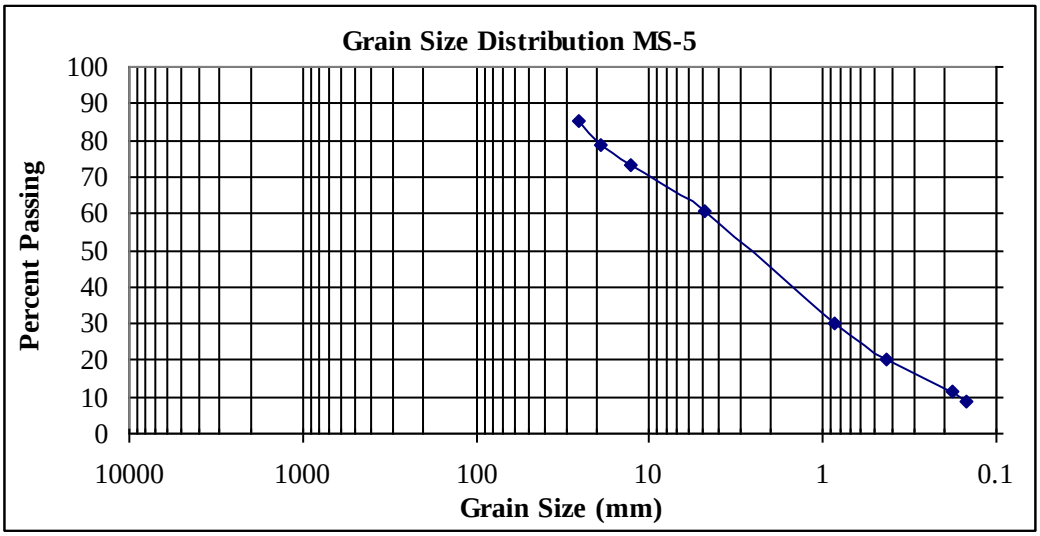

Site ID	Site	% finer than #100	D50 (mm)	D84 (mm)	USCS Classification
MS-5	Mountainside	8.6	2.5	11.5	SW - SM

Figure C.5 Grain Size Distribution for MS-5

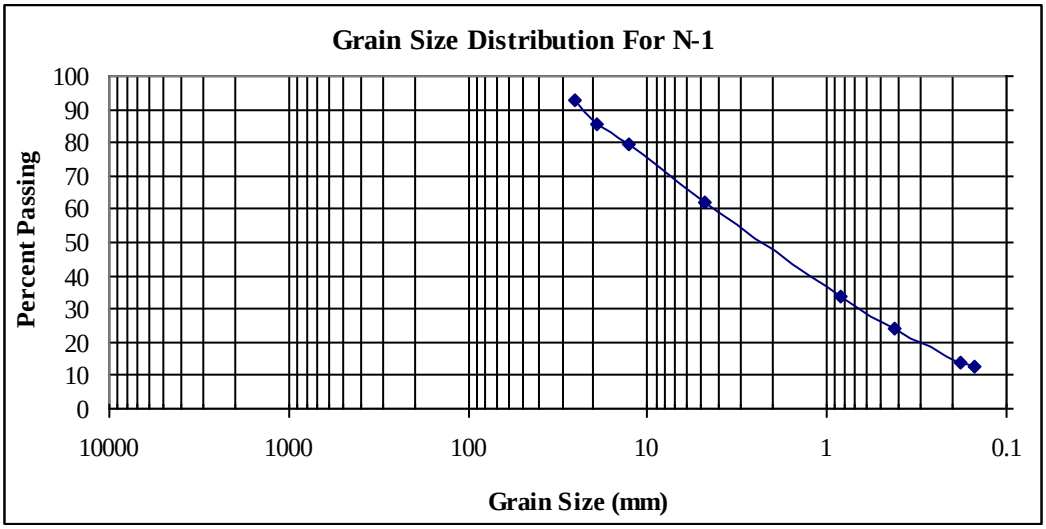

Site ID	Site	% finer than #100	D50 (mm)	D84 (mm)	USCS Classification
N-1	National	12.9	2	11	SW - SM

Figure C.6 Grain Size Distribution for N-1

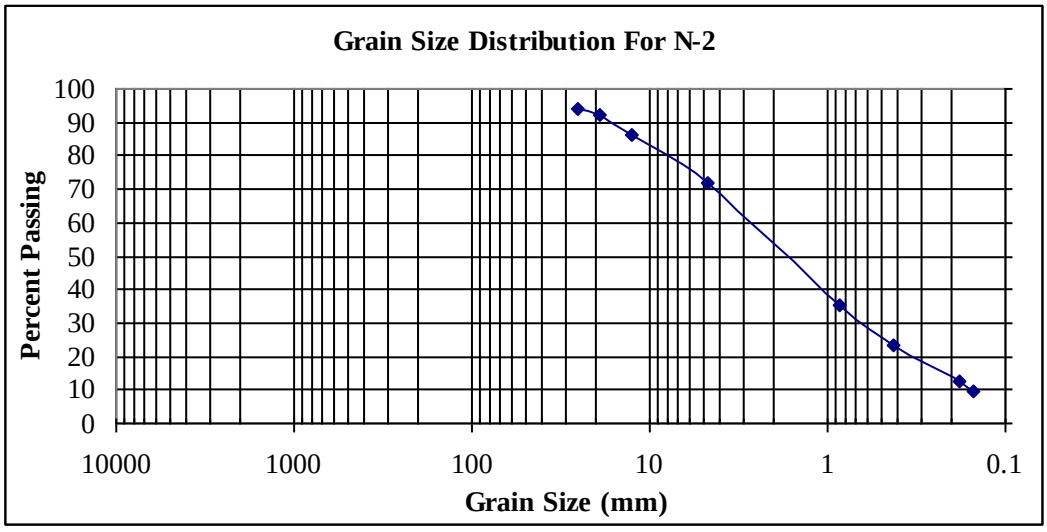

Site ID	Site	% finer than #100	D50 (mm)	D84 (mm)	USCS Classification
N-2	National	9.7	1.5	10	SW - SM

Figure C.7 Grain Size Distribution for N-2

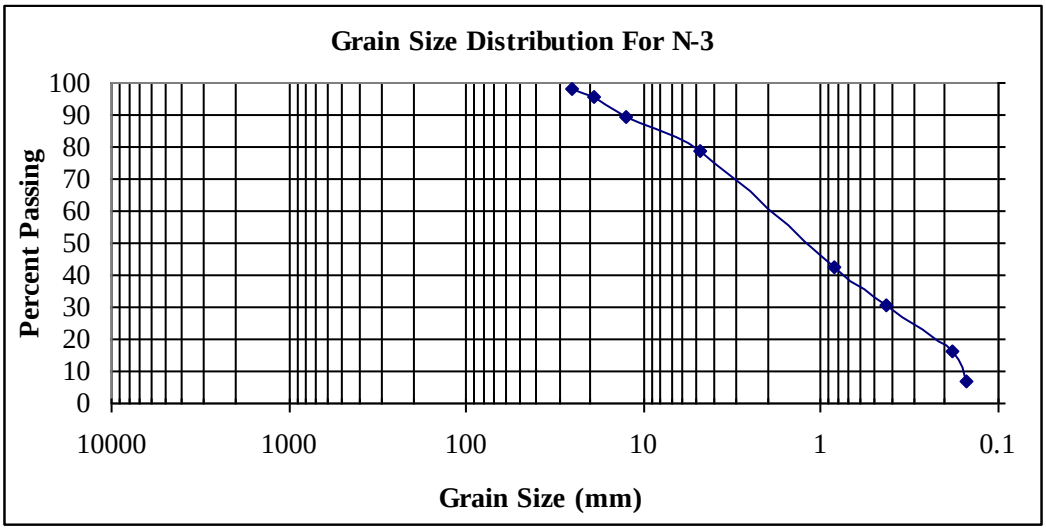

Site ID	Site	% finer than #100	D50 (mm)	D84 (mm)	USCS Classification
N-3	National	7.2	1.5	6.5	SW - SM

Figure C.8 Grain Size Distribution for N-3

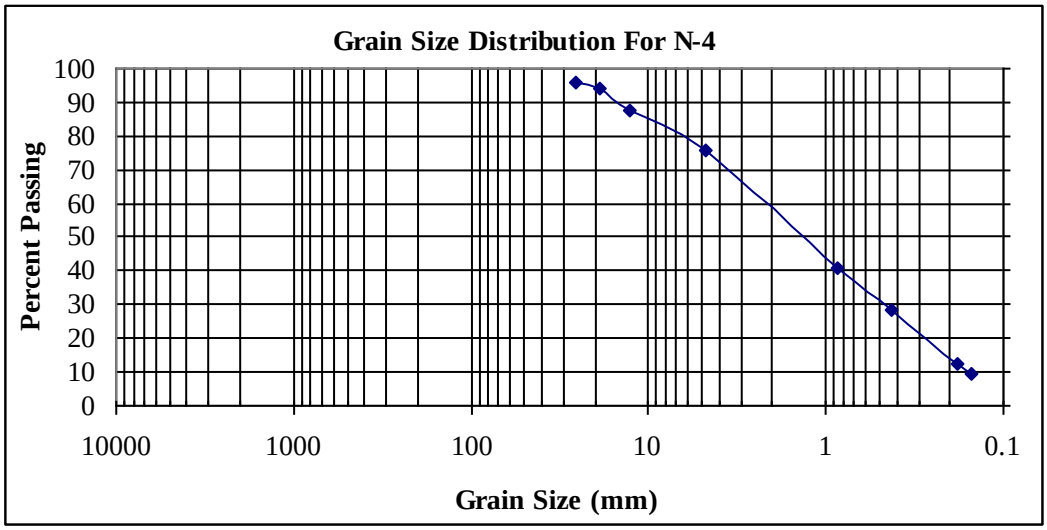

Site ID	Site	% finer than #100	D50 (mm)	D84 (mm)	USCS Classification
N-4	National	9.3	1.5	9	SW - SM

Figure C.9 Grain Size Distribution for N-4

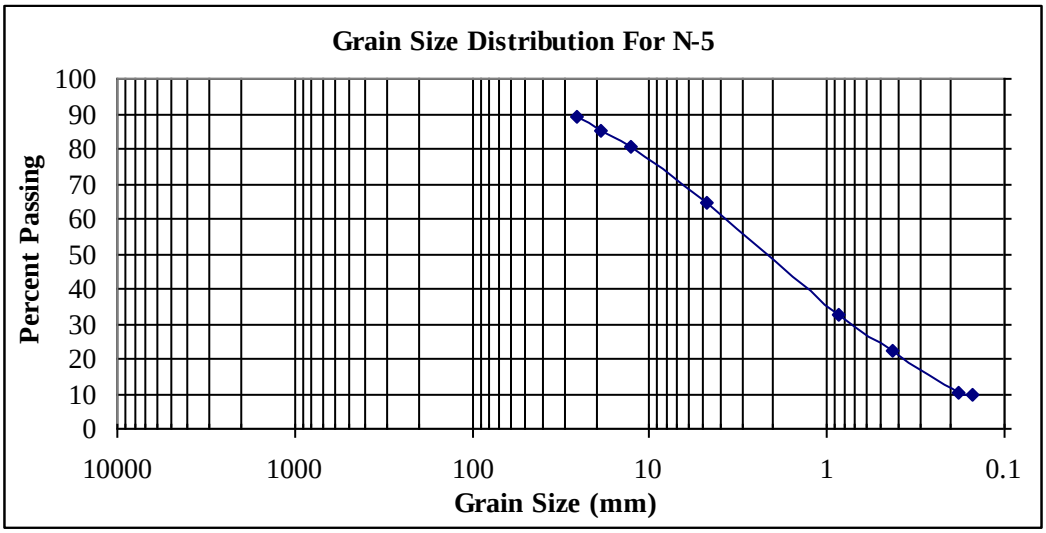

Site ID	Site	% finer than #100	D50 (mm)	D84 (mm)	USCS Classification
N-5	National	9.6	2	11	SW - SM

Figure C.10 Grain Size Distribution for N-5

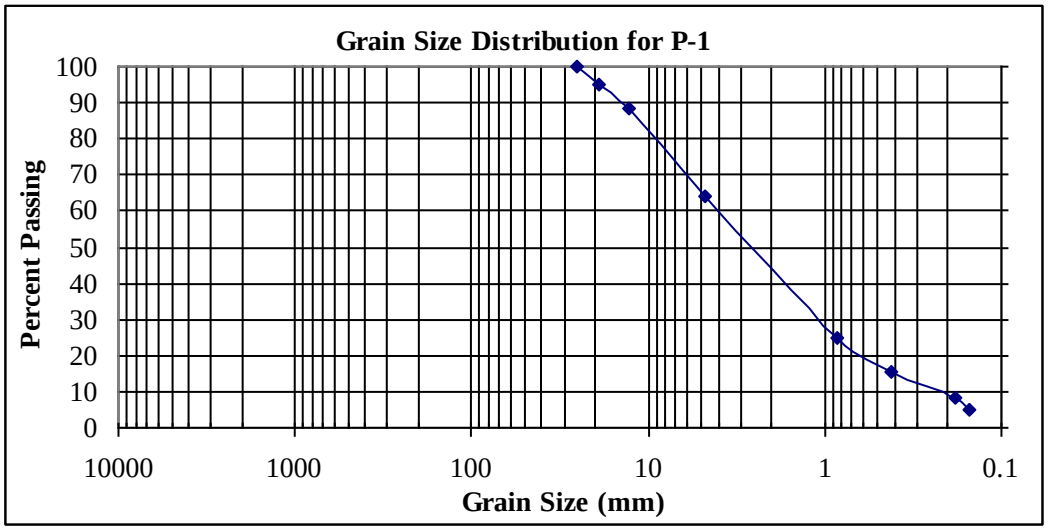

Site ID	Site	% finer than #100	D50 (mm)	D84 (mm)	USCS Classification
P-1	Premium	5.2	2.5	10	SW

Figure C.11 Grain Size Distribution for P-1

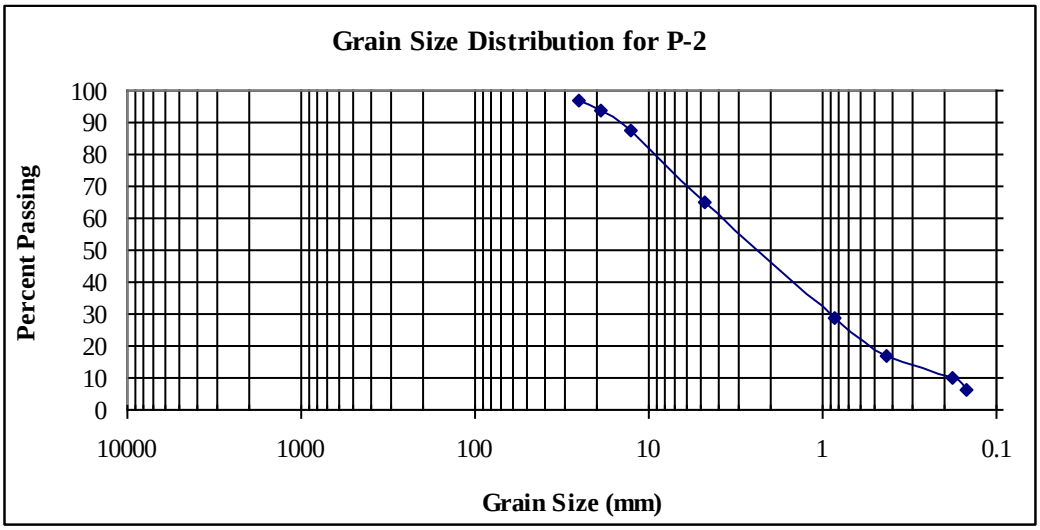

Site ID	Site	% finer than #100	D50 (mm)	D84 (mm)	USCS Classification
P-2	Premium	6.1	2.5	10	SW

Figure C.12 Grain Size Distribution for P-2

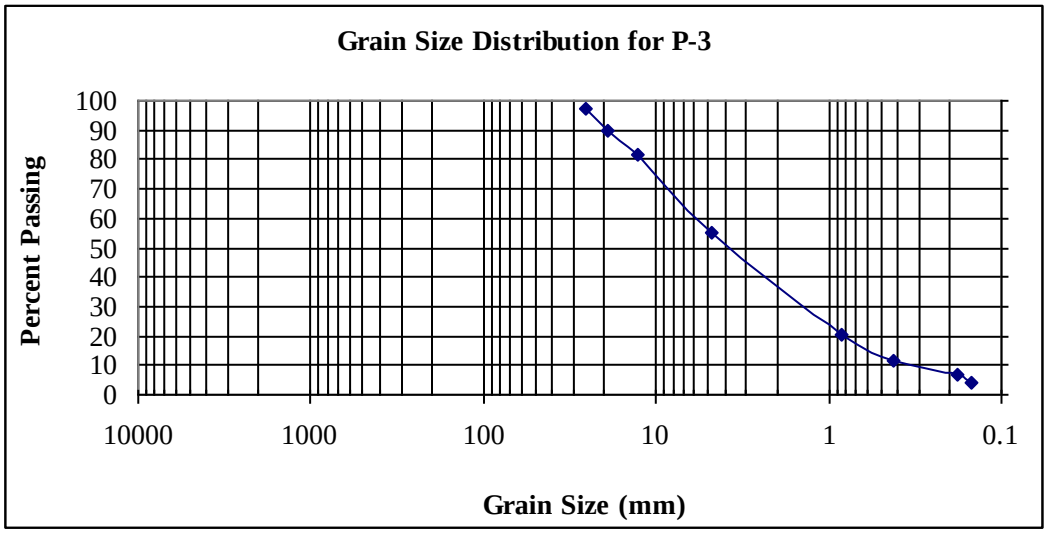

Site ID	Site	% finer than #100	D50 (mm)	D84 (mm)	USCS Classification
P-3	Premium	4.3	3.5	10.5	SW

Figure C.13 Grain Size Distribution for P-3

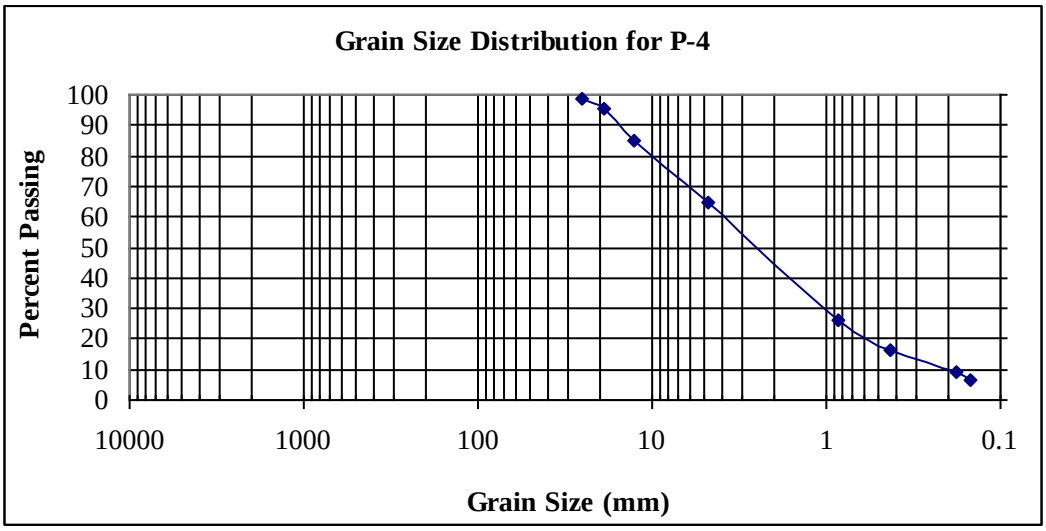

Site ID	Site	% finer than #100	D50 (mm)	D84 (mm)	USCS Classification
P-4	Premium	6.6	2.5	10.5	SW

Figure C.14 Grain Size Distribution for P-4

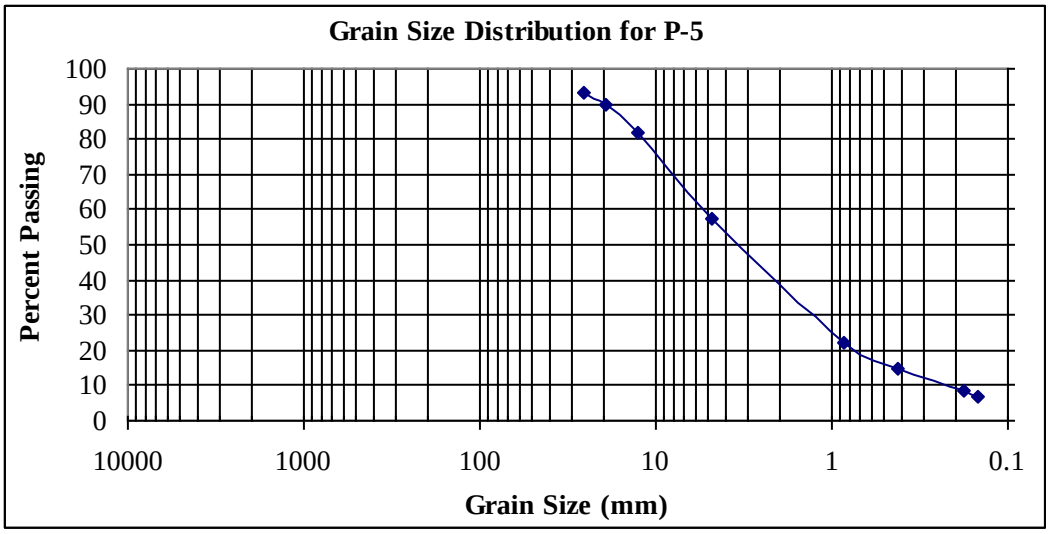

Site ID	Site	% finer than #100	D50 (mm)	D84 (mm)	USCS Classification
P-5	Premium	6.8	3	10	SW

Figure C.15 Grain Size Distribution for P-5

Appendix D: Angle of Repose Pictures

Note: **Slope length for Premium Coal Site ≈ 75 feet**
Slope length for National Coal Site ≈ 75 feet
Slope length for Mountainside Coal Site ≈ 100 feet

Figure D.1 Premium Coal Site Angle of Repose Number One

Figure D.2 Premium Coal Site Angle of Repose Number Two

Figure D.3 Premium Coal Site Angle of Repose Number Three

Figure D.4 Premium Coal Site Angle of Repose Number Four

Figure D.5 National Coal Site Angle of Repose Number One

Figure D.6 National Coal Site Angle of Repose Number Two

Figure D.8 National Coal Site Angle of Repose Number Three

Figure D.9 National Coal Site Angle of Repose Number Four

Figure D.10 Mountainside Coal Site Angle of Repose Number One

Figure D.11 Mountainside Coal Site Angle of Repose Number Two

Figure D.11 Mountainside Coal Site Angle of Repose Number Three

Figure D.12 Mountainside Coal Site Angle of Repose Number Four

Appendix E: Geographic Coordinates

Table E.1 Geographic Coordinates for Premium Coal Site

Point #	North	West
1	36° 06' 22.067"	84° 19' 26.444"
2	36° 06' 21.550"	84° 19' 26.640"
3	36° 06' 20.291"	84° 19' 26.822"
4	36° 06' 19.493"	84° 19' 27.120"
5	36° 06' 18.671"	84° 19' 27.782"
6	36° 06' 19.043"	84° 19' 28.658"
7	36° 06' 19.660"	84° 19' 28.310"
8	36° 06' 20.675"	84° 19' 28.130"
9	36° 06' 21.461"	84° 19' 28.046"
10	36° 06' 22.349"	84° 19' 28.052"

Table E.2 Geographic Coordinates for National Coal Site

Point #	N	W
1	36° 30' 37.144"	84° 16' 14.960"
2	36° 30' 36.538"	84° 16' 15.200"
3	36° 30' 35.836"	84° 16' 15.548"
4	36° 30' 34.900"	84° 16' 16.136"
5	36° 30' 34.300"	84° 16' 16.046"
6	36° 30' 33.958"	84° 16' 14.330"
7	36° 30' 34.522"	84° 16' 13.900"
8	36° 30' 35.266"	84° 16' 13.862"
9	36° 30' 36.088"	84° 16' 13.358"
10	36° 30' 37.228"	84° 16' 13.400"

Table E.3 Geographic Coordinates for Mountainside Coal Site

Point #	N	W
1	36º 31' 30.680"	83º 57' 23.256"
2	36º 31' 30.060"	83º 57' 23.382"
3	36º 31' 29.230"	83º 57' 23.610"
4	36º 31' 28.530"	83º 57' 23.420"
5	36º 31' 27.900"	83º 57' 23.385"
6	36º 31' 27.642"	83º 57' 21.888"
7	36º 31' 28.400"	83º 57' 21.642"
8	36º 31' 29.300"	83º 57' 21.790"
9	36º 31' 30.010"	83º 57' 21.780"

10	36° 31' 30.650"	83° 57' 21.786"

Appendix F: Grid Pictures and Grain Size Distribution Estimates

Figure F.1 Five Meter Square Grid Photograph at Mountainside Coal Site

Figure F.2 Five Meter Square Grid Photograph at Premium Coal Site

Figure F.3 Five Meter Square Grid Photograph at National Coal Site

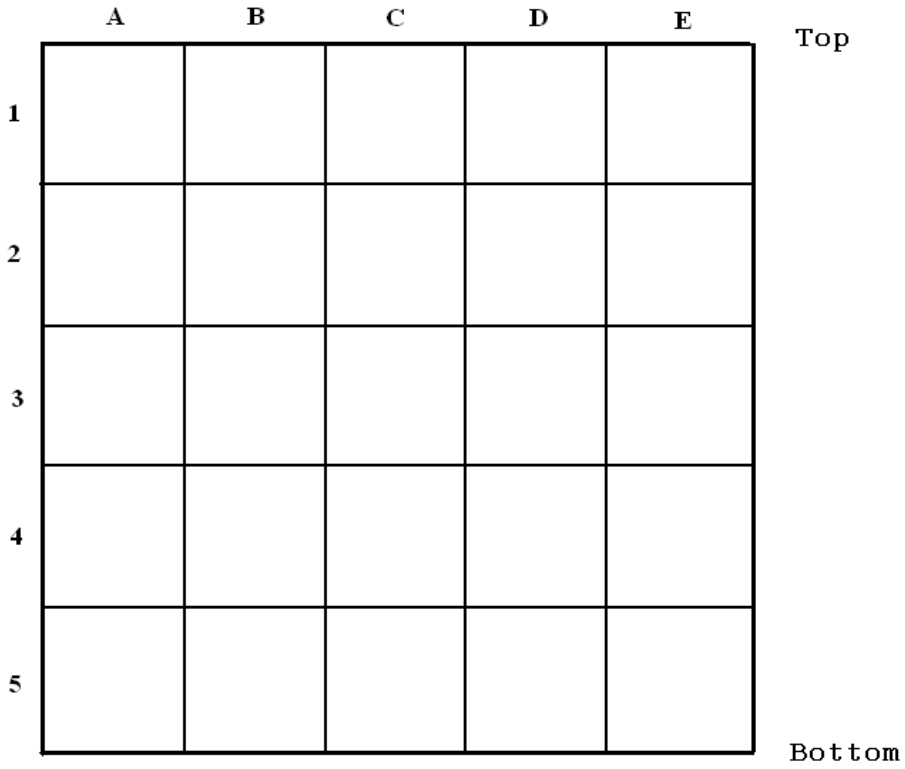

Figure F.4 Reference Chart for Grain Size Approximation Photos

Figure F.5 Photo A-1 for Mountainside Coal Site

Figure F.6 Photo A-2 for Mountainside Coal Site

Figure F.7 Photo A-3 for Mountainside Coal Site

Figure F.8 Photo A-4 for Mountainside Coal Site

Figure F.9 Photo A-5 for Mountainside Coal Site

Figure F.10 Photo B-1 for Mountainside Coal Site

Figure F.11 Photo B-2 for Mountainside Coal Site

Figure F.12 Photo B-3 for Mountainside Coal Site

Figure F.13 Photo B-4 for Mountainside Coal Site

Figure F.14 Photo B-5 for Mountainside Coal Site

Figure F.15 Photo C-1 for Mountainside Coal Site

Figure F.16 Photo C-2 for Mountainside Coal Site

Figure F.17 Photo C-3 for Mountainside Coal Site

Figure F.18 Photo C-4 for Mountainside Coal Site

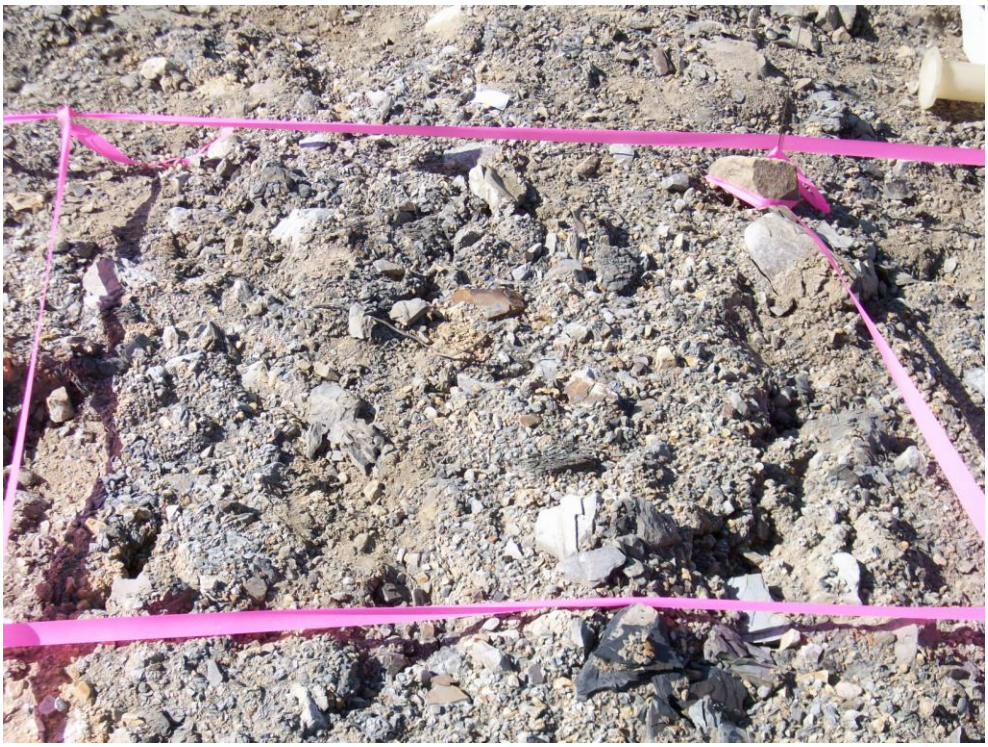

Figure F.19 Photo C-5 for Mountainside Coal Site

Figure F.20 Photo D-1 for Mountainside Coal Site

Figure F.21 Photo D-2 for Mountainside Coal Site

Figure F.22 Photo D-3 for Mountainside Coal Site

Figure F.23 Photo D-4 for Mountainside Coal Site

Figure F.24 Photo D-5 for Mountainside Coal Site

Figure F.25 Photo E-1 for Mountainside Coal Site

Figure F.26 Photo E-2 for Mountainside Coal Site

Figure F.27 Photo E-3 for Mountainside Coal Site

Figure F.28 Photo E-4 for Mountainside Coal Site

Figure F.29 Photo E-5 for Mountainside Coal Site

	A	B	C	D	E	
1	50	35	25	25	35	Top
2	60	50	30	25	35	
3	10	15	35	60	35	
4	20	15	30	35	60	
5	40	25	35	60	40	Bottom

Figure F.30 2" Particles Size Percentage Estimates for Mountainside Coal Site

	A	B	C	D	E	
1	40	20	10	5	15	Top
2	40	20	5	15	15	
3	5	5	5	5	15	
4	5	5	10	15	15	
5	10	5	5	5	5	Bottom

Figure F.31 12" Particles Size Percentage Estimates for Mountainside Coal Site

Figure F.32 Photo A-1 for Premium Coal Site

Figure F.33 Photo A-2 for Premium Coal Site

Figure F.34 Photo A-3 for Premium Coal Site

Figure F.35 Photo A-4 for Premium Coal Site

Figure F.36 Photo A-5 for Premium Coal Site

Figure F.37 Photo B-1 for Premium Coal Site

Figure F.38 Photo B-2 for Premium Coal Site

Figure F.39 Photo B-3 for Premium Coal Site

Figure F.40 Photo B-4 for Premium Coal Site

Figure F.41 Photo B-5 for Premium Coal Site

Figure F.42 Photo C-1 for Premium Coal Site

Figure F.43 Photo C-2 for Premium Coal Site

Figure F.44 Photo C-3 for Premium Coal Site

Figure C.F.45 Photo C-4 for Premium Coal Site

Figure F.46 Photo C-5 for Premium Coal Site

Figure F.47 Photo D-1 for Premium Coal Site

Figure F.48 Photo D-2 for Premium Coal Site

Figure F.49 Photo D-3 for Premium Coal Site

Figure F.50 Photo D-4 for Premium Coal Site

Figure F.51 Photo D-5 for Premium Coal Site

Figure F.52 Photo E-1 for Premium Coal Site

Figure F.53 Photo E-2 for Premium Coal Site

Figure F.54 Photo E-3 for Premium Coal Site

Figure F.55 Photo E-4 for Premium Coal Site

Figure F.56 Photo E-5 for Premium Coal Site

	A	B	C	D	E	
1	50	25	10	15	15	Top
2	50	25	20	30	35	
3	45	25	25	25	30	
4	45	40	15	35	15	
5	30	25	40	15	20	Bottom

Figure F.57 2” Particles Size Percentage Estimates for Premium Coal Site

	A	B	C	D	E	
1	20	5	0	5	5	Top
2	15	5	5	15	10	
3	10	15	5	5	10	
4	25	15	0	15	5	
5	5	5	20	0	10	Bottom

Figure F.58 12” Particles Size Percentage Estimates for Premium Coal Site

Figure F.59 Photo A-1 for National Coal Site

Figure F.60 Photo A-2 for National Coal Site

Figure F.61 Photo A-3 for National Coal Site

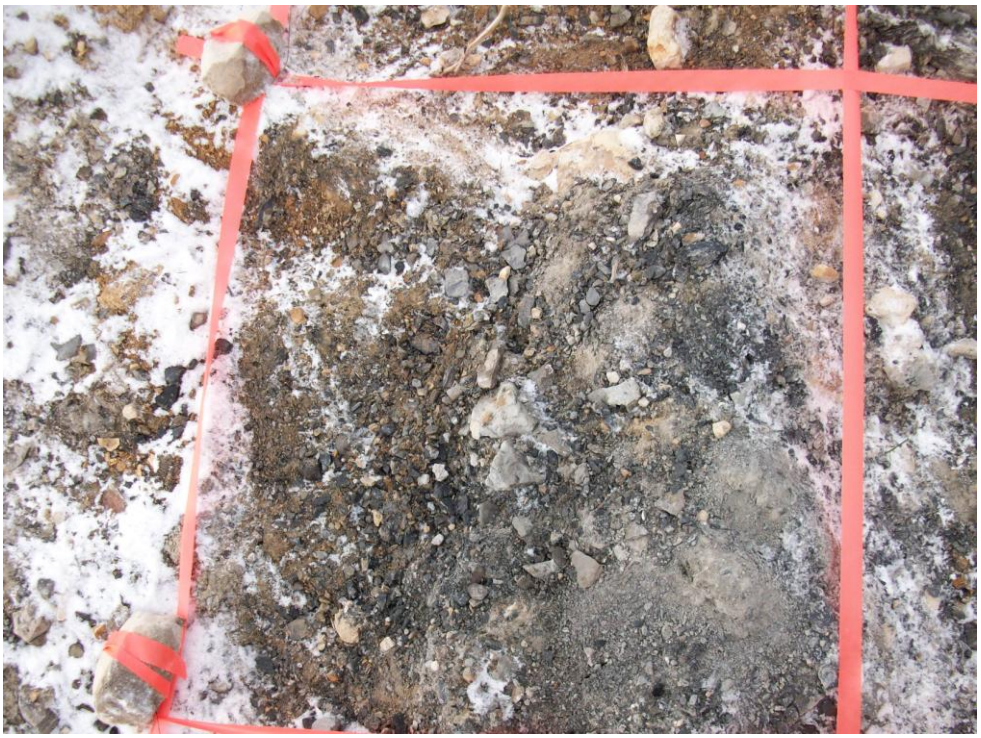

Figure F.62 Photo A-4 for National Coal Site

Figure F.63 Photo A-5 for National Coal Site

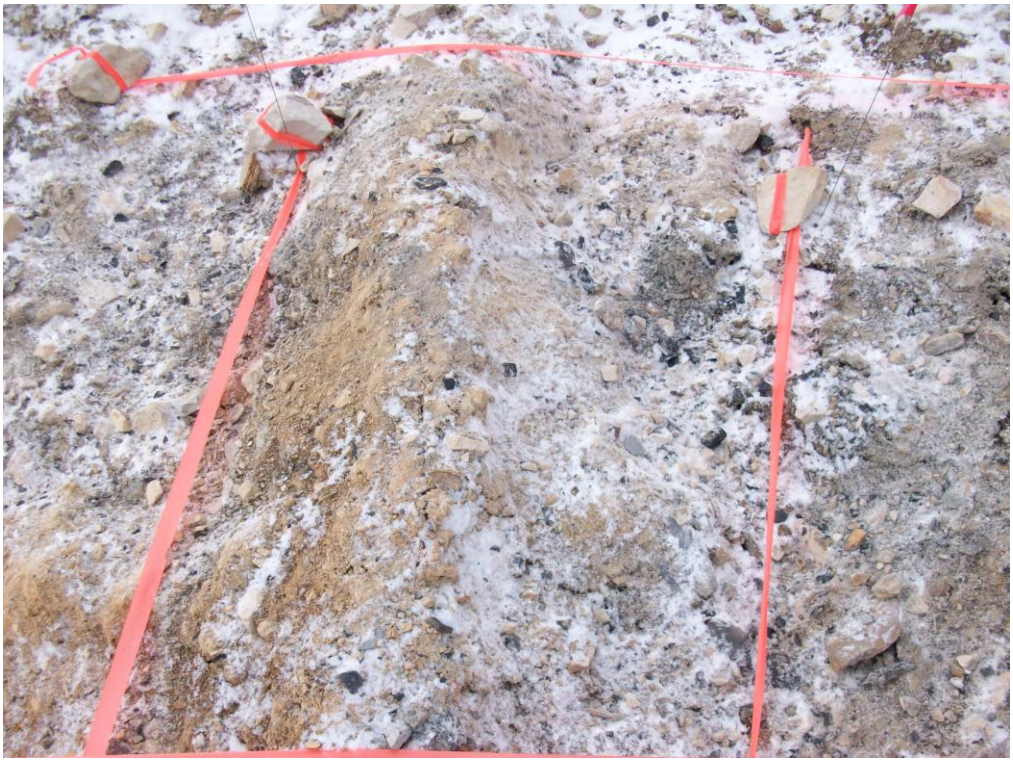

Figure F.64 Photo B-1 for National Coal Site

Figure F.65 Photo B-2 for National Coal Site

Figure F.66 Photo B-3 for National Coal Site

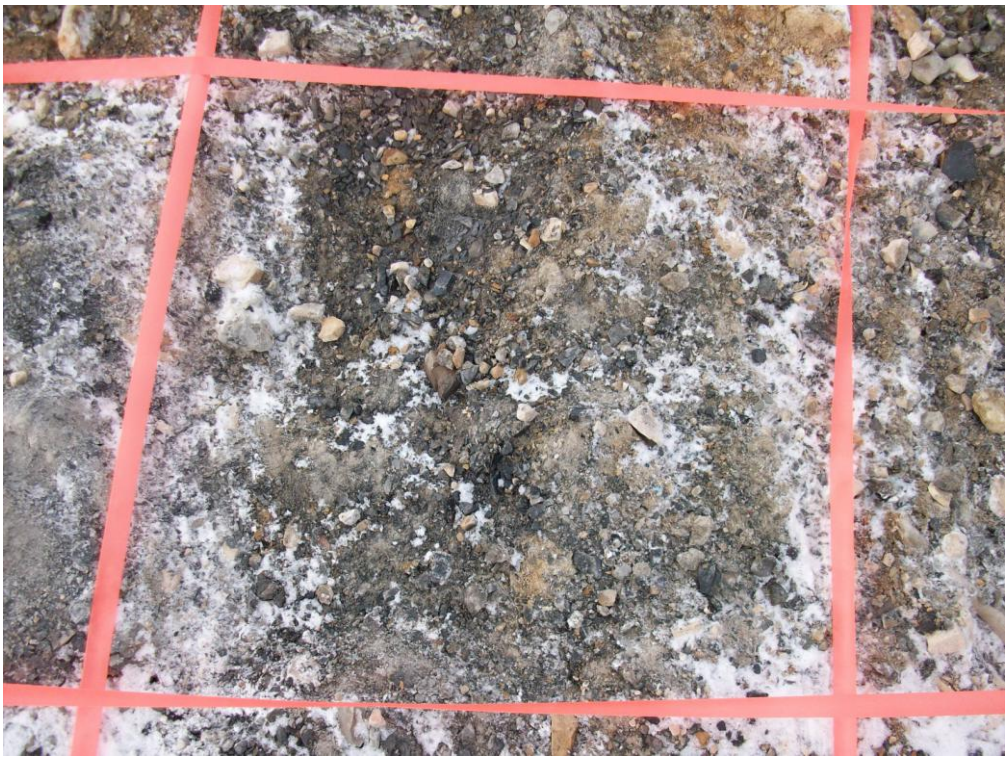

Figure F.67 Photo B-4 for National Coal Site

Figure F.68 Photo B-5 for National Coal Site

Figure F.69 Photo C-1 for National Coal Site

Figure F.70 Photo C-2 for National Coal Site

Figure F.71 Photo C-3 for National Coal Site

Figure F.72 Photo C-4 for National Coal Site

Figure F.73 Photo C-5 for National Coal Site

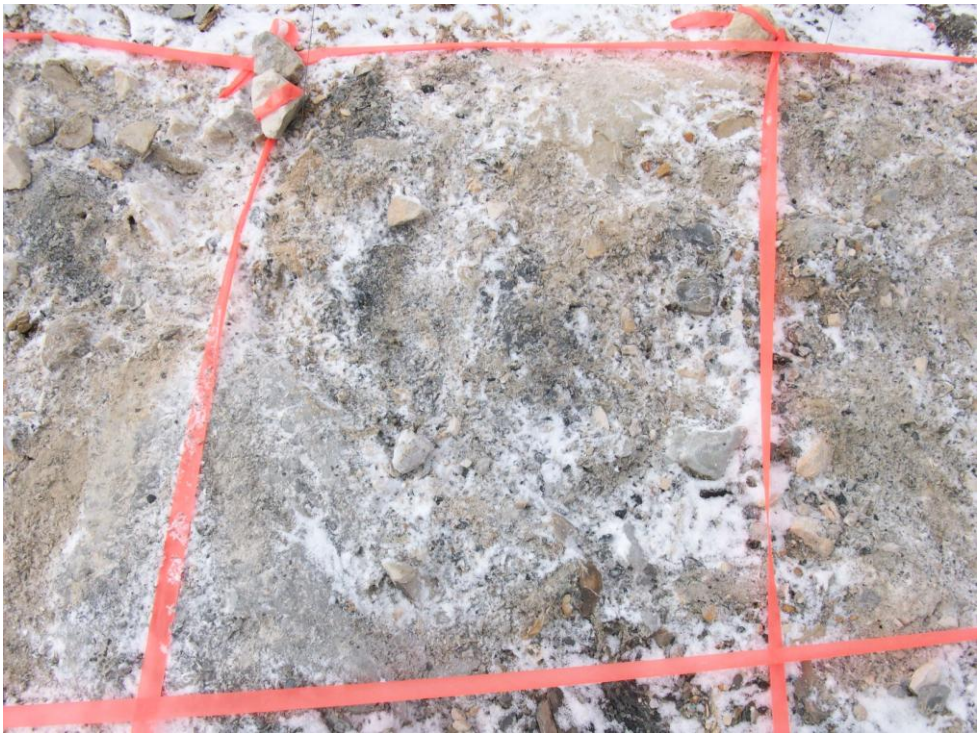

Figure F.74 Photo D-1 for National Coal Site

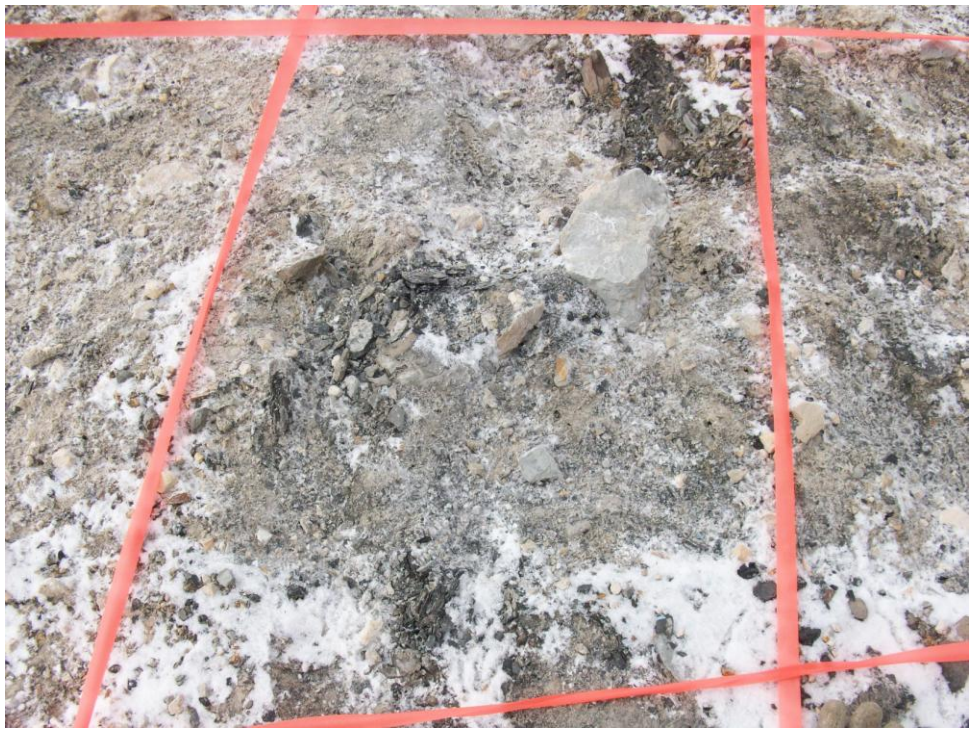

Figure F.75 Photo D-2 for National Coal Site

Figure F.76 Photo D-3 for National Coal Site

Figure F.77 Photo D-4 for National Coal Site

Figure F.78 Photo D-5 for National Coal Site

Figure F.79 Photo E-1 for National Coal Site

Figure F.80 Photo E-2 for National Coal Site

Figure F.81 Photo E-3 for National Coal Site

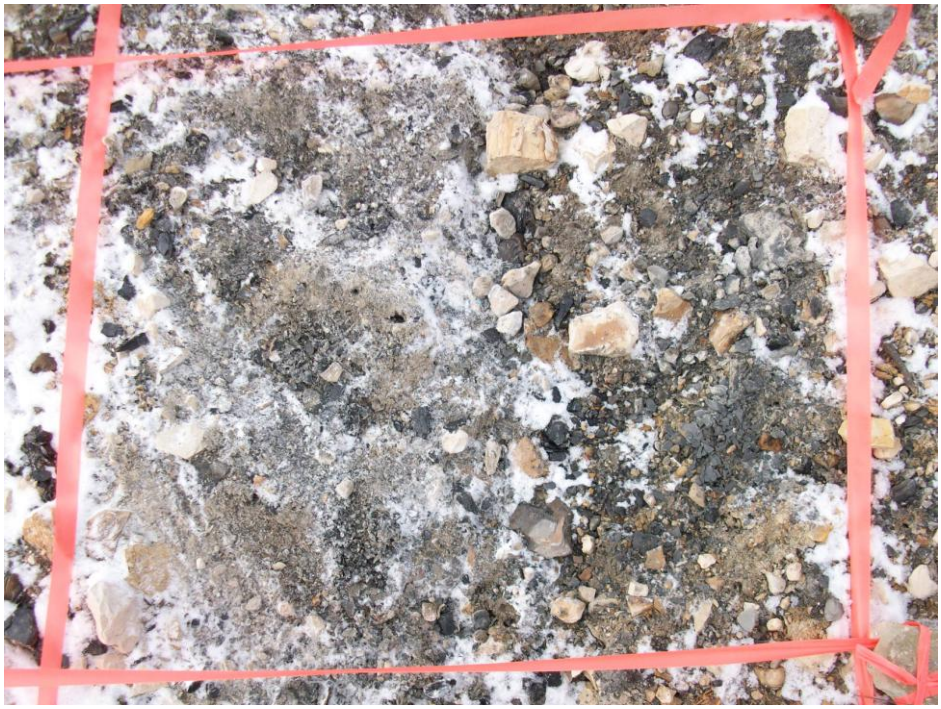

Figure F.82 Photo E-4 for National Coal Site

Figure F.83 Photo E-5 for National Coal Site

	A	B	C	D	E	
1	20	15	35	40	25	Top
2	20	15	15	25	20	
3	20	20	35	15	20	
4	20	20	25	20	25	
5	15	15	25	30	35	Bottom

Figure F.84 2" Particle Size Estimates for National Coal Site

	A	B	C	D	E	
1	0	0	10	5	5	Top
2	5	5	0	10	0	
3	0	5	5	0	5	
4	5	0	0	5	5	
5	5	0	5	10	5	Bottom

Figure F.85 12" Particle Size Percentage Estimates for National Coal Site

Vita

Patrick White was born and raised in Jackson, Tennessee. He attended North Side High School, and upon graduation in May of 2003, he enrolled in the Civil Engineering program at the University of Tennessee. Patrick received his Bachelors Degree in Civil and Environmental Engineering in May 2008, and enrolled in the Masters Degree program at the University of Tennessee with his concentration in geotechnology and infrastructure materials. Mr. White plans on graduating from the Masters Program in May of 2009.